GLOBAL JOURNAL

OF RESEARCHES IN ENGINEERING: A

Mechanical & Mechanics Engineering

Aspect Ratio and Installation

Effects of Ageing on Mechanical

} Highlights {

Flow Heat Transfer Performance

Critical Appraisal of Conventional

Discovering Thoughts, Inventing Future

Global Journal of Researches in Engineering: A

Mechanical and Mechanics Engineering

Global Journals Inc.

Publisher's Headquarters office

Global Journals® Headquarters
945th Concord Streets,
Framingham Massachusetts Pin: 01701,
United States of America
USA Toll Free: +001-888-839-7392
USA Toll Free Fax: +001-888-839-7392

Offset Typesetting

Global Journals Incorporated
2nd, Lansdowne, Lansdowne Rd., Croydon-Surrey,
Pin: CR9 2ER, United Kingdom

Packaging & Continental Dispatching

Global Journals Pvt Ltd
E-3130 Sudama Nagar, Near Gopur Square,
Indore, M.P., Pin:452009, India

Find a correspondence nodal officer near you

To find nodal officer of your country, please email us at *local@globaljournals.org*

eContacts

Press Inquiries: *press@globaljournals.org*
Investor Inquiries: *investors@globaljournals.org*
Technical Support: *technology@globaljournals.org*
Media & Releases: *media@globaljournals.org*

Pricing (Excluding Air Parcel Charges):

Yearly Subscription (Personal & Institutional)
250 USD (B/W) & 350 USD (Color)

Dr. Sofoklis S. Makridis

B.Sc(Hons), M.Eng, Ph.D. Professor Department of Mechanical Engineering University of Western Macedonia, Greece

Dr. Steffen Lehmann

Faculty of Creative and Cultural Industries Ph.D., AA Dip University of Portsmouth United Kingdom

Dr. Wenfang Xie

Ph.D., Department of Electrical Engineering, Hong Kong Polytechnic University, Department of Automatic Control, Beijing University of Aeronautics and Astronautics China

Dr. Hai-Wen Li

Ph.D., Materials Engineering, Kyushu University, Fukuoka, Guest Professor at Aarhus University, Japan

Dr. Saeed Chehreh Chelgani

Ph.D. in Mineral Processing University of Western Ontario, Adjunct professor, Mining engineering and Mineral processing, University of Michigan United States

Belen Riveiro

Ph.D., School of Industrial Engineering, University of Vigo Spain

Dr. Adel Al Jumaily

Ph.D. Electrical Engineering (AI), Faculty of Engineering and IT, University of Technology, Sydney

Dr. Maciej Gucma

Assistant Professor, Maritime Univeristy of Szczecin Szczecin, Ph.D.. Eng. Master Mariner, Poland

Dr. M. Meguellati

Department of Electronics, University of Batna, Batna 05000, Algeria

Dr. Haijian Shi

Ph.D. Civil Engineering Structural Engineering Oakland, CA, United States

Dr. Chao Wang

Ph.D. in Computational Mechanics Rosharon, TX, United States

Dr. Joaquim Carneiro

Ph.D. in Mechanical Engineering, Faculty of Engineering, University of Porto (FEUP), University of Minho, Department of Physics Portugal

Dr. Wei-Hsin Chen

Ph.D., National Cheng Kung University, Department of Aeronautics, and Astronautics, Taiwan

Dr. Bin Chen

B.Sc., M.Sc., Ph.D., Xian Jiaotong University, China. State Key Laboratory of Multiphase Flow in Power Engineering Xi?an Jiaotong University, China

Dr. Charles-Darwin Annan

Ph.D., Professor Civil and Water Engineering University Laval, Canada

Dr. Jalal Kafashan

Mechanical Engineering Division of Mechatronics KU Leuven, Belglum

Dr. Alex W. Dawotola

Hydraulic Engineering Section, Delft University of Technology, Stevinweg, Delft, Netherlands

Dr. Shun-Chung Lee

Department of Resources Engineering, National Cheng Kung University, Taiwan

Prof. (LU), (UoS) Dr. Miklas Scholz

Cand Ing, BEng (equiv), PgC, MSc, Ph.D., CWEM, CEnv, CSci, CEng, FHEA, FIEMA, FCIWEM, FICE, Fellow of IWA, VINNOVA Fellow, Marie Curie Senior, Fellow, Chair in Civil Engineering (UoS) Wetland Systems, Sustainable Drainage, and Water Quality

Dr. Kitipong Jaojaruek

B. Eng, M. Eng, D. Eng (Energy Technology, Asian Institute of Technology). Kasetsart University Kamphaeng Saen (KPS) Campus Energy Research Laboratory of Mechanical Engineering

Dr. Yudong Zhang

B.S., M.S., Ph.D. Signal and Information Processing, Southeast University Professor School of Information Science and Technology at Nanjing Normal University, China

Dr. Burcin Becerik-Gerber

University of Southern Californi Ph.D. in Civil Engineering Ddes, from Harvard University M.S. from University of California, Berkeley M.S. from Istanbul, Technical University

Dr. Minghua He

Department of Civil Engineering Tsinghua University Beijing, 100084, China

Hiroshi Sekimoto

Professor Emeritus Tokyo Institute of Technology Japan Ph.D., University of California Berkeley

Dr. Philip G. Moscoso

Technology and Operations Management IESE Business School, University of Navarra Ph.D. in Industrial Engineering and Management, ETH Zurich M.Sc. in Chemical Engineering, ETH Zurich, Spain

Dr. Shaoping Xiao

BS, MS Ph.D. Mechanical Engineering, Northwestern University The University of Iowa, Department of Mechanical and Industrial Engineering Center for Computer-Aided Design

Dr. Stefano Mariani

Associate Professor, Structural Mechanics, Department of Civil and Environmental Engineering, Ph.D., in Structural Engineering Polytechnic University of Milan Italy

Dr. A. Stegou-Sagia

Ph.D., Mechanical Engineering, Environmental Engineering School of Mechanical Engineering, National Technical University of Athens, Greece

Dr. Ciprian Lapusan

Ph. D in Mechanical Engineering Technical University of Cluj-Napoca Cluj-Napoca (Romania)

Diego Gonzalez-Aguilera

Ph.D. Dep. Cartographic and Land Engineering, University of Salamanca, Avilla, Spain

Dr. Francesco Tornabene

Ph.D. in Structural Mechanics, University of Bologna Professor Department of Civil, Chemical, Environmental and Materials Engineering University of Bologna, Italy

Dr. Maria Daniela

Ph.D in Aerospace Science and Technologies Second University of Naples, Research Fellow University of Naples Federico II, Italy

Dr. Omid Gohardani

Ph.D. Senior Aerospace/Mechanical/ Aeronautical, Engineering professional M.Sc. Mechanical Engineering, M.Sc. Aeronautical Engineering B.Sc. Vehicle Engineering Orange County, California, US

Dr. Paolo Veronesi

Ph.D., Materials Engineering, Institute of Electronics, Italy President of the master Degree in Materials Engineering Dept. of Engineering, Italy

CONTENTS OF THE ISSUE

Effect of Aspect Ratio and Installation Direction on Channel Flow Heat Transfer Performance under a wide Range of Reynolds Number

By Shunichi Sakuragi & Daisuke Torii

Abstract- In recent years, in the cooling technology for high-power electronic devices such as power transistors used for drive motor control of electric vehicles and hybrid vehicles, a method of flowing a cooling fluid to a cooling substrate having a fin structure has become the main technology. The structure of the cooling fluid flow path is a channel flow through multiple narrow plate gaps to secure a heat transfer area. In this study, the heat transfer characteristics when the aspect ratio of the channel having a flat rectangular cross-section was changed were investigated in detail by experiments. Moreover, the difference in the heat transfer characteristic at the time of making a rectangular flow path into vertical installation and horizontal installation was also investigated.

Keywords: channel flow, forced convection, natural convection, aspect ratio, synergistic effect, cooling device, power electronics device.

GJRE-A Classification: FOR Code: 091399

Strictly as per the compliance and regulations of:

Effect of Aspect Ratio and Installation Direction on Channel Flow Heat Transfer Performance under a wide Range of Reynolds Number

Shunichi Sakuragi [α] & Daisuke Torii [σ]

Abstract- In recent years, in the cooling technology for high-power electronic devices such as power transistors used for drive motor control of electric vehicles and hybrid vehicles, a method of flowing a cooling fluid to a cooling substrate having a fin structure has become the main technology. The structure of the cooling fluid flow path is a channel flow through multiple narrow plate gaps to secure a heat transfer area. In this study, the heat transfer characteristics when the aspect ratio of the channel having a flat rectangular cross-section was changed were investigated in detail by experiments. Moreover, the difference in the heat transfer characteristic at the time of making a rectangular flow path into vertical installation and horizontal installation was also investigated. As a result, we have clarified the general nature and characteristics of channel flow heat transfer. In particular, in the case of vertical flow, it has been confirmed that the synergetic effect of forced convection and natural convection achieves a maximum heat transfer coefficient in a constant channel width region.

Keywords: channel flow, forced convection, natural convection, aspect ratio, synergistic effect, cooling device, power electronics device.

I. Introduction

With the spread of hybrid vehicles and electric vehicles, the development of a high-efficiency cooling device for high output power electronic devices such as power transistors for controlling high output motors has become one of the important technical issues (Taguchi and Sakuragi, 2014). To achieve high cooling capacity in a limited space volume, it is considered that the design of a cooling system utilizing channel flow is an effective method.

Channel flow is widely used in various cooling devices, heat exchangers, etc., and so far, performance evaluation has been conducted by many experimental studies (Mehta and Khandekar, 2013, Forrest et al., 2014, Ashraf et al., 2016) and simulations on its heat transfer characteristics (Kawamura et al., 2000, Mollik et al., 2017, Uchino et al., 2017). However, there are very few research examples in which heat transfer characteristics are systematically pursued in response to a wide Reynolds number region of the cooling flow and various aspect ratios of the flow channel cross-

section. In particular, the optimization of fin thickness and fin spacing is very important to achieve high cooling capacity in a small space (Tanaka et al., 2015). For this purpose, it is also necessary to investigate in detail the effect of the gap width of the channel on the heat transfer performance.

In this study, we fabricated an evaluation system of heat transfer performance that can change the gap width and height of the channel with a rectangular cross-section. And the evaluation data of heat transfer performance were systematically acquired about various channel gap width and aspect ratio. We also acquired data in a wide range of Reynolds numbers of 4,000 to 110,000. Furthermore, the difference in heat transfer characteristics was also evaluated when the channel flow path was placed vertically and horizontally.

From these series of experiments, it was revealed that in the case of the vertically disposed flow passage, there is a flow passage gap width at which the heat transfer coefficient takes a maximum value. In this case, it was confirmed that the heat transfer coefficient could be accurately approximated by a function including both Reynolds number and Grashof number. It is considered that these results obtained in this study can be a useful indicator in the design of high-performance cooling systems for various heat generators.

Nomenclature
D: channel width
d: tube diameter
dh: equivalent diameter of channel cross-section
Gr: Grashof number
H: channel height
L: length of the water-cooled surface of a heat transfer substrate
Nu: Nusselt number
P: static pressure of the flow
Q: flow rate of cooling water
Qa: the amount of heat absorbed by cooling water
Qh: heat generation output of a heater
q: heat flux
Re: Reynolds number
S: heat transfer area
T: temperature

Author α: Department of Mechanical Engineering, Shizuoka Institute of Science and Technology 2200-2 Toyosawa, Fukuroi city, Shizuoka 437-8555, Japan. e-mail: sakuragi.shunichi@sist.ac.jp
Author σ: Yamaha Motor Co., Ltd. 2500 Shingai, Iwata city, Shizuoka 438-8501, Japan.

Tin: temperature of cooling water at the inlet of the test section

Tout: temperature of cooling water at the outlet of the test section

Ts: temperature of the substrate

Tw: temperature of cooling water

W: substrate thickness

α: heat transfer coefficient

λ: thermal conductivity of the substrate

ρ: fluid density

II. Experimental Apparatus and Method

a) Evaluation device of heat transfer performance

Figure 1 shows a schematic diagram of the evaluation device of heat transfer performance. Two pure copper heat transfer substrates are inserted oppositely from both sides of a case made of SUS304, and sandwiching the two spacers at the top and bottom of the substrates, the gap between the two substrates can be adjusted. Five types of gap values *D* (= 1.2, 1.8,

2.4, 3.0, 3.6 mm) were set by the thickness of the spacer.

Two plate heaters (100 V, 200 W) (210 mm × 30 mm × 2 mm in thickness) are attached to the outside of the heat transfer substrate via a heat transfer rubber sheet, and a total heat load of 400 W is generated. Also, three insertion holes for inserting a sheath type thermocouple are provided at equal intervals of 65 mm on the side surface portion of the heat transfer substrate. The substrate temperature at the center of the channel height is measured at a total of six locations on the two substrates, and the substrate average temperature *Ts* (= (*T*1 + *T*2 +.. + *T*6) / 6) is determined. Further, the height *H* of the water-cooled surface of the heat transfer substrate was prepared to be 20 mm and 30 mm. The lengths *L* of the water-cooled surfaces of the heat transfer substrates in the flow direction are all 180 mm.

Figure 2 shows two installation states of the channel flow path. Vertical placement and horizontal placement are shown.
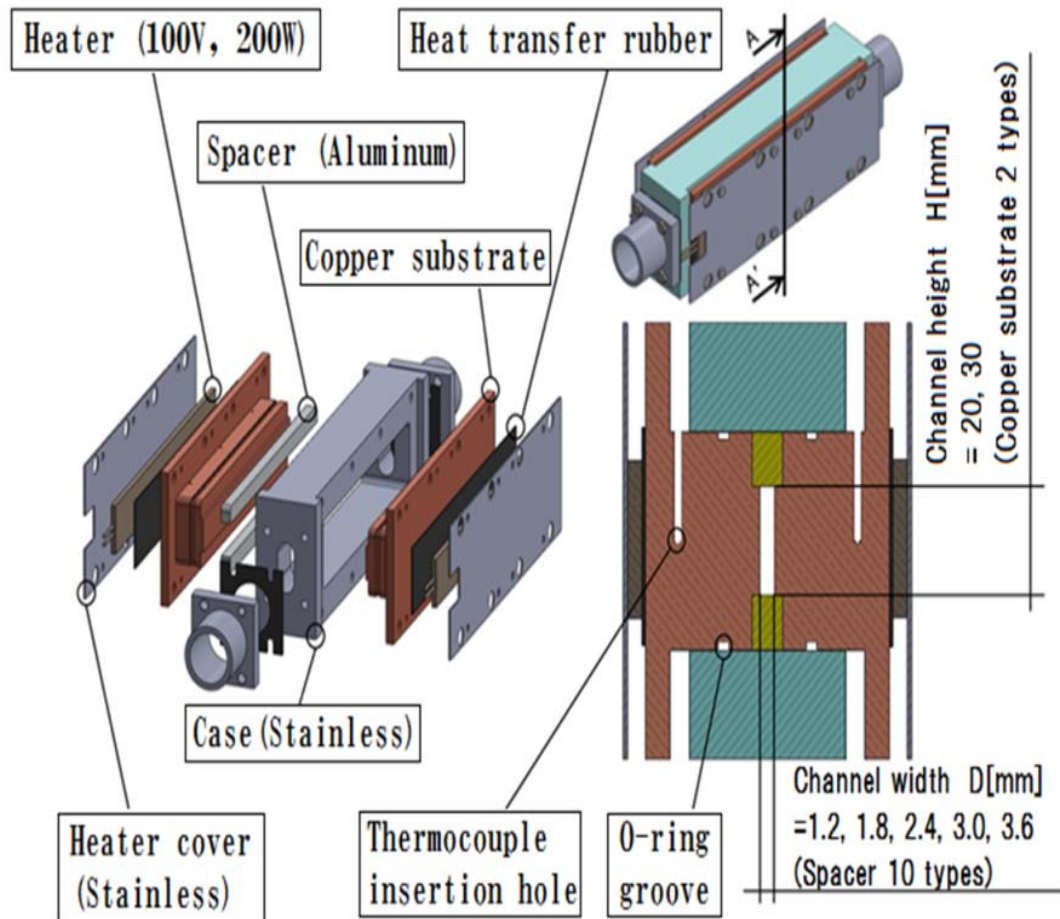
Figure 1: Structure of the evaluation device of heat transfer performance for channel flow.

(a) Vertical placement

(b) Horizontal placement
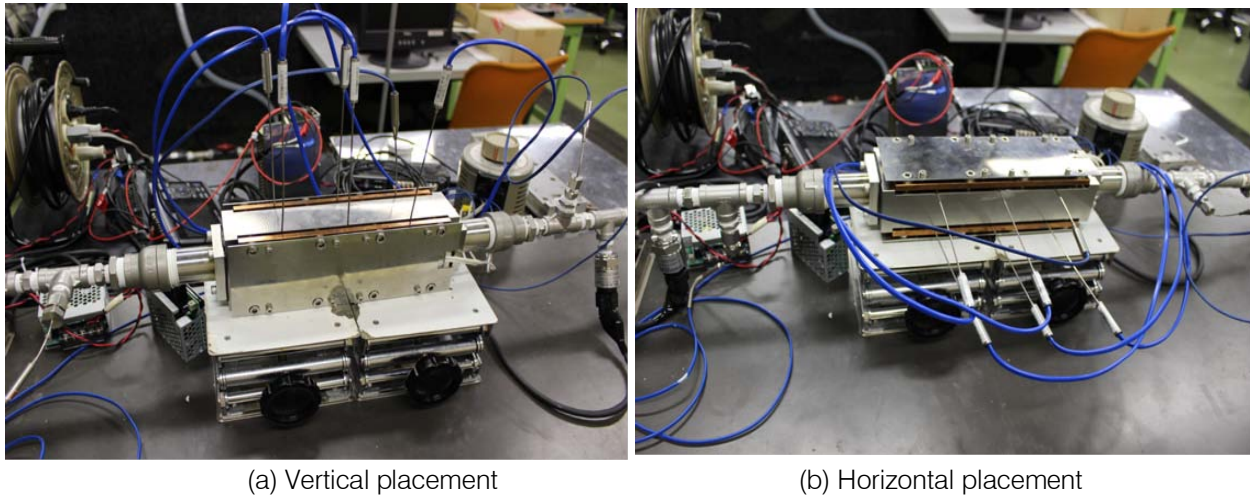
Figure 2: Two installation methods of the channel flow path

In this experiment, to obtain an accurate heat transfer coefficient between the cooling water and the substrate, it is necessary to accurately know the substrate surface temperature in contact with the cooling water. In this apparatus, the distance between the heating surface of the substrate and the water-cooled surface is 30 mm, and the substrate temperature is measured at the approximate center of the substrate thickness. Therefore, it is necessary to estimate the difference between the measured temperature and the water cooling surface temperature. The maximum temperature difference is calculated as follows.

In order to estimate the maximum temperature difference ΔT $(= Tsh - Tsw)$ between the substrate surface temperature Tsh in contact with the heater and the substrate surface temperature Tsw in contact with the cooling water, it is assumed that all the heat Qh emitted from the heater passes through the water cooling area $(= H \times L)$ one-dimensionally. The passing heat flux q is calculated by the following equation.

$$q = Q_h / (H\, L) = \lambda\, (\Delta T / W) \quad (1)$$

Here, Qh is the heat generation output of the heater (W), H is the water-cooled surface height (m), L is the water-cooled surface length (m), λ is the substrate thermal conductivity (W / (mK)), W is substrate thickness (m). From this, ΔT is calculated as follows.

$$\Delta T = Q_h\, W/(\lambda\, H\, L) = 200 \times 30 \times 10^{-3}/(400 \times 20 \times 10^{-3} \times 180 \times 10^{-3}) = 4.2\ ^{\circ}\mathrm{C} \quad (2)$$

Therefore, it can be seen that the temperature difference between the measured average temperature Ts and the temperature Tsw in contact with the cooling water is about $\Delta T/2 = 2.1\ ^{\circ}\mathrm{C}$ at the maximum. In the following discussion, we will consider the measured average temperature Ts as the substrate representative temperature and proceed with the discussion.

b) Configuration of measurement system

Figure 3 shows the measurement system. In the evaluation device of heat transfer performance shown in Fig. 1, water at 20 $^{\circ}$C is always supplied from the chiller unit, heat is absorbed in the test section, and the heated water is returned to the chiller unit again and cooled.

To accurately estimate the amount of heat absorbed by the cooling water, it is necessary to evaluate the measurement accuracy of the flow meter. This is because the flow meter often has a relatively large measurement error as compared to other sensors.
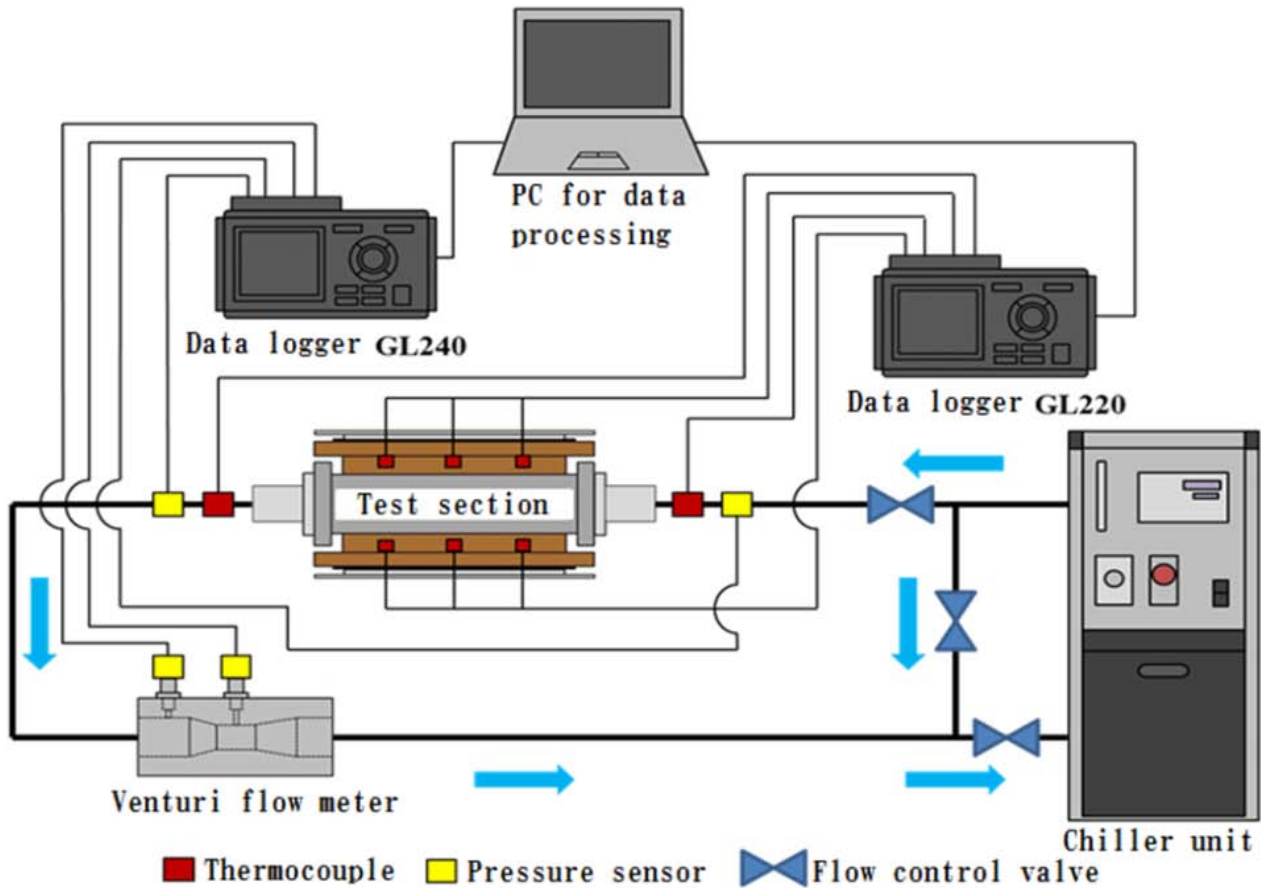
Figure 3: Measurement system for performance data acquisition

The specifications of the Venturi flow meter used in the coolant circuit are shown in Fig. 4. The theoretical flow rate determined from the pressure difference measured by the Venturi flow meter is given by the following equation (Daugherty et al., 1985).

$$Q = \frac{\pi d_1^2}{4\sqrt{(d_1/d_2)^4 - 1}} \sqrt{\frac{2(P_1 - P_2)}{\rho}} \tag{3}$$

Here, $d1$ and $d2$ represent the pipe diameter of each pressure measurement location.

On the other hand, to investigate the relationship between the actual passing flow rate and the measured pressure difference, the flow rate test was performed by the method shown in Fig. 5. Water was supplied from the tap of the water supply to the inlet of the Venturi flow meter, the passed water was collected with a large beaker, and the time until reaching a predetermined volume was measured to determine the actual flow rate.

The theoretical flow rate and the measured flow rate are plotted in Fig. 6. From the figure, it can be seen that the two match with good accuracy. In the actual flow rate measurement, the method of calculating the flow rate by substituting the pressure difference measured by the Venturi flowmeter into Eq. (3) was adopted.
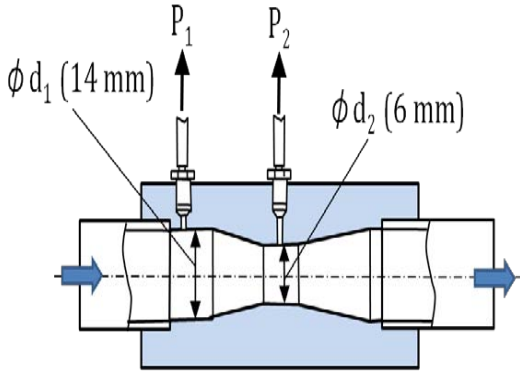
Figure 4: Specifications of the Venturi flowmeter.
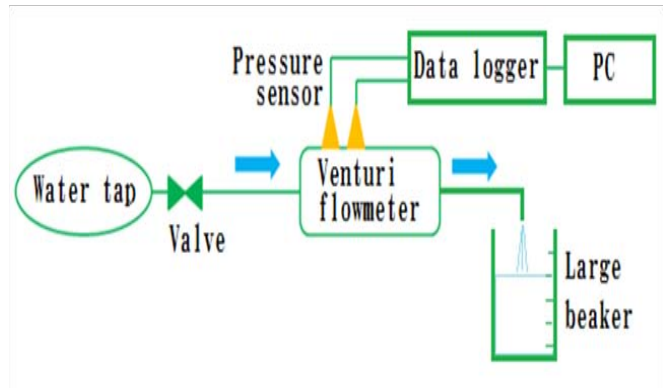
Figure 5: Measurement accuracy verification method of Venturi flow meter
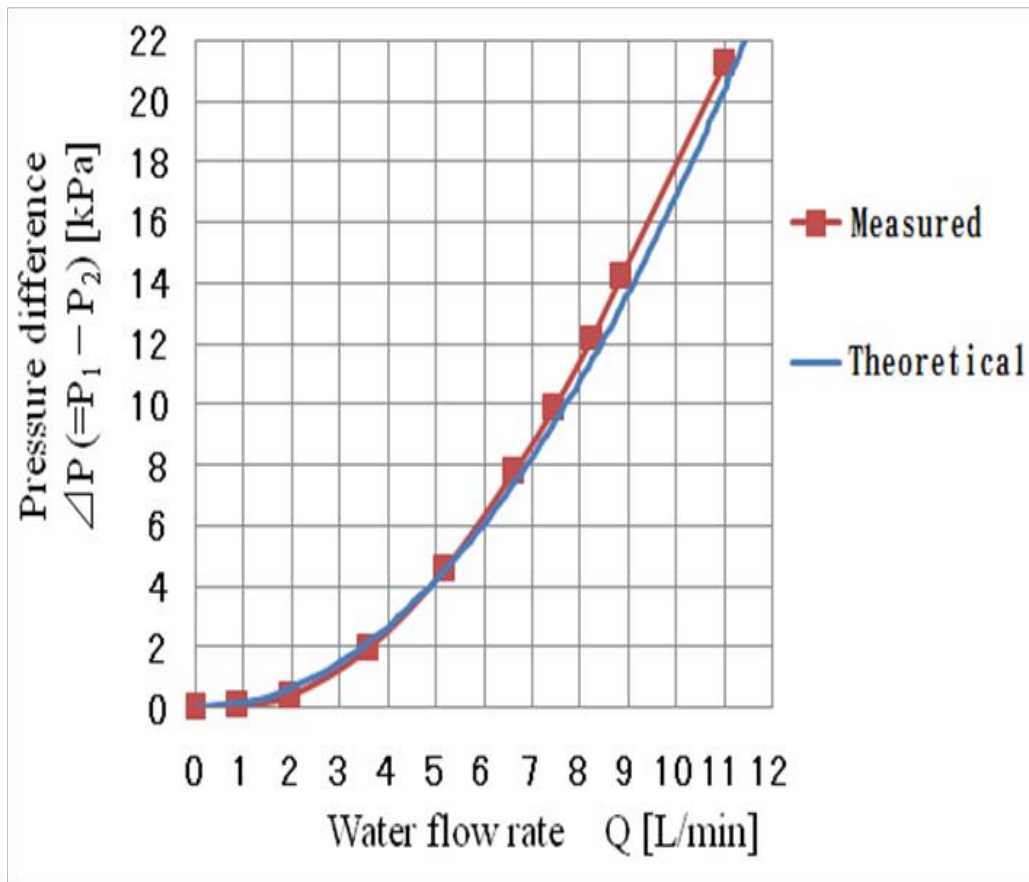
Figure 6: Comparison of the theoretical flow rate of the Venturi flow meter and the measured flow rate

c) *Evaluation method of heat transfer performance*

The amount of heat Qa absorbed by the cooling water in the test section is expressed by the following equation.

$$Q_a = \dot{m}c(T_{out} - T_{in}) \qquad (4)$$

Here, m is the mass flow rate of water c is the specific heat of water, $Tout$ is the temperature of water at the outlet of the test section and Tin is the temperature of water at the inlet of the test section.

Further, the average heat transfer coefficient α on the surface of the heat transfer substrate is defined by the following equation.

$$\overline{\alpha} = \frac{Q_a}{S\,(\overline{T_s} - \overline{T_w})} \qquad (5)$$

Here, S is a heat transfer area, Tw is average water temperature, and is defined by $Tw = (Tout + Tin) / 2$. Also, the equivalent diameter dh of the flow path shape was used as the value of the representative length required for the calculation of the Reynolds number and the Grashof number of the dimensionless parameters related to the heat transfer performance. dh is defined by the following formula (Nakayama, 1998).

$$d_h = 2DH/(D+H) \qquad (6)$$

Here, D is the channel width, and H is the channel height (see Fig. 1).

III. Experimental Results and Discussion

a) *Amount of heat absorbed by cooling water and substrate temperature*

Figures 7 and 8 show the relationship between the flow rate of cooling water and the amount of heat absorbed by cooling water when the channel flow path height H is 20 mm and 30 mm, respectively. In each of the graphs, measurement results in the case where the flow path is set vertically and horizontally with the flow path width D as a parameter is shown.

In both figures, the larger the flow path width D, the larger the absorbed heat amount tends to be. Further, when H is 20 mm, the absorbed heat amount is relatively smaller than when H is 30 mm, and it is presumed that the amount of heat leakage to the outside of the apparatus is large.

In the case of $H = 20$ mm, no significant difference is observed between the vertical and horizontal placement at any D value. However, at $H = 30$ mm, it can be seen that the amount of heat absorbed in the vertical position significantly exceeds the amount of heat absorbed in the horizontal position when $D = 1.8$ and 2.4 mm.
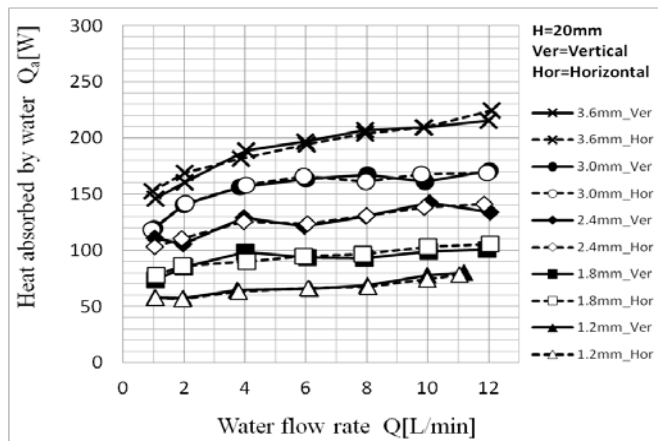
Figure 7: Relationship between cooling water flow rate and absorbed heat quantity (*H*=20mm)
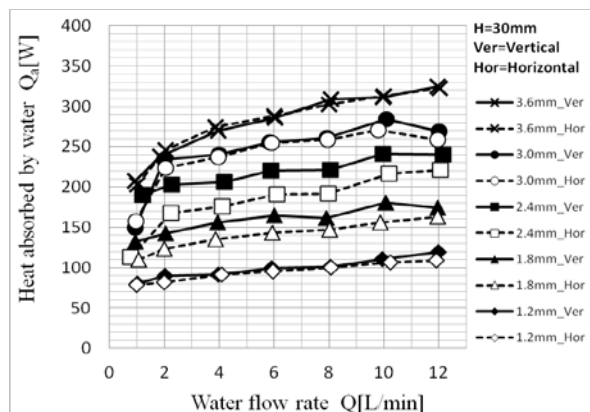
Figure 8: Relationship between cooling water flow rate and absorbed heat quantity (*H*=30mm)

Figures 9 and 10 show the relationship between the cooling water flow rate and the average substrate temperature when the channel height H is 20 mm and 30 mm, respectively. In both graphs, the average substrate temperature tends to decrease in inverse proportion to the cooling water flow rate. When H is 20 mm, a significant difference between vertical and horizontal placement is not seen. However, when H is 30 mm, horizontal placement tends to lower the substrate temperature.
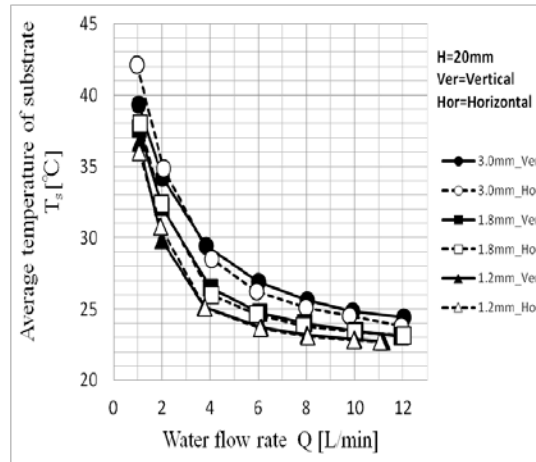
Figure 9: Relationship between cooling water flow rate and average substrate temperature (H=20mm)
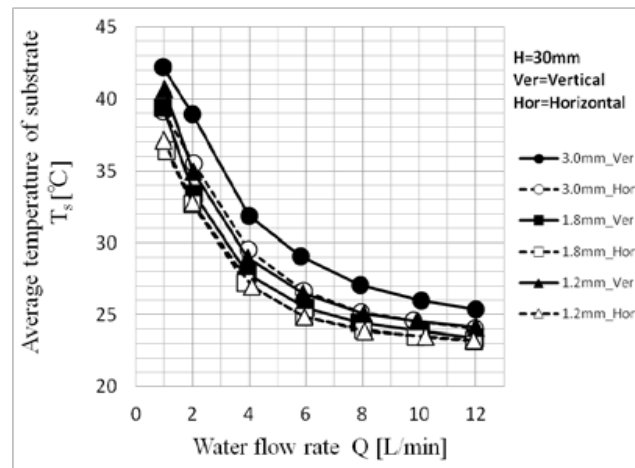
Figure 10: Relationship between cooling water flow rate and average substrate temperature (H=30mm).

b) *Relationship between Reynolds number of cooling water flow and heat transfer coefficient*

Figures 11 and 12 show the relationship between the Reynolds number of the cooling water flow and the average heat transfer coefficient when the channel height H is 20 mm and 30 mm, respectively. In both figures, the heat transfer coefficient increases as the Re number increases. Also, the larger the value of D, the larger the rate of increase.

Comparing Fig. 11 and Fig. 12, it can be seen that when the aspect ratio $D/H = 0.06$, the heat transfer coefficients in the vertical and horizontal placements have the same value over almost all Re number regions. At other aspect ratios, the heat transfer coefficient becomes larger in almost all cases when it is placed horizontally.
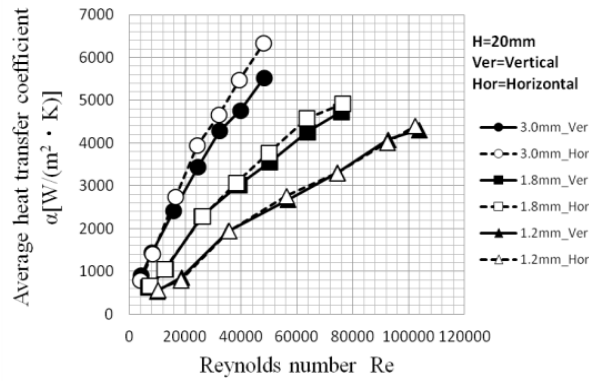
Figure 11: Relationship between *Re* number of flow and average heat transfer coefficient (*H*=20mm)
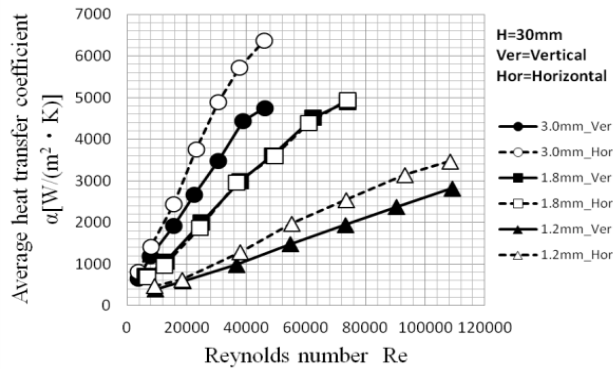
Figure 12: Relationship between *Re* number of flow and average heat transfer coefficient (*H*=30mm)

c) *Influence of natural convection effect*

Figure 13 shows the relationship between the water flow rate and the *Gr* number when the channel height *H* = 30 mm. In the case of the channel width *D* = 1.2 mm and 1.8 mm, the *Gr* number has a substantially constant value regardless of the flow rate. Further, in this case, the *Gr* number values become equal in the vertical placement and the horizontal placement. Therefore, in

the case of having these values of *D*, it is inferred that the influence of natural convection is strongly limited by the influence of strong viscosity. When *D* is larger than 1.8 mm, the value of the *Gr* number rapidly increases with the decrease of the flow rate, and a difference occurs in the value between the vertical placement and horizontal placement. Also, the same tendency is shown in the case of the flow path height *H* = 20 mm.
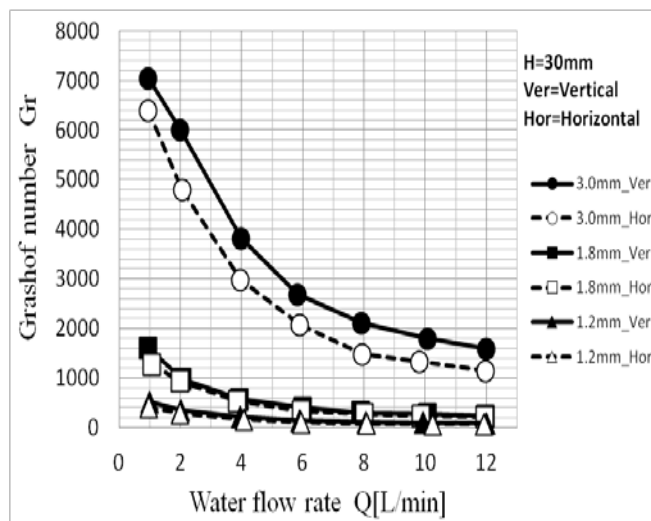
Figure 13: Relationship between cooling water flow rate and *Gr* number.

d) Effects of channel width on the heat transfer coefficient

Figure 14 shows the relationship between the *D* value and the average heat transfer coefficient when cooling water with a constant flow rate is supplied at each channel width when *H* = 30 mm. From the figure, it can be seen that the heat transfer coefficient takes a maximum value at *D* = 2.4 mm in the case of a vertically placed flow. It is also noteworthy that at this *D* value, the value of the heat transfer coefficient is greater at all flow rates than at the horizontally placed flow case.

The peculiar behavior of the heat transfer coefficient observed in the vertical placement is considered to occur in the region where forced convection and natural convection coexist. Therefore, to formulate the heat transfer coefficient in this flow region, it is necessary to obtain a function type including both the Reynolds number and the Grashof number.

It has been found that this heat transfer phenomenon can be approximated relatively well by the following equation in the range of 1.8 mm ≤ *D* ≤ 3.6 mm (see Appendix).

$$\overline{\alpha} = C_1 \cdot C_2 /(Re^{0.5} \cdot Gr^{0.08}) \tag{7}$$

Here, *C1* is a constant determined by the flow rate *Q*, and *C2* is a constant determined by the flow path width *D*, and is expressed by the following equations, respectively.

$$C_1 = 0.2Q - 0.3 \quad [\times 10^6 \ W/(m^2 K)] \tag{8}$$

$$C_2 = 0.479D^3 - 3.898D^2 + 10.14D - 7.402 \tag{9}$$

In the above equations, the unit of *Q* is (L/min), and the unit of *D* is (mm). Also, *C2* is a dimensionless number. The comparison between the values calculated by Eq. (7) and the measured values are shown in Fig.15.
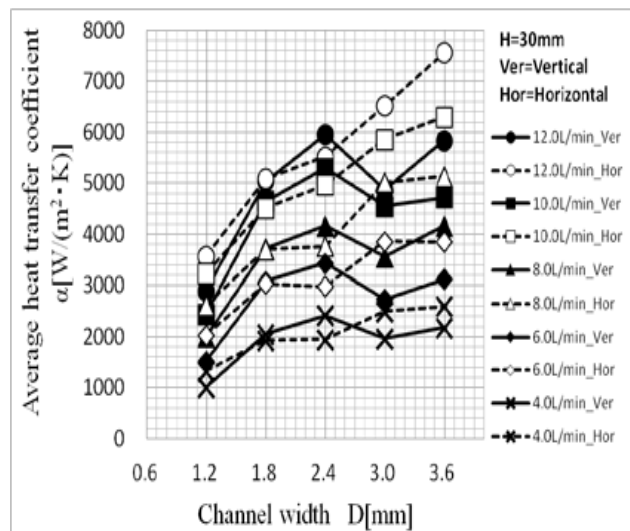
Figure 14: Relationship between channel width and average heat transfer coefficient
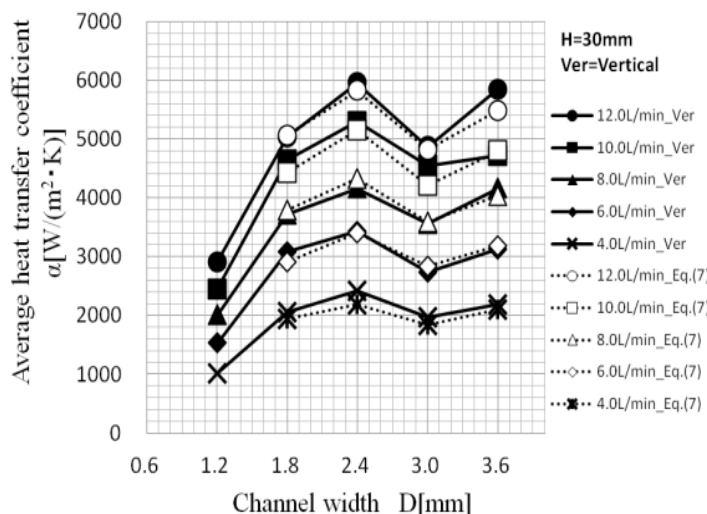
Figure 15: Functional approximation of heat transfer coefficient by Eq. (7) and comparison with the measured values

It is predicted that this unique heat transfer phenomenon is strongly influenced by both Re number and Gr number. And it is thought that the synergistic effect of forced convection and natural convection appears most effectively in the vicinity of the channel width of 2.4 mm.

In the future, it is desired to clarify the detailed physical mechanism of the heat transfer phenomenon of channel flow approximated by Eq.(7).

As an effective utilization of high heat transfer phenomenon due to mixed convection whose existence has been confirmed in this research, it is expected to be applied to the development of high-performance cooling devices with excellent cooling capacity per volume. This is because in the design of a cooling device composed of a plurality of cooling fins, the optimum design of fin thickness and fin gap width is the most important index governing performance. By determining the optimum fin gap width, the optimum relationship between fin thickness and total heat transfer area can be identified.

IV. Conclusions

In this study, the heat transfer phenomenon in the channel flow was examined in detail by changing the channel width and the channel height by experiment. We also examined the difference between vertical and horizontal placement. The following shows the conclusions obtained in this study.

1. When the aspect ratio of the flow path is $D / H = 0.06$, the heat transfer coefficients in the case of vertical installation and horizontal installation has equal values in a wide Re number range.
2. When the channel width is $D = 1.8$ mm or less, the Gr number is a small value of an almost constant value independent of the flow rate regardless of vertical and horizontal placement. In this case, it is considered that the effect of the viscous force is very large, and the effect of the natural convection is suppressed to a small value.
3. When a fixed flow rate of cooling water is supplied in a vertical installation, the heat transfer coefficient tends to take maximum value when $D = 2.4$ mm. The vicinity of this flow passage width is considered to be a region where the synergetic effect of forced convection and natural convection appears most effectively, and the phenomenon can be well approximated as a heat transfer coefficient function, including both Re number and Gr number.

Appendix

About the method for finding the approximation function

The heat transfer characteristics on a flat plate are generally expressed by the following equations when the change of the Prandtl number of the cooling fluid due to temperature is small. That is, forced convection heat transfer is expressed by the Eq. (A1), and natural convection heat transfer is expressed by the Eq. (A2) (Chapman, 1987).

$$Nu = k_1 Re^m \quad (k_1, m : constant) \quad \text{(A1)}$$

$$Nu = k_2 Gr^n \quad (k_2, n : constant) \quad \text{(A2)}$$

The formulation of the phenomena that natural convection heat transfer and forced convection heat transfer are thought to coexist is assumed as the following equation.

$$Nu = k_3 Re^s Gr^t \quad (k_3, s, t : constant) \quad \text{(A3)}$$

Accordingly, the average heat transfer coefficient α is expressed by the following equation.

$$\overline{\alpha} = C Re^x Gr^y \quad (C, x, y : constant) \quad \text{(A4)}$$

Next, the coefficients C, x, and y in the Eq. (A4) are determined to perform curve fitting with a minimum error as compared with the measured value of the average heat transfer coefficient.

As the first step, at each flow rate Q, when the value of α in equation (A4) matches the measured value in the range of 1.8 mm $\leq D \leq$ 3.6 mm, the values of x and y were determined to satisfy the condition that the value of C is constant without depending on the value of D. As a result, it was found that when the values of x and y are represented by Eq. (A5) at all flow rates, the value of C corresponding to each D value takes a minimum error. The results are shown in Table A1.

$$(x, y) = (-0.5, -0.08) \quad \text{(A5)}$$

Table A1: Value of C at each flow rate [(x,y) = (-0.5, -0.08)]

	D [mm]	1.8	2.4	3.0	3.6	Average
	4.0	0.524	0.599	0.466	0.493	0.521
	6.0	0.942	0.987	0.751	0.837	0.879
Q [L/min]	8.0	1.261	1.354	1.120	1.269	1.251
C [×10⁶ W/(m²K)]	10.0	1.765	1.894	1.594	1.583	1.709
	12.0	2.066	2.328	1.841	2.119	2.089

In the data of Table A1, when the relationship between the average value of C and the flow rate Q is graphed, it becomes as shown in Fig. A1, and it can be understood that C can be approximated by a linear function of Q. That is,

$$C \approx f(Q) = 0.2Q - 0.3 \quad [\times 10^6 \text{ W/(m}^2\text{K)}] \quad (A6)$$

Next, we compare the measured average heat transfer coefficient and the average heat transfer coefficient calculated from the Eq. (A4) using the values of x, y, and C defined by the Eq. (A5) and Eq. (A6). The results are shown in Fig. A2.
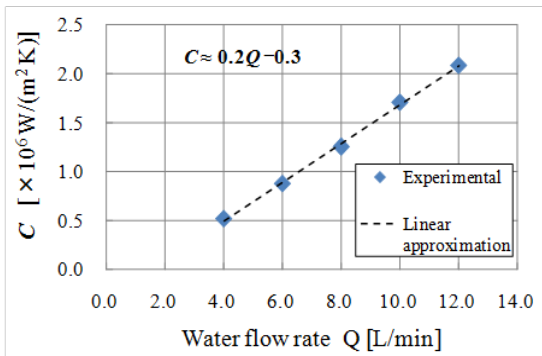
Figure A1: Relationship between the water flow rate Q and the average value of C
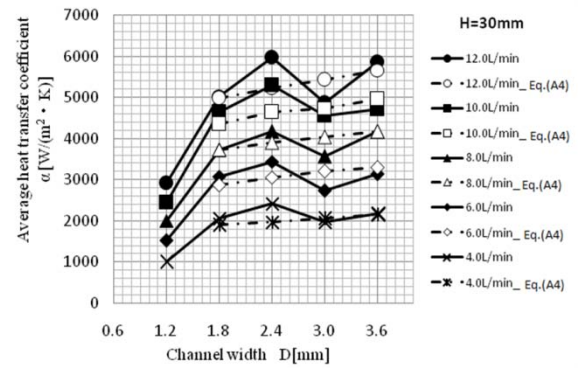
Figure A2: Comparison of the values calculated by the Eq. (A4) with the measured values

From the figure, it can be seen that the result calculated using the value of C determined by the Eq. (A6) shows a set of average values of heat transfer coefficients in the range of 1.8 mm $\leq$ D $\leq$ 3.6 mm.

Therefore, C should be considered as a coefficient determined by the two factors of the flow rate Q and the flow path width D in order to make the approximation of the heat transfer coefficient more accurate. That is,

$$C = C_1 \cdot C_2 = f(Q) \cdot g(D) \quad (A7)$$

However, it is

$$C_1 = f(Q) = 0.2Q - 0.3 [\times 10^6 \text{ W/(m}^2\text{K)}] \quad (A8)$$

Here, the values of $C_2 = C / C_1 = C / f(Q)$ are as shown in the following Table A2.

Table A2: Value of C_2 at each channel width D.

	D [mm]	1.8	2.4	3.0	3.6
	4.0	1.048	1.199	0.931	0.987
	6.0	1.046	1.096	0.835	0.930
Q [L/min]	8.0 ($C_2 = C/C_1$)	0.970	1.041	0.862	0.976
	10.0	1.038	1.114	0.937	0.931
	12.0	0.984	1.109	0.877	1.009
Average		1.017	1.112	0.888	0.967
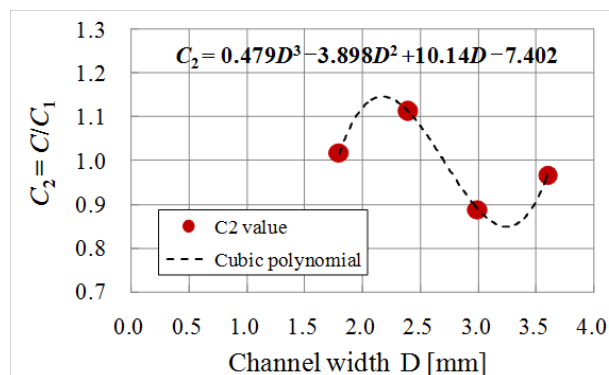
Figure A3: Relationship between the mean value of C2 and channel width D

Figure A3 plots the relationship between the mean value of $C2$ and D, and approximates it with a third-order polynomial. From this, the approximate expression of $C2$ is expressed as the following equation.

$$C_2 = g(D) = 0.479D^3 - 3.898D^2 + 10.14D - 7.402 \tag{A9}$$

From the above, $C1$ and $C2$ can be expressed by the Eq. (8) and Eq. (9) respectively, and an approximate expression of the average heat transfer coefficient in the flow path width range 1.8mm $\leq$ D $\leq$ 3.6mm can be expressed by the Eq. (7).

References Références Referencias

1. Ashraf, A., Mohammed, S. N., Thoufeeq, A., Bibin, S. and Arun, S., Experimental Analysis of Performance Characteristics of Mini Channel Heat Exchangers, International Journal of Research in Mechanical Engineering, Vol. 4, Issue 3, (2016), pp. 39–43.
2. Chapman, A. J., Fundamentals of heat transfer (1987), pp. 311–379, Macmillan.
3. Daugherty, R. L., Franzini. J. B. and Finnemore, E. J., Fluid Mechanics with Engineering Applications, eighth edition (1985), p. 420, Mc Graw-Hill.
4. Forrest, E. C., Hu, L. W., Buongiorno, J. and McKrell, T. J., Convective Heat Transfer in a High Aspect Ratio Mini-Channel Heated on One Side, Journal of Heat Transfer, SAND2014-18834J, pp. 1–57.
5. Kawamura, H., Abe, H. and Shingai, K., DNS of turbulence and heat transport in a echannel flow with different Reynolds and Prandtl numbers and boundary conditions, Proceedings of the 3rd Int. Symp. on Turbulence, Heat and Mass Transfer, (2000), pp. 1–18.
6. Mehta, B. and Khandekar, S., Local experimental heat transfer of single-phase pulsating flow in a square mini-channel, Proceedings of the ASME 2013 4th Micro/Nanoscale Heat & Mass Transfer International Conference, pp. 1–7.
7. Mollik, T., Roy, B. and Saha, S., Turbulence modeling of channel flow and heat transfer: A comparison with DNS data, 10th International Conference on Marine Technology, ELSEVIER Procedia Engineering 194 (2017), PP. 450–456.
8. Nakayama, Y., Dynamics of fluid (revised edition) (1998), p. 107, Youkendou (in Japanese).
9. Taguchi, T. and Sakuragi, S., Experimental study on high efficiency cooling mechanism of power electronic devices, Proceedings of the 1st IPEJ Chubu District Conference on Research achievements, (2014), pp. 17 20 (in Japanese).
10. Tanaka, Y., Yamaji, K. and Sakuragi, S., Optimization study of cooling substrate fin structure, Proceedings of the 2nd IPEJ Chubu District Conference on Research achievements, (2015), pp. 5–8 (in Japanese).
11. Uchino, K., Mamori, H. and Fukagata, K., Heat transfer in fully developed turbulent channel flow with streamwise traveling wave-like wall deformation, Journal of Thermal Science and Technology, Vol.12, No.1 (2017), pp.1–11.

Effects of Ageing on Mechanical Behaviour of Homogenized Twin Rolled 8011 Type Al-Fe-Si Alloy

By A. O. Ogunsanya, P. S. Olayiwola & D. O. Daramola

Bells University of Technology

Abstract- The use of aluminium-iron alloy sheet is of great importance depending on service requirements for specific application as these materials provide a light weight alternative to steel sheet grades but have limitations in the area of mechanical strength. Exploring ways of improving its mechanical properties particularly its strength has led to development of strength-induce forming processes. In this paper, the effect of ageing on the mechanical properties and morphological structure of homogenized twin rolled 0.85% Fe Al alloy 8011 for potential use in orthopaedic devices was investigated. Mechanical properties of homogenized, cold rolled, hot rolled prior to ageing at 175 0C of twin rolled Al-Fe- Si alloy was characterized.

Keywords: aluminum alloy, cold rolling, orthopaedic, homogenization, characterization.

GJRE-A Classification: FOR Code: 090399

EFFECTSOFAGEINGONMECHANICALBEHAVIOUROFHOMOGENIZEDTWINROLLED8011TYPEALFESIALLOY

Strictly as per the compliance and regulations of:

Effects of Ageing on Mechanical Behaviour of Homogenized Twin Rolled 8011 Type Al-Fe-Si Alloy

A. O. Ogunsanya [α], P. S. Olayiwola [σ] & D. O. Daramola [ρ]

Abstract- The use of aluminium-iron alloy sheet is of great importance depending on service requirements for specific application as these materials provide a light weight alternative to steel sheet grades but have limitations in the area of mechanical strength. Exploring ways of improving its mechanical properties particularly its strength has led to development of strength-induce forming processes. In this paper, the effect of ageing on the mechanical properties and morphological structure of homogenized twin rolled 0.85% Fe Al alloy 8011 for potential use in orthopaedic devices was investigated. Mechanical properties of homogenized, cold rolled, hot rolled prior to ageing at 175 $^{\circ}$C of twin rolled Al-Fe-Si alloy was characterized. The result shows that cold rolled sample has better ultimate strength (160MPa) and hardness (60.31HBN) with decrease in impact energy of 3.383joules has compared to as-homogenized and hot rolled samples. Ageing decreases slightly the ultimate strength and hardness with increase in impact energy during 2 - 6 hrs of cold worked samples but it was observed that after 8 hrs, there was increase in ultimate strength and hardness of 166MPa and 54.72HBN respectively with slight decrease in impact energy. Internal residual stresses resulting from working processes are prevented by employing ageing (low temperature annealing) thereby preventing stress corrosion cracking.

Keywords: aluminum alloy, cold rolling, orthopaedic, homogenization, characterization.

I. Introduction

Selections of metallic material for particular applications are governed by the working conditions to which it is subjected, ease of manufacturing and cost. Pure metals are not usually regarded as engineering materials because they are difficult to produce in pure conditions resulting to failure in service. Failure of engineering materials are undesirable for reasons of safety, economy and reliability which may occur due to improper materials selection, casting discontinuities, improper manufacturing process Manufacturing process employed determine the material structure and as a result determine its properties, performance and application in service. Furthermore, changes in one are inseparably related to change in the others [1, 2].

The use of metallic materials has grown drastically in orthopedic devices intended for orthopedic surgery, including permanent implants (total joint replacement, hip prosthesis etc.) and temporary implants (pins, bone plates, screws etc.) [3,4]. Orthopedic surgery in recent times depends profoundly on the development of biomaterials used for fixation of fractures and joint replacement. Owing to their mechanical strength, metallic materials have been widely used in orthopedic applications of which commonly used are: stainless steel, cobalt-chromium alloy and titanium alloy etc. Development of metallic biomaterials has gained interest and has contributed significantly to the improvement of the health and well-being of mankind. However, the biggest drawback is the non-degradability of these materials in the body physiological environment leading to the demand of secondary surgical procedure for the removal of implants after the bone heals [4].

Presently, a great amount of research is focused on developing biodegradable, low density and highly bioactive implants without compromising on strength. One such material which meets these requirements is magnesium (Mg) and its alloys [5-8]. Mg and alloys modulus and density is very close to that of the human bones [9]. There use reduce the shielding effect of implants and they are lighter than other medical metal, but they are difficult to process, they corrode rapidly and are less biocompatible [10].

Aluminium and its alloys, are the second most commonly used material after steel, exhibits poor casting and mechanical properties which can be improved by the addition of alloying elements such as Mg, Si, Cu, Zn, Mn, Fe, and other element [11], thermal treatment, working process or combination of both [12]. An analysis of both the scientific and branch literature has shown trends of the development and advancement of products made of aluminum and its alloys for electrical, construction, automotive, food, packaging, heat ex-changer and medical implant applications [13] and are widely used in structures and components where light weight or corrosion resistance is required [14]. A thin aluminum strip can be produced by two different processes: (i) Direct chill casting (ii) Continuous casting/Twin roll casting. An ideal twin rolled casting has

Author α σ ρ: Department of Mechanical & Biomedical Engineering, Bells University of Technology, Ota, Ogun State, Nigeria.
e-mails: olyinkabbey@gmail.com, olayiwola_patrickshola@yahoo.com, dodaramola@bellsuniversity.edu.ng

been reported [15]. In 1950, continuous strip casting for aluminum and its alloys has also been reported [16]. In twin rolled casting process, molten metal was directly converted into thick strip. Annealing and cold rolling operations were performed on this thick strip to get the required size, shape as well as mechanical properties [17, 18]. In Twin roll casting, centre-line segregation of second phase particles was most commonly found for high alloying content materials [19–25].

Aluminium alloy 8xxx series have been found to have broader usage as in medical implant applications because of their good physical and chemical properties such as formability, corrosion, light weight as well as the possibility of controlling micro structural composition of the alloy by means of specific thermal and mechanical treatments [26]. The iron composition of AA 8011 ranges from 0.6 – 1% has greatly influenced the mechanical properties of the alloy [27]. Large numbers of iron containing intermetallic phases have been identified in the microstructures depending on solidification conditions and alloy composition and so it tends to combine with other elements to form intermetallic phase particles of various types. In the absence of silicon, the dominant phases that is formed are Al_3Fe and Al_6Fe, but when Si is present, the dominant phases are Al_8Fe_2Si (α-phase) and Al_5FeSi (β-phase). If Mg and Mn are present respectively with Si alternative phase calledπ -phase, $Al_8FeMg_3Si_6$ and Al_{15} $(Fe,Mn)_3Si_2$ are confusingly known as α-phase. There are also other rarer phases which form when other elements are present, example are Ni, Co, Cr, Be. When these low symmetry compounds crystallize, they are prone to grow into long needles/plates that are extremely detrimental to both strength and ductility [28].

During metal working, the optimum level of the iron that will not impact any negative effect on the ductility of the alloy is highly required in order to avoid defects such as cracking due to the low level of material ductility. The processing capabilities and final wrought product strength of the aluminium alloy are greatly affected by the iron level content [29].

Mbuya *et al.* investigated the effect of iron content on the mechanical properties of Al alloys [30]. The result revealed that increased iron content lead decrease in ductility of Al-Si based alloys accompanied by increase in tensile strength. However, the yield stress becomes unaffected by level of iron content, unless the ductility were affected so much that the alloy cannot even reach yield point before brittle fracture occurs. According to Miller *et al.*, deep drawing process (DDP) finds application in numerous fields such as in automobile industries where the trend is towards safety and fuel economy [31]. However, the stability of spread of extensively drawn aluminium alloys is often a major problem.

Investigation on the effect of intensive forced melt convection on mechanical properties of Fe-containing Al-Si based alloys was carried out [32]. Their report revealed that, as the equilibrium solid solubility of iron in the aluminium solid solution (α-Al) decreases, iron exists in aluminium alloys in the form of iron-bearing intermetallic compounds. In commercial Al-Si based cast alloys, these compounds are often of the morphologies either as long needles or large plates, which drastically reduce the ductility of the alloys. Chemically, the detrimental effect of iron in aluminium alloys can be minimized by limiting the maximum content of the iron impurity, or by alloying with other element such as manganese [33]. Alloying with 0.9% Mn will results in apparent fragmentation of the β-Al_5FeSi-needles [34]. The investigation on the effect of iron in Al-Si casting alloys by [35] concluded that, iron level in Al-Si alloys should be kept at the bearable minimum level in order to avoid the detrimental effect on mechanical properties, mostly ductility and fracture toughness.

Investigation on the effect of cold rolling on bending and tensile behavior of 7075 aluminium alloy report showed that after 58% cold rolling, there was rapid increase in yield strength of 119.25% due to high density of dislocations. Furthermore, increase in the tensile strength and hardness value with decrease in percentage elongation of the rolled material was reported [36]. The effect of hot cumulative roll bonding process on the mechanical properties of AA 5058 revealed that the strength of the sheet increased as a result of work hardening which was caused by an increase in dislocation density and sub-grains [37].

With extensive data available on the thermal treatment of AA 8011 with conventional alloying elements, not much has been documented on the ageing characteristics after homogenized, cold and hot rolling of the alloy, particularly with high iron content reinforcement for medical applications. Hence, the need for research on this area is justified. The main aim of the current research is to study the ageing characteristics of Aluminium Alloy 8011 and its potential use for orthopaedic devices. Twin rolled aluminium alloy 8011 were homogenized at 500 ^{0}C, cold rolled at ambient temperature, and hot rolled below and above recrystallization temperature at 200 ^{0}C and 400 ^{0}C respectively prior to ageing at 175^{0}C. Mechanical properties and morphological structure were investigated. The effect of ageing on homogenized, cold and hot roll twin rolled AA 8011 was then characterized.

II. Problem Analysis

Theoretical modelling of the material strength and capability makes use of some parameters' values deductible from the experimental analysis. It is therefore important to present the theoretical analysis as follows.

a) Theoretical Analysis

In two-dimensions, stresses are functions of the independent variables x and y, while the transverse stresses are zero, that is;

$$\sigma_{xx} = \sigma_{xx}(x, y)$$

$$\sigma_{yy} = \sigma_{yy}(x, y)$$

$$\sigma_{xy} = \sigma_{xy}(x, y)$$

$$\sigma_{zz} = \sigma_{xz} = \sigma_{yz} = 0$$

The stress-strain relations from Hooke's law now reduce to;

$$\epsilon_{xx} = \frac{1}{E}\left(\sigma_{xx} - v\sigma_{yy}\right) + \alpha(T - T_o)$$

$$\epsilon_{yy} = \frac{1}{E}\left(\sigma_{yy} - v\sigma_{xx}\right) + \alpha(T - T_o) \qquad (2)$$

$$\epsilon_{xy} = \frac{1}{2G}\sigma_{xy}$$

On solving for the stresses, we deduce that;

$$\sigma_{xx} = \frac{E}{1 - v^2}\left[\left(\epsilon_{xx} - \vartheta\epsilon_{yy}\right) - \alpha(1 + v)(T - T_o)\right]$$

$$\sigma_{yy} = \frac{E}{1 - v^2}\left[\left(\epsilon_{yy} - \vartheta\epsilon_{xx}\right) - \alpha(1 + v)(T - T_o)\right]$$

$$\sigma_{xy} = \frac{E}{1 + v}\epsilon_{xy} \qquad (3)$$

On introducing Airy stress function, ϕ, and ignoring the body force and inertia terms since the process is stationary, we define as follows;

$$\sigma_{xx} = \frac{\partial^2\phi}{\partial y^2}$$

$$\sigma_{yy} = \frac{\partial^2\phi}{\partial x^2}$$

$$\sigma_{xy} = -\frac{\partial^2\phi}{\partial_x\partial_y} \qquad (4)$$

Substituting equation (4) into equation (3)

$$\left(\frac{\partial^2}{\partial x^2} + \frac{\partial^2}{\partial y^2}\right)(\sigma_{xx} + \sigma_{yy}) + E\alpha\nabla^2 T = 0 \qquad (5)$$

So that, the governing equation in terms of Airy stress function for the plane stress is;

$$\nabla^2\nabla^2\Phi + E\alpha\nabla^2 T = 0 \qquad (6)$$

Also for the plane strain, it is given by;

$$\nabla^2\nabla^2\Phi + \frac{E\alpha}{1 - v}\nabla^2 T = 0 \qquad (7)$$

The stress function, ϕ, is obtained by integrating the equation (7) knowing the distribution of the temperature. The constants of integration in the expression for the stress function are obtained by application of known physical traction on kinematics boundary conditions of the problem.

b) Experimental Analysis

i. Materials

The material used for the study was two (2) coil slabs of twin rolled AA 8011 with dimensions 1200mm × 140mm × 6.80mm, weighing 2kg obtained from Aluminium Rolling Mills (ARM) Ota, Ogun State, Nigeria. Table 1 show the percent composition with 0.85% Fe present.

Table 1: Chemical Composition of AA 8011

Element	Fe	Si	Mn	Cu	Zn	Ti	Mg	Pb	Sn	Al
% composition	0.85	0.50	0.08	0.07	0.07	0.02	0.02	0.01	0.01	98.37

ii. Methods

The two (2) slabs of AA 8011 were sectioned into 8 samples of dimension 300mm × 140mm × 6.80mm using cutting machine. Samples were homogenize at 500 °C for 1 hr, soaked for 2 hrs followed by cold water quenching to obtain a uniform distribution and homogenous composition throughout the alloy and also to improve workability. Samples were further prepared for various characterizations. Two samples were cold rolled in five passes to 50% reduction in thickness (3.4mm thickness) using Two-High Mill. Two samples each were hot rolled below and above recrystallation temperature of the alloy at 200°C and 400°C in four and three passes respectively to 50%

reductions in thickness. The remaining samples were kept as as-homogenized samples. Cold rolling was carried out on the samples to 50% cumulative thickness reduction at ambient temperature (32°C). Samples were prepared in accordance to ASTM standard dimensions for non-proportional rectangular test pieces, for the subsequent mechanical test and morphological analysis.

A ductile non-ferrous metal such as aluminium has great tendency to deform plastically to a very large extent during machining operation.

Center lathe machine was used to obtain the samples for tensile test, hardness test, impact test, and

morphological analysis (see Figure 1). Four prepared samples each from as-homogenized, cold rolled, thermal treated at 200°C and 400°C were aged at low annealing temperature of 175°C called strain-ageing for 2, 4, 6 & 8 hrs respectively before been normalized in air.

Figure 1: Prepared Sample in ASTM standard dimension

Tensile test samples were shaped in such a way that fracture occurs within the gauge length tested on table top Instron Universal Tensile Testing Machine of Engineering Development Management Institute (EDMI), Akure at strain rate of 10 mm/min. The tensile test samples with gauge dimension 100mm x 40mm x 8mm from as-homogenized, cold rolled, and hot rolled were obtained prior to ageing.

Impact test samples were shaped creating V-notched of 2mm depth at angle 45o tested on Avery Impact Testing Machine of capacity 25J. The test samples were machined into 8mm wide and 100mm long respectively.

WP 300 Gunt Brinell Hardness Tester with 1⁄16 inch diameter (1.588 mm) steel sphere and 100kg load of Federal Institute of Industrial Research Oshodi (FIRO, Lagos) was used to obtain the hardness value of all samples.

The morphological state of the experiment was investigated using standard metallographic procedures. Each sample were ground and polished before being etched in 2g of Sodium Hydroxide (NaOH) (Pellets) in 100 ml of water (H2O) with 15 secs of etching time. Etched samples were washed under running tap of water to remove excessive etchant from the surface before drying in air. Photographic image of the structures were obtained using the digital metallurgical microscope of magnification of X100 with α-aluminum phase as white colour, Mg2Si crystal as dark colour and the Al-Fe-Si crystal as brown colour. crystal as dark colour and the Al-Fe-Si crystal as brown colour.

III. Results and Discussion

a) Aluminium Alloy Sample with Homogenization

The stress-strain curves shown in Figure 2 revealed that the ultimate tensile strength (UTS) of the as-homogenized sample are in the range of 100MPa - 112Mpa while the aged samples for 2, 4, 6 & 8 h have the values of 108MPa, 114MPs, 110MPa and 112MPa respectively. The variation of ductility with percentage elongation (Figure 3) showed that ductility increased as compared to investigation by [38] but slightly decreased during ageing for 2 h, increases for the next 6 h and started to decrease with 8 h of ageing time. The graph showed an increase in hardness values with increase ageing time (Figure 4). Table 2 showed the hardness values obtained for as-homogenized, cold rolled, hot rolled below and above recrystallization temperature before and after ageing.

The impact strength showed better result but decreases progressively with increased ageing time (Figure 5). Table 3 showed the impact strength values obtained for as-homogenized, cold rolled, hot rolled below and above recrystallization temperature before and after ageing.
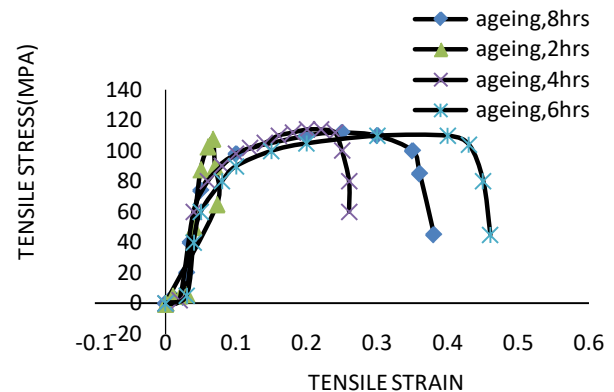
Figure 2: Stress-Strain Curve of As-homogenized Samples with 2 - 8 hrs of Ageing Time
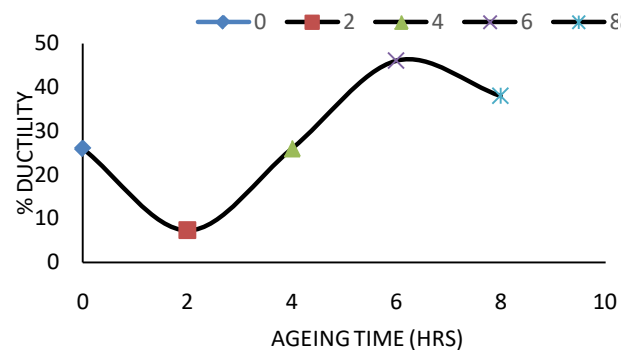
Figure 3: Variation of % Ductility with Ageing Time for As-homogenized Samples
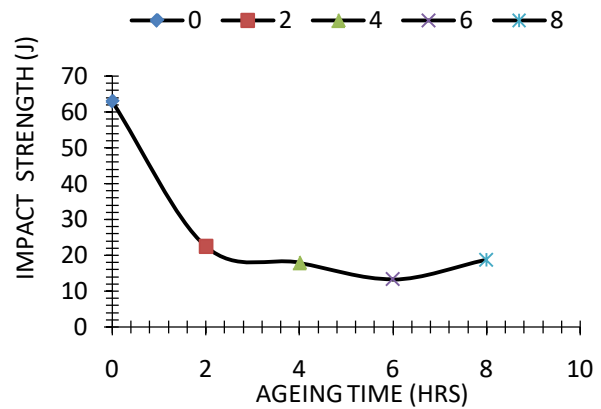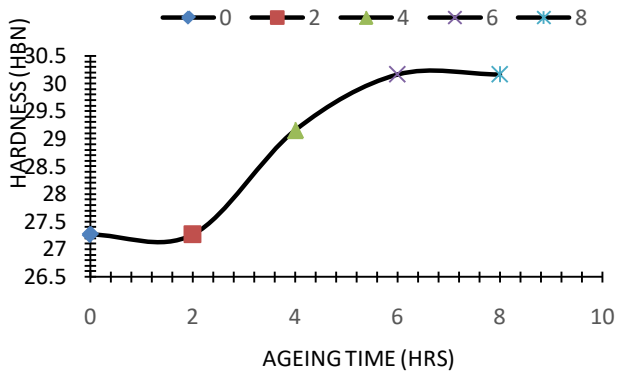
Figure 4: Variation of Hardness with Ageing Time for As-homogenized Samples.

Figure 5: Variation of Impact Energy (J) with Ageing Time for As-homogenized

Table 2: Hardness values of as-homogenized sample, cold rolled sample, hot rolled at 200°C and at 400°C samples before and after ageing

Samples	No-ageing	2hrs	4hrs	6hrs	8hrs
As-homogenized (HBN)	27.27	27.27	29.16	30.16	30.16
Cold Rolled (HBN)	60.31	54.61	54.61	53.59	54.72
Thermal treated at 200°C (HBN)	59.12	57.93	53.59	49.58	43.685
Thermal treated at 400°C (HBN)	54.70	49.25	48.07	48.02	46.525

Table 3: Impact Strength of as-homogenized sample, cold rolled sample, hot rolled at 200°C and at 400°C sample before and after ageing

Samples	No-ageing	2hrs	4hrs	6hrs	8hrs
As-homogenized	62.92 J	22.46 J	17.95 J	13.26 J	18.67 J
Cold Rolled	3.38 J	6.76 J	7.60 J	8.25 J	8.17 J
Thermal treated at 200°C	3.85 J	5.14 J	8.12 J	8.71 J	9.85 J
Thermal treated at 400°C	3.65 J	5.01 J	5.44 J	5.92 J	6.14 J

b)   *Aluminium Alloy Sample with Cold Rolled*

Figure 6 showed that the samples deformed at 50% revealed the UTS of 160MPa while UTS displayed decreased for 2 - 6 h of ageing but there was shape increase in UTS to 166MPa after 8 h ageing samples. The graph displayed increase in ductility with 2 h ageing and further decrease with increase in ageing time (Figure 7). The hardness values of the samples deformed at 50% increased then decreased with increased ageing time (Figure 8). Figure 9 revealed increased impact energy with increased ageing time.
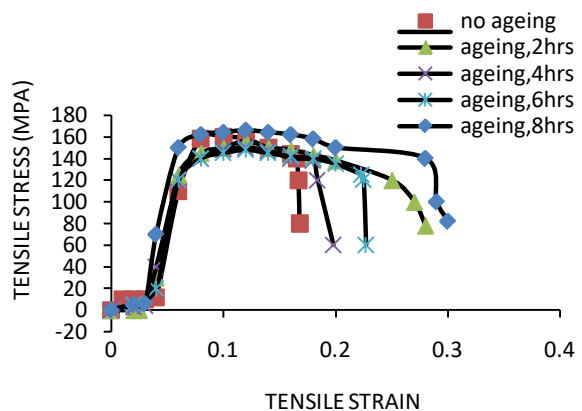
Figure 6: Stress-Strain Curve of Cold Rolled Samples with 2 - 8 hrs of Ageing.

18
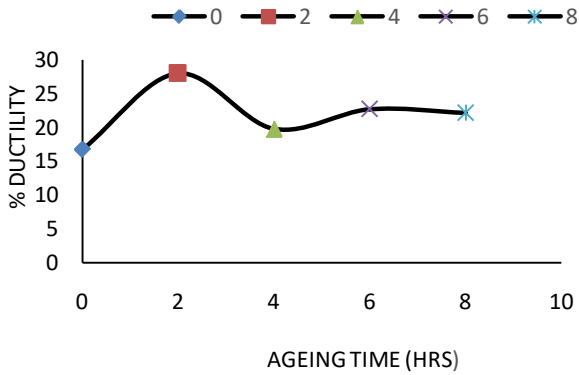
Figure 7: Variation of % Ductility with Ageing Time of Cold Rolled Samples.

Figure 8: Variation of Hardness with Ageing Time of Cold Rolled Samples.

Figure 9: Variation of Impact Energy with Ageing Time of Cold Rolled Samples.

c) *Aluminium Alloy Sample with Hot Rolled below Recrystallation*

The samples deformed at 50% revealed values of UTS of 143MPa (Figure 10) and decrease in strength with increased ageing time. The graph displayed decreased in ductility at 50% deformation and then showed increase in ductility with increased ageing time (Figure 11). Both hardness and impact strength decreased with increased ageing time (Figure 12 & Figure 13) but show a better result as compared to cold rolled samples in term of impact strength.

Figure 10: Stress-Strain Curves for Thermal Treatment at 200 °C with Ageing Time.

Figure 11: Variation of % Ductility with Aging Time for Thermal Treatment at 200 °C.

Figure 12: Variation of Hardness Values with Ageing Time for Thermal Treatment at 200 °C.
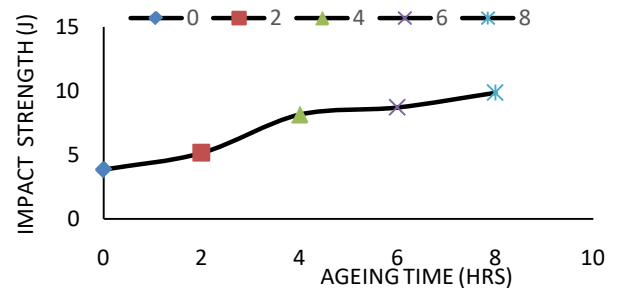
Figure 13: Variation of Impact Strength with Ageing Time for Thermal Treatment at 200 °C.

d) Aluminium Alloy Sample with Hot Rolled above Recrystallation

The value of 120MPa was displayed by sample deformed at 50% while the other samples for ageing are in a range of 116MPa - 125MPa respectively (Figure 14). The ductility increased with increased ageing time (Figure 15). Hardness values decreased with increased ageing time (Figure 16) while Figure 17 revealed that the impact strength increases with increased ageing time.
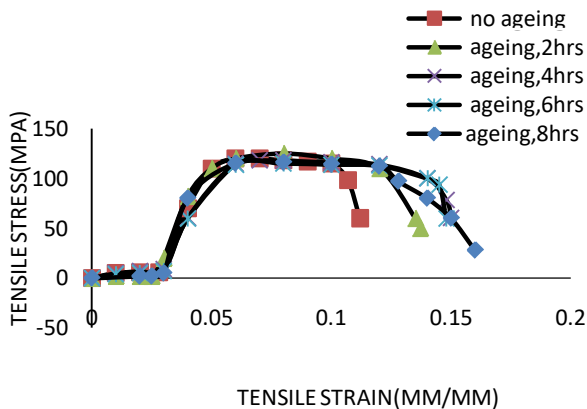
Figure 14: Stress-Strain Curves of Thermal Treatment Samples at 400 ^{0}C with Ageing Time
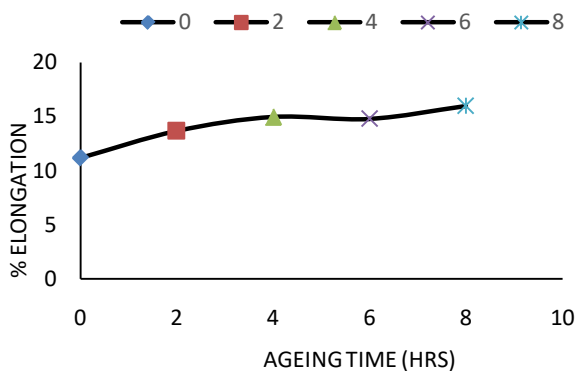
Figure 15: Variation of % Ductility with Ageing Time for Thermal Treatment at 400 ^{0}C
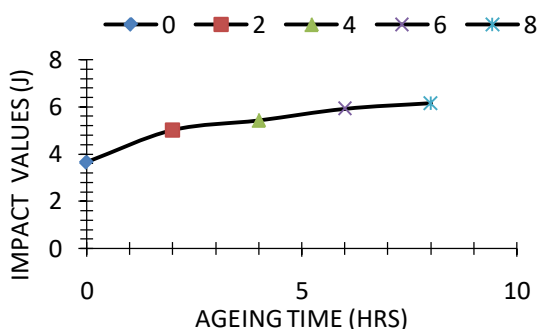
Figure 16: Variation of Hardness with Ageing Time for Thermal Treatment at 400°C.
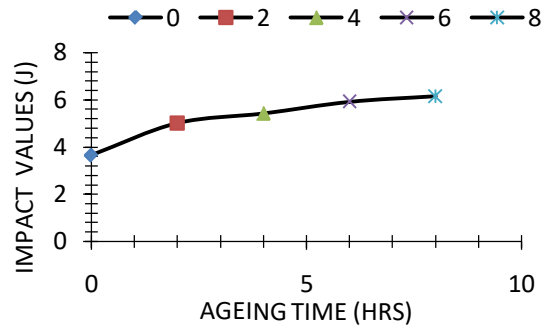
Figure 17: Variation of Impact Energy (J) against Ageing Time for Thermal Treatment at 400°C.

e) Effect of Plastic Deformation and Ageing on Ultimate Tensile Strength of Homogenized AA 8011

Elastic behaviour occurs at a strain of about 2×10^{-3} and maximum tensile strength of 110MPa was achieved for As-homogenized (Figure 2). The effect of ageing improved the Ultimate Tensile Strength to 114MPa. The slight improvement in strength might be due to Guinier-Preston (GP) zones and precipitating second phase particles from solid solution obtained from quenching clustering together resisting the movement of dislocations that generate elastic strain in the surrounding matrix lattice that resisted dislocation slip and thereby increase the strength. Figure 18 shows the heat treatment of the aluminium alloy. The solid solubility limit decreases with decrease in temperature that is the phase diagram show solvus forming supersaturated solid solution and then, reject finely dispersed precipitates at the heat treatment temperature of 500 ^{0}C. The aluminium-iron system rich in α-Aluminium was a typical precipitation-hardening system that exists as a homogeneous α-solid solution at high temperatures but on cooling becomes saturated with respect to the second phase (Al-Fe-Si), forming coarse precipitates and occur at the grain boundaries of α-Aluminium matrix and this might be the reason for any improvement in mechanical properties of AA 8011. Rapid quenching of the alloy suppresses the separation of the second phase and no time available for the diffusion to occur to bring about composition changes. The ageing of the alloy for a sufficient length of time at slightly higher temperature of 175 ^{0}C caused fine precipitation to occur inside the grain. Due to limited diffusion rates at these low temperature, the solute atoms move through only few interatomic distance giving rise to extremely fine precipitation that can occur by nucleation and growth process. The fluctuation in the solute concentration provides smaller clusters of solute atoms in the crystal lattice of the aluminium which act like nuclei foe the precipitation. The growth rate of these nuclei is controlled by the rate of atomic migration, so that precipitation increases with the increasing temperature. However, the size of the precipitates

become finer as the ageing temperature at which precipitation occur is lowered. As the precipitate size increases, loss of coherency at the interface occurs when equilibrium precipitate Al-Fe-Si forms by then over-ageing had already occur.
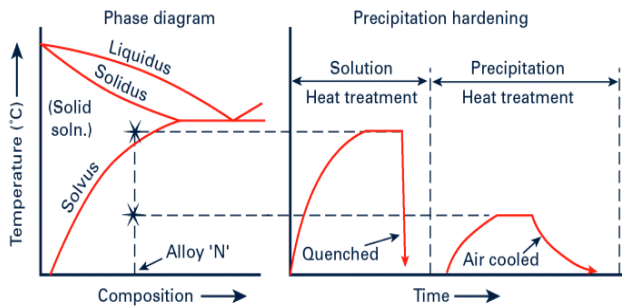
Figure 18: Heat Treatment of Aluminium Alloy.

The effect of plastic deformation at ambient temperature contributes greatly to the mechanical properties of the metal. At 50% percentage deformation, there was progressive increase in UTS from 108MPa to 160MPa and elastic behaviour of 4×10^{-3} respectively (Figure 6). The increase in strength was due to the interaction between the dislocations and precipitate particles, hindering the motions of dislocation there by leading to strength increment. The rapid increased in the value of the UTS of the cold rolled sample up to 50% deformation was attributed to the array of defects such as high density of dislocation produced in the alloy [38]. The very high density of GP zones generates a sufficiently high internal strain to impede dislocation movement. The coherent precipitate (second phase particles) caused further improvement in strength because higher internal strain generated than GP zones. As this particles grow in size, they provide greater resistance to the movement of dislocation slip that cut through and continues to move through the matrix. Deterioration displayed during the 2 - 6 h of ageing might be due to the released of stress carried by coherent precipitate. Cracks that occurs in this particles affect the load bearing capacity of the alloy, thereby limiting its work hardening behavior. Higher level of load transfer to the second phase intermetallic particles lead to flow stress increase in the matrix as previously reported by [39]. Rapid improvement in UTS of 166MPa after 8 h of ageing was attributed to precipitates having large coherency strains or interfacial energies, defect such as the dislocations, sub-grains and grain boundaries acting as the sites for nucleation of the precipitates. Because of the interactions between dislocations and precipitates are on a much finer scale than interactions between dislocations and grain and sub-grain boundaries, the effect of plastic deformation at temperature below (200 ^{0}C) and above (400 ^{0}C) recrystallization has effect on the strength of the alloy

(Figure 10). Hot rolling and deformation prior ageing causes deterioration in strength owing to coarsening in the incoherent particles. The degree of recrystallization normally affects the crystallographic texture, which does affect strength and anisotropy of the properties of the aluminium alloy (Figure 14).

f) Effect of Plastic Deformation and Ageing on the Ductility of Homogenized AA 8011

The variation of ductility with 50% deformation showed increase in ductility (Figure 3). The simultaneous increase in ductility of the alloy which could attributed to the micro structural changes. The fine grains formed during deformation might facilitate an increased in grain boundaries sliding and hence grain rotation which could improve ductility. The increase at 50% deformation therefore should have been linked to grain boundaries sliding as previously reported by [40]. Deformation at ambient temperature displayed decrease in ductility and this might be due to dislocations generation which interacted and impeded each other, hindering their motion thereby decreasing the ductility of the alloy [30]. Decreased in ductility were also seen during ageing (Figure 7). Deformation below and above recrystallization temperature of the alloy showed increased in ductility. Ductility increased as the ageing time increased (Figure 11 and Figure 15).

g) Effect of Plastic Deformation and Ageing on the Hardness of Homogenized AA 8011

The Brinell Hardness values of the investigated AA 8011 samples with As-homogenized, cold rolled to 50 % deformation, hot rolled to 50 % deformation at 200 ^{0}C and 400 ^{0}C revealed that cold sample showed highest hardness value followed by hot rolled at 200 ^{0}C while As-homogenized sample showed the lowest value. But during ageing, as-homogenized samples revealed increased in hardness values but the same cannot be said of cold rolled samples, hot rolled samples at 200 ^{0}C and 400 ^{0}C which showed decreased in hardness values (Figure 4, 8, 12, 16). The increased in the hardness value of cold rolled sample could be attributed to high dislocation density (strain Hardening tendency) there by increasing the stacking faults of the alloy under investigation where as decreased in hardness value after ageing of the alloy was as a result of decrease in dislocation density in the interior sub-grains. The rearrangement of the dislocations was assisted by the thermal activation that is ageing temperature, that causes slip, cross-slip and climbing of dislocation over small distance. This observation is in agreement with the previous report by [41].

h) Effect of Plastic Deformation and Ageing on the Impact Strength of Homogenized AA 8011

The impact strength sample of as-homogenized showed an improved value but decreased in impact

strength were revealed during ageing of the samples (Figure 5). This could be due dislocation generation and interaction. During cold and hot rolling of the alloy, dislocation density increases at 50 % deformation; causing fragmentation of interdenditic particles in the alloy that showed a deficient in the impact strength of the samples. Whereas deformation prior to ageing of the samples revealed increased impact strength. This is attributed to the interaction provided by the precipitates with the dislocation in the alloy.

i) Effect of Plastic Deformation and Ageing on the Microstructure of Homogenized AA 8011

The micro structural analysis reveals homogenous and even distribution of both Al-Fe-Si crystals with more of the crystals and coarse grains structure and the α-Aluminium crystals (see Plate 1a). Homogenization, quenching in water and ageing produce fine and small volume of Al-Fe-Si crystals in α-Aluminium matrix for enhanced strength, hardness and ductility (see Plate 2: a-d).

In the cold rolled sample, the Al-Fe-Si crystals are found at grain boundaries, distorted and in the rolling direction and are finely distribution, which serves as obstacles to the motion of dislocation leading to pile-up of dislocations at the grain boundaries during plastic deformation. The fine and smaller volume fraction of intermetallic phase (Al-Fe-Si phase) precipitated exceeds that of α-Aluminium phase that has some of its crystals diffused into the matrix consequent upon the applied rolled load (Plate 1b). These features promote strength and hardness while sacrificing ductility and toughness. Homogenization, quenched rapidly in water, cold rolled and ageing leads to the annihilation, polygonisation and rearrangement of dislocations of the Al-Fe-Si crystals and α-Aluminium exhibiting decrease in rate of strain-hardening that is strength and hardness decreased but enhanced ductility and impact energy as a result of consequence of dynamic recovery leading reduction in lattice energy occurring without a significant change in the microstructure (see Plate 3: a-d). In the hot rolled below recrystallization temperature sample, distortion of Al-Fe-Si crystals is less pronounced has compared to the cold rolled sample, with a considerable decreased strength and hardness while slight increase in impact energy and ductility (see Plate 1c).

Hot rolled above recrystallization temperature, revealed fine and recrystallized crystals of Al-Fe-Si crystals, α-Aluminium crystals and other intermetallic crystals are seen in Plate 1d.
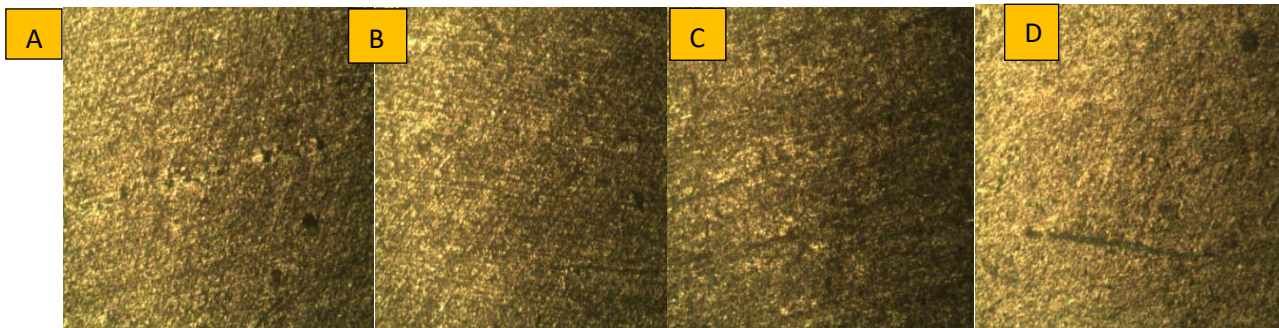
Plate 1: Optical micrographs of (a) as-homogenized (b) cold rolled (c) hot rolled at 200^0C (d) hot rolled at 400^0C; White spots (second phase particles): Al-Fe-Si, yellowish back ground: α-Aluminium, Black spots: Al-Fe. X100
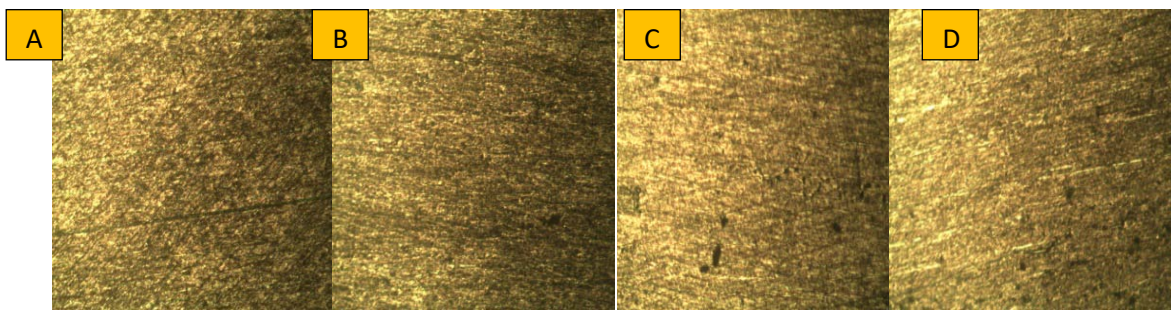
Plate 2: Optical micrographs of As-homogenized Aged at (a) 2hrs (b) 4hrs (c) 6hrs (d) 8hrs; White spots, the interdendritic of intermetallic particles been distributed in α-Aluminium (yellowish back ground), Black spots are Al-Fe. X100
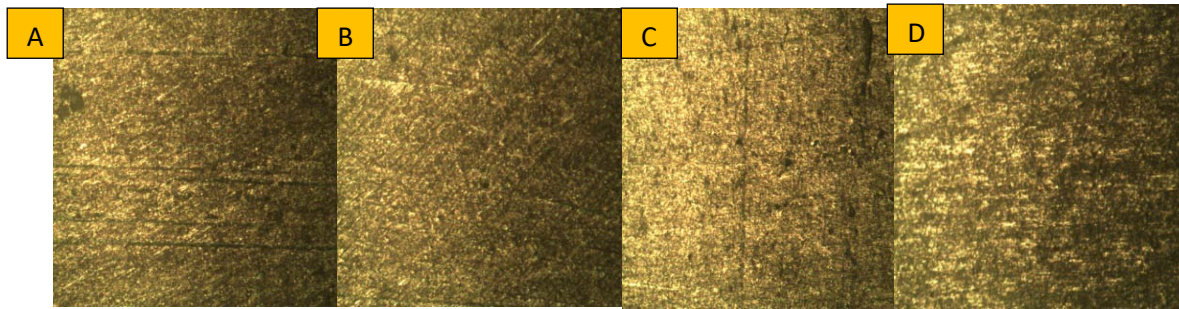
Plate 3: Optical micrographs of cold rolled samples, aged at (a) 2hrs (b) 4hrs (c) 6hrs (d) 8hrs; White spots are interdendritic particles elongated along rolled direction in the Aluminium matrix (yellowish back ground), Black spots are particles of Al-Fe. X100

Homogenization, quenched in water, hot rolled below and above recrystallization temperature prior to ageing rearranged the distorted Al-Fe-Si crystals and α- Aluminium leading to decreased in strength and hardness while promoting or enhancing ductility and impact energy (see Plate 4 &5).
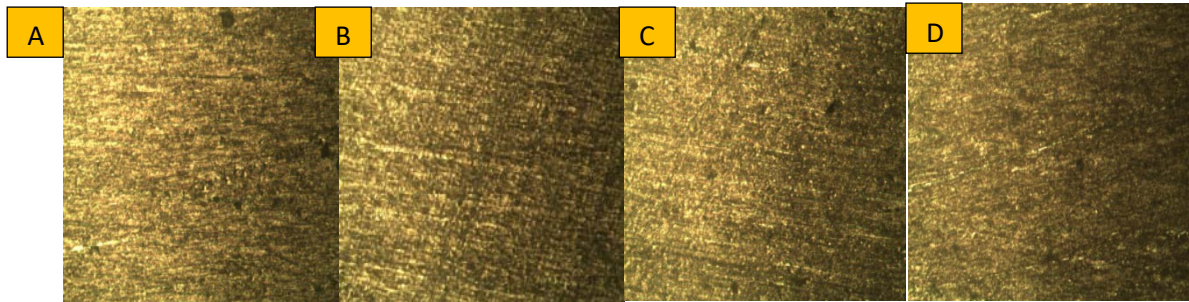
Plate 4: Optical micrographs of hot rolled samples below recrystallization temperature, aged at (a) 2hrs (b) 4hrs (c) 6hrs (d) 8hrs; White (second phase particles): Al-Fe-Si, Brown: α-Aluminium, Black: Iron (Fe). X100
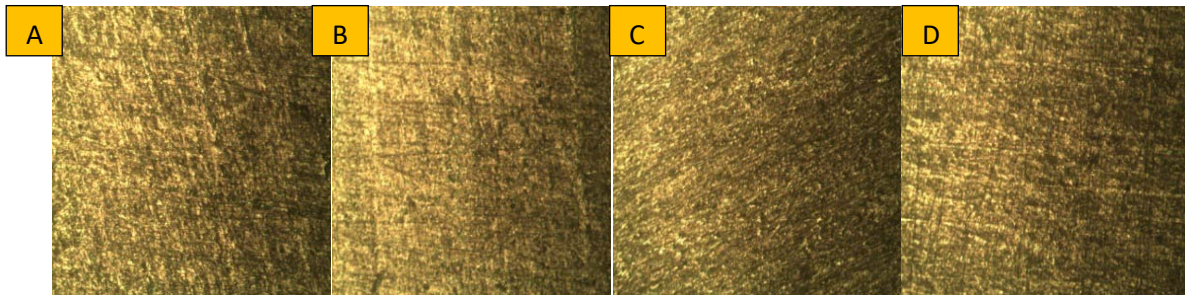
Plate 5: Optical micrographs of hot rolled samples above recrystallization temperature, aged at (a) 2hrs. (b) 4hrs. (c) 6hrs. (d) 8hrs; White (second phase particles): Al-Fe-Si, Brown: α-Aluminium, Black: Iron (Fe). X100

IV. Conclusion

Based on the research finding, the following conclusions were drawn.

i. It can be seen that cold rolling increased; tensile strength, hardness and decreased ductility and toughness.
ii. Hot rolling below and above recrystallization temperature also decreased strength and hardness of the alloy and increased ductility and toughness.
iii. Homogenizing time has more influence on the tensile strength and hardness of the alloy to the other two parameters, viz., aging temperature and aging time.
iv. Homogenizing time (500 ^{0}C), aging temperature (175 ^{0}C), aging time (8 hrs) was found out to achieve the maximum tensile strength of 166 MPa and hardness of 54.72 HBN.
v. Ageing temperature remove internal residual stresses due to the working process that can lead to stress corrosion cracking.

vi. Lattice energy occurring at the recovery stage during ageing lead to slight decreased in tensile strength and hardness while ductility and toughness increased.

vii. The effective utilization of tensile for AA 8011 for achieving the optimal combination of enhanced tensile strength has been attempted.

viii. The alloys also possess excellent ductility as a results of its soften characteristics.

ix. Hot/cold working process helps to improve the mechanical property of Al-Fe-Si alloy and severe plastic deformation techniques will improved the corrosion resistance.

x. The choose of suitable materials and processing techniques by highlighting the recent trends in the emerging area of Al-Fe-Si based materials for orthopedic implants.

References Références Referencias

1. Willian D. Callister Jr. "Fundamentals of materials Science and Engineering (5th ed), 2006.

2. Adeosun S. O.: "Class note MME 506", 2010/2011 Session, Second Semester, Faculty of Engineering, University of Lagos, Akoka, Yaba, Lagos, Nigeria, 2011.

3. J. P. DeAngelis, B.D. Browner, A.E. Caputo, J.W. Mast, M.W. Mendes, B.D. Browner, A. Levine, J. Jupiter, P. Trafton, C. Krettek (Eds.), Skeletal Trauma (4th ed.), W.B. Saunders Company, Philadelpia, 2008.

4. R. Radha, D. Sreekanth. "Insight of magnesium alloys and composites for orthopedic implant applications: a review", *Journal of Magnesium and Alloy,* vol. 5(3), pp. 286-312, 2017.

5. Witte, F., Abeln, I., Switzer, E., Kaese, V., Meyer-Lindenberg, A., Windhagen, H. "Evaluation of the skin sensitizing potential of biodegradable magnesium alloys," *Journal of Biomedical Materials Research - Part A*, vol. 86(4), pp. 1041-1047, 2008.

6. Williams, D."New interests in magnesium", *Medical device technology*, vol. 17(3), pp. 9-10, 2006.

7. Kirkland, N. T., Kolbeinsson, I., Woodfield, T., Dias, G., Staiger, M.P." Processing-property relationships of As-Cast magnesium foams with controllable architecture," *International Journal of Modern Physics B*, vol. 23(6-7), pp. 1002-1008, 2009.

8. Kirkland, N. T., Kolbeinsson, I., Woodfield, T., Dias, G., Staiger, M.P. "Synthesis and properties of topologically ordered porous magnesium," *Materials Science and Engineering B: Solid-State Materials for Advanced Technology*, vol. 176(20), pp. 1666-1672, 2011.

9. Y. Yun, Z. Dong, D. Yang, M.J. Schulz, V.N. Shanov, S. Yarmolenko, Xu, Z., Kumta, P., Sfeir, C., "Biodegradable Mg corrosion and osteoblast cell culture studies," *Mater. Sci. Eng. C*, vol. 29(6), pp. 1814-1821, 2009.

10. López, H. Y., Cortés, D. A., Escobedo, S., Mantovani, D."In vitro bioactivity assessment of metallic magnesium," *Key Engineering Materials*, Volume 309-311 I, pp. 453-456, 2006.

11. Rafiq A. Siddiqui, Hussein A. Abdullah, Khamis R. Al-Belushi. "Inference of aging parameters on the mechanical properties of 6063 aluminum alloy", *Journal of Materials Processing Technology*, vol. 102, pp. 234–240, 2000.

12. Aalco, "Aluminium alloy: Introduction to Aluminium and its alloys", www.aalco.co.uk/datasheets/Aalco-Metal, 2010.

13. Sanders Jr. R. E., Hollinshead P. A., Simielli E. A. "Industrial Development of Non-Heat Treatable Aluminum Alloys". *Materials Forum*, vol. 28, pp. 53-64, 2004.

14. Alumatter Aluminium. "Materials science and Engineering", Alloying and Wrought Aluminium alloys Classification, pp. 2/22, 2010.

15. H. Bessember. "Improvement in the Manufacture of Iron and Steel; US patent: 49053. July 25, 1865.

16. R. Cook, P. G. Growcock, P. M. Thomas, D. V. Edmonds, J.D. Hunt. "Development of Twin Roll Casting Process", *Journal of Materials Processing Technology*, vol.55, pp. 76–84, 1995.

17. Martin Lentz, Galyna Laptyeva, Olaf Engler. "Characterization of second-phase particles in two aluminium foil alloys", *Journal of Alloys and Compounds*, vol. 660, pp. 276–288, 2016.

18. Yücel B. "Response to annealing treatments of twin-roll cast thin Al–Fe–Si strips", *Journal of Alloys and Compounds*, vol. 458, pp. 265–270, 2008.

19. Ghosh. "Segregation in Cast Products; Sadhana", vol. 26, Parts 1 & 2, pp. 5–24, 2001.

20. Ozgul Keles, Murat Dundar. "Aluminum foil: Its typical quality problems and their causes", *Journal of Materials Processing Technology*, vol. 186, pp. 125-137, 2007.

21. Ch. Gras, M. Meredith, J. D. Hunt. "Micro-defects formation during the twin-roll casting of Al–Mg–Mn aluminum alloys", *Journal of Materials Processing Technology*, vol. 167, pp. 62-72, 2005.

22. Ranjeet Kumar, Aman Gupta, Amit Kumar, R.N. Chouhan, Rajesh K. K. "Microstructure and texture development during deformation and recrystallization in strip cast AA8011 aluminum alloy", *Journal of Alloys and Compounds*, vol. 742, pp. 369-382, 2018.

23. H. westengen. "Twin-roll casting of aluminum: The occurrence of structure in homogeneity and defects in as cast strip", *Light Metals, J.P. McGee, Editor*, pp. 972-980, 1984.

24. R. E. Sanders Jr., P. A. Hollinshead, E. A. Simielli. "Industrial Development of Non-Heat Treatable

Aluminum Alloys", *9th International Conference on Aluminium Alloys*, Institute of Materials Engineering Australasia Ltd, pp. 53-64, 2004.

25. Aziz Dursun, Beril Çorlu, Canan İnel, S. Levent Aktuğ, Murat Dündar. "Effect of Homogenization Treatment on Microstructural Evolution of 1050 and 1200 TRC Aluminum Alloys", *Assan Aluminum*, Tuzla, Istanbul, 34940 Turkey.

26. Xing Z. P., Kang S. B. and Kim H. W. "Softening Behavior of 8011 Alloy Produced by Accumulative Roll Bonding Process", *Scripta Material*, vol. 45, pp. 597-604, 2001.

27. O. H. Yakubu, I. Usman, A. Aliyu and O. O. Emmanuel. "Influence of Iron Content & Plastic Deformation on Mech. Prop. of 8011-Type Al-Fe-Si Alloy", *Nigerian Journal of Technology (Nijotech)*, vol. 35 (1), pp. 122-128, 2016.

28. Zhang H. "Effect of Iron on the Microstructure and Mechanical Properties of Al-Si Alloys", *Minerals, Metals and Materials Society*, Shanghai, China, pp. 775-780, 2007.

29. John A. T. "The Effect of Iron in Al-Si Casting Alloy", *Cooperative Research Centre for Cast Metals Manufacturing (CAST)*, the University of Queensland, Brisbane, Australia, pp. 1-10, 2009.

30. Mbuya T. O., Odera B. O. and Nganga S. P. "Influence of Iron on Castability and Properties of Aluminium Silicon Alloys", *International Journal of Cast Metals Research*, vol. 16 (5), pp 45-465, 2003.

31. W. Miller, J. Zhuang, A. Bottema, P. Witterbrood, P. De Smet, A. Haszler and A. Vieregge. "Recent Development in Aluminium Alloys for the Automotive Industry", *Materials Science and Engineering*, vol. 280, (1), 2000, pp. 37-49, 2000.

32. Fang X., Shao G., Liu Y. Q. and Fan Z. "Effects of Intensive Forced Melt Convection on the Mechanical Properties of Fe-containing Al-Si based Alloys" *Brunel Centre for Advanced Solidification Technology (BCAST)*, Brunel University, Uxbridge, Middlesex, UB8 3PH, UK, pp. 1-11, 2011.

33. Lu L. and Dahel A. K. "Iron-rich Intermetallic Phases and their Role in Casting Defect Formation in Hypoeutectic Al-Si Alloys", *Metallurgical and Materials Transactions*, vol. 36A, pp. 819–835, 2005.

34. Shabestari S. G., Mohammed M., Emamy M. and Campbell J. "Effect of Mn and Sr on Intermetallics in Fe-rich Eutectic Al-Si Alloys", *International Journal of Cast Metal Research*, vol. 15(1), pp. 17-24, 2002.

35. John A. T. "The Effect of Iron in Al-Si Casting Alloy", *Cooperative Research Centre for Cast Metals Manufacturing (CAST),* the University of Queensland, Brisbane, Australia, pp. 1-10, 2009.

36. Tajally M., Huda Z. and Masjuki H. H. "Effect of cold rolling on bending and tensile behaviour of 7075 aluminum alloy", *Journal of Applied Sciences*, vol. 9, pp. 3888-3893, 2009.

37. Hassan S. and Ebrahim P. "Effect of hot cumulative roll bonding on the mechanical properties of AA 5058", *Open Journal of Metal*, vol. 1, pp. 12-15, 2011.

38. O. H. Yakubu, I. Usman, A. Aliyu and O. O. Emmanuel. "Influence of Iron Content and Plastic Deformation on the Mechanical Properties of 8011-Type Al-Fe-Si Alloy", *Nigerian Journal of Technology*, vol. 35 (1), pp. 122-128, 2016.

39. Salem S.: "The Influence of Iron on the Microstructure and Mechanical Properties of Cast Al-Si Alloys", Unpublished Ph.D Thesis, Jonkoping University, the School of Engineering Component Technology, Sweden, 2007.

40. Akshap G. P. and Ibrahim M.: "Mechanical Properties of Zn-9%-3%Cu Alloy after Equal Channel Angular Extrusion", *Proceedings of the Xth International Congress and Exposition*, Society for Experimental Mechanics inc. Orlando, Florida USA, pp. 1-7, 2008.

41. Chang, J. Y. and Shan, A.:"Microstructure and Mechanical Properties of AlMgSi Alloys after Equal Channel Angular Pressing at Room Temperature", *Materials Science and Engineering Journal*, A327, pp. 165-170, 2003.

A Critical Appraisal of Conventional Methodology used to Determine Heat Transfer Correlations, and Alternate Methodology

By Eugene F. Adiutori

Abstract- This article describes alternate methodology for determining heat transfer correlations from experimental programs. In conventional methodology, the form of heat transfer correlations is determined before the experiment by deduction, and the experiment is performed in order to quantify constants in the deduced correlation form. In the proposed alternate methodology, the form of heat transfer correlations is determined after the experiment by induction.

Three examples in the text apply the alternate methodology to data in the literature, and compare the resultant correlations to widely accepted correlations based on conventional methodology and the same data. The correlations that result from the alternate methodology agree with the underlying data much more accurately than correlations that result from conventional methodology. The difference in accuracy reflects the fact that deduction is much more difficult than induction, and therefore much more likely to include errors, and less likely to accurately describe the underlying data.

GJRE-A Classification: FOR Code: 290501

CRITICALAPPRAISALOFCONVENTIONALMETHODOLOGYUSEDTODETERMINEHEATTRANSFERCORRELATIONSANDALTERNATEMETHODOLOGY

Strictly as per the compliance and regulations of:

A Critical Appraisal of Conventional Methodology used to Determine Heat Transfer Correlations, and Alternate Methodology

Eugene F. Adiutori

Abstract- This article describes alternate methodology for determining heat transfer correlations from experimental programs. In conventional methodology, the *form* of heat transfer correlations is determined *before* the experiment by *deduction*, and the experiment is performed in order to quantify constants in the deduced correlation form. In the proposed alternate methodology, the *form* of heat transfer correlations is determined *after* the experiment by *induction*.

Three examples in the text apply the alternate methodology to data in the literature, and compare the resultant correlations to widely accepted correlations based on conventional methodology and the *same data*. The correlations that result from the alternate methodology agree with the underlying data much more accurately than correlations that result from conventional methodology. The difference in accuracy reflects the fact that deduction is much more difficult than induction, and therefore much more likely to include errors, and less likely to accurately describe the underlying data.

One of the examples concerns film heating/cooling, a process widely used to deice airplanes in flight, and to cool internal components in gas turbines. The other two examples concern the relationship between heat flux and boundary layer temperature difference in the nucleate boiling region, and in the transition boiling region.

I. Reviews of Film Heating/Cooling Studies

Kays (1966) presents a brief review of film cooling/heating effectiveness studies. Kays states:

. . . there is a considerable body of experimental data, the results of which can be presented in a simple manner. . . . It is found that η is primarily a function of a blowing rate parameter m . . . the width (or height) of the injection slot s, and the distance x. . . Wieghardt (1946) presents the correlation . . .

$$\eta = 21.8(x/ms)$$
$$0.22 < m < 0.74 \quad x/s > 100 \quad (1)$$

Acharya and Kanani (2017) present a comprehensive review of film cooling/heating studies made since 1946. All correlations in the review are based on the group parameter x/ms, including correlations by Bunker (2006) and Colban et al (2011). Most correlations are in the form of Eq. (2). Several are in the form of Eq. (3).

Author: e-mail: efadiutori@aol.com

$$\eta = f\{x/ms\} \quad (2)$$
$$\eta = f\{m, x/ms\} \quad (3)$$

Wieghardt's (1946) pioneering study of film heating, and the conventional methodology that typically underlies the form of film heating/cooling correlations.

In a pioneering study, Wieghardt (1946) determined a correlation for film heating. Data were obtained from a system in which film heating air entered the mainstream from a tangential slot. Data were obtained at m values from 0.22 to 1.90, a slot height of 10 mm, mainstream air velocities of 16 and 32 m/sec, heating air velocities of 8 to 40 m/sec, and temperature differences of 30 to 60 C between mainstream air and film heating air.

Wieghardt *a priori*:

- Deduced that the important parameters in film heating are η, x, m, and s.
- Deduced that equations in the form of Eq. (4) correlate film heating data.

$$\eta = f\{x\}f\{m\}f\{s\} \quad (4)$$

- Deduced that each function in Eq. (4) is the parameter raised to an exponent, as in Eq. (5).

$$\eta = ax^b m^c s^d \quad (5)$$

- Because it is assumed that rational equations are dimensionally homogeneous, deduced that d and b in Eq. (5) are equal, resulting in Eq. (6).

$$\eta = ax^b m^c s^{-b} \quad (6)$$

- Deduced that, because the s exponent equals the negative of the x exponent, and because the data include a wide range of x values, the s exponent can be determined from the $\eta\{x\}$ data, and therefore the experiment requires only one value of s.

Note that, before any data were obtained, everything about the film heating correlation had been deduced except the values of the constants in Eq. (6).

The constants in Eq. (6) were quantified after the experiment by induction, and Eq. (7) resulted.

$$\eta = 21.8(x/ms)^{-8} \quad x \geq 100s \quad m \leq 1.0 \quad (7)$$

The restrictions on the application of Eq. (7) are required because:

- Eq. (7) does *not* agree with the data if x is less than 100s.
- The data indicate that, at x = 100s, dη/dm becomes *negative* at m = 1.0.

Note that in Eq. (7), η is inversely related to x. Therefore Eq. (7) indicates that η equals *infinity* at x = 0, whereas η cannot exceed 1.000.

The problem with the a priori deduction that η depends on x, m, and s

It is axiomatic that a parametric correlation should be expressed in terms of *independent* parameters so that the correlation is affected by *every* parameter in the correlation.

The problem with the *a priori* deduction that η depends on x, m, and s is that m is *not* independent of s. m is inversely proportional to s, and consequently the *product* ms does *not* depend on m or s. Therefore the parameter group x/ms does *not* depend on m or s, and consequently Eq. (7) seems to state that η depends on m and s, when in fact Eq. (7) states that η does *not* depend on m or s. Note that:

- Identity (8) indicates that m is inversely proportional to s.

$$m \equiv G_{slot}/G_{ms} \equiv (W_{slot}/sw_{slot})/G_{ms} \equiv W'_{slot}/(G_{ms}s) \quad (8)$$

- Identity (9) indicates that, in terms of *independent* parameters, ms is W'_{slot}/G_{ms}. In other words, the *product* ms does *not* depend on m or s. It depends on W'_{slot} and G_{ms}.

$$ms \equiv (W'_{slot}/(G_{ms}s))s \equiv W'_{slot}/G_{ms} \quad (9)$$

- Identity (10) indicates that, in terms of *independent* parameters, x/ms is xG_{ms}/W'_{slot}.

$$x/ms \equiv xG_{ms}/W_{slot} \quad (10)$$

- Combining Identity (10) and Eq. (7) results in Eq. (11). Eqs. (7) and (11) are *identical*. *Both* equations state that η depends on x, G_{ms}, and W'_{slot}. *Both* equations state that η does *not* depend on m or s.

$$\eta = 21.8 \, (xG_{ms}/W'_{slot})^{-.8} \quad x \geq 100s \; m \leq 1.0 \quad (11)$$

- Eq. (11) should replace Eq. (7) because Eq. (7) seems to state that η depends on m and s, when in fact it states that η does *not* depend on m or s. *Both* equations state that η depends on x, G_{ms}, and W'_{slot}.
- Because Eqs. (7) and (11) state that η does *not* depend on m, any effect that m has on η necessarily contributes to the disagreement between the data and Eqs. (7) and (11). (Recall that s was *not* varied in the experiment, and therefore variation in s could not have contributed to the disagreement between the data and Eqs. (7) and (11).)

In summary, the problem with the *a priori* deduction that η depends on x, m, and s is that this deduction is largely responsible for Eq. (7), an equation that appears to state that η depends on x, m, and s, when in fact it states that η depends on x, $G_{ms, and}W'_{slot}$

The problem with the a priori deduction that equations in the form of Eq. (4) correlate film heating data

The problem with the *a priori* deduction that an equation in the form of Eq. (4) best correlates film heating data is that there is no sound reason to conclude that film heating data are best correlated by an equation that indicates η is a function of the product of each parameter raised to an exponent.

The problem with the a priori deduction that equations in the form of Eq. (6) correlate film heating data

The problem with the *a priori* deduction that equations in the form of Eq. (6) correlate film heating data is that η is inversely related to x, and therefore Eq. (6) states that η equals *infinity* at x = 0, whereas η *cannot* be greater than 1.00.

Note that Eqs. (7) and (11) are in the form of Eq. (6), and they do *not* correlate the data if x is less than 100s. For example, if the slot height is 10 mm as in Wieghardt (1946), Eqs. (7) and (11) do *not* correlate film heating data in the first *1000 mm* directly downstream of the slot exit.

The problem with the a priori deduction that the relationship between η and s can be experimentally determined without varying s

The only way to experimentally determine the relationship between η and s is to test more than one value of s. Because the Wieghardt test program included only one value of s, the test data do *not* establish the relationship between η and s. Therefore Eq. (7) should either:

- *Not* include parameter s, and be accompanied by the statement "s = 10 mm." to inform the user that the correlation is based on data obtained at s = 10 mm.
- Or include parameter s *and* be accompanied by the statement "s = 10 mm." to inform the user that the η\{s\} functionality in the correlation is *not* supported by data.

The film heating correlation by Hartnett, Birkebak, and Eckert (1961)

Hartnett, Birkebak, and Eckert (1961) performed a film heating experiment using a tangential slot similar to that used by Wieghardt, a slot height of 3.12 mm, an m value of 0.28, a mainstream velocity of 51 m/sec, and temperatures differences of 5 to 80 C between the film air and the mainstream air. The authors state:

> *The usual choice of parameters was made to represent the data. These same parameters are suggested in a semiempirical analysis presented in the Appendix . . .*

It was *a priori* deduced or assumed that an equation in the form of Eq. (7) would best correlate their film heating data. The authors plotted their data on the log log chart in their Fig. (24), drew a line through their data, and concluded that the line indicates that the coefficient in Eq. (7) should be 16.9 rather than the 21.8, resulting in Eq. (12).

$$\eta = 16.9(x/ms)^{-0.8}$$
$$x/s > 17 \quad m = .28 \quad s = 3.12 \text{ mm.} \tag{12}$$

Note that Eq. (7) closely correlates its underlying data only if x/s is greater than 100, whereas Eq. (12) closely correlates its underlying data if x/s is greater than 17.

With regard to the discrepancy between coefficients 21.8 and 16.9 in Eqs. (7) and (12), Hartnett, Birkebak, and Eckert (1961) state:

. . . we would expect that the value of Wieghardt's constant (21.8) *would be less than 16.9 as found in this investigation . . .This inconsistency may possibly be the result of an inaccurate measurement by Wieghardt of the entering injectant air temperature T_{slot} . . .*

However, as noted above, Eqs. (7) and (12) state that m and s have *no effect* on η. Therefore, if m or s *does* affect η, the difference in m or s values between the two studies could explain the inconsistency noted above.

In the Wieghardt study, s was 10 mm, and the correlation was based on m values from 0.22 to 1.0. In the Hartnett, Birkebak, and Eckert study, s was 3.12 mm and m was 0.28. Note that there is a factor of 3 difference between s values, and a factor of 2 difference in average m values. Hartnett, Birkebak, and Eckert state:

If Wieghardt's correlation is modified to represent only his lower blowing rates, m ≤ 0.40 . . ., the constant is changed from 21.8 . . . to 19.5.

This statement indicates that:

- The value of m or s *does* affect η.
- m should be a parameter in film heating correlations. (Note that several correlations cited in Acharya and Kanani (2017) are in the form η = *f* {m, x/ms}, indicating that m *does* affect η.)
- The discrepancy between coefficients 21.8 and 16.9 in Eqs. (7) and (12) resulted, at least in part, because m and s in the two studies were vastly different, whereas Eqs. (7) and (12) state that η does *not* depend on m or s.

Using alternate methodology to determine the best correlation for the data presented in Hartnett, Birkebak, and Eckert (1961)

The film heating experiment by Hartnett, Birkebak, and Eckert (1961) included only one value of G_{ms} and one value of W'_{slot}. Consequently the data provide information about η{x}, but no information about η{x/ms}. Therefore we can determine the best η{x/ms} correlation for the subject data only if the analysis is based on the *a priori* conclusion that the best correlation form for film heating data is η{x/ms}.

In order to determine the best η{x/ms} correlation for the subject data, it is necessary to determine the η{x/ms} correlation that best describes the line drawn by the authors through their x/ms data plotted on the log log chart in their Fig. (24). Since η cannot exceed 1.00, the best film heating correlation *must* be in a form in which the calculated value of η cannot exceed 1.00. Equation (13) is a correlation form in which η cannot exceed 1.00. Eq. (13) is plotted on the log log data chart in Fig. (24), and the optimum value of c is determined by trial and error.

$$\eta = 1/(1.00 + c(x/ms)) \tag{13}$$

Eq. (14) is the resultant correlation. Adiutori (1974) states that Eq. (14) correlates *all* of the subject data so well that it is not possible *to distinguish between Eq. (14) and the curve drawn by the authors through their experimental points* plotted on their Fig. 24.

$$\eta = 1/(1.00 + .0142(x/ms))$$
$$x \geq 0 \quad m = 0.28 \quad s = 3.12 \text{ mm.} \tag{14}$$

Eq. (14) is much more accurate than Eq. (12) because Eq. (14) closely agrees with *all* of the data presented in Hartnett, Birkebak, and Eckert (1961), whereas Eq. (12) closely agrees with the data only at x/s values greater than 17.

It is important to note that Eq. (14) describes the relationship between x, m, and s (ie. x, G_{ms}, and W'_{slot}) at only one value of m and one value of s. Consequently Eq. (14) in fact describes only the relationship between η and x.

II. Boiling Heat Transfer Study by Nukiyama (1934)

Nukiyama (1934) was a pioneering study of boiling heat transfer in which nucleate boiling and film boiling heat transfer data were obtained from electrically heated wires and flat surfaces immersed in water at atmospheric pressure. The data were plotted on linear coordinates, and the resultant charts indicate the following:

- In fully developed nucleate boiling, the relationship between heat flux q and boundary layer temperature difference ΔT is usually quite *linear*, and is described by equations in the form of Eq. (15). Note that q_{ofnb} is the heat flux at the onset of fully developed nucleate boiling, and ΔT_{ofnb} is the temperature difference at the onset of fully developed nucleate boiling. ΔT_{DNB} is the

temperature difference at the departure from nucleate boiling.

$$q_{nb} = q_{ofnb} + a(\Delta T - \Delta T_{ofnb})$$
$$\Delta T_{ofnb} \leq \Delta T \leq \Delta T_{DNB} \qquad (15)$$

- In fully developed nucleate boiling, the relationship between q and ΔT is sometimes slightly nonlinear, and is described by equations in the form of Eq. (16) in which $n \cong 0.8$.

$$q_{nb} = q_{ofnb} + a(\Delta T - \Delta T_{ofnb})^n$$
$$\Delta T_{ofnb} \leq \Delta T \leq \Delta T_{DNB} \qquad (16)$$

A priori deduction or assumption that results in the widely accepted conclusion that nucleate boiling heat transfer data describe highly nonlinear power laws

In spite of Nukiyama's data that documented highly *linear* behavior in the nucleate boiling region, for almost 100 years it has been widely agreed in American engineering literature that nucleate boiling heat transfer data describe highly *nonlinear* power laws[1] in the form of Eq. (17), such as the widely accepted Rohsenow correlation in which n = 3.

$$q = f\{\Delta T^n\} \qquad (17)$$

The graphical methodology that results in highly nonlinear power laws is described in Cryder and Finalbargo (1937). This methodology is based on the *a priori* deduction or assumption that nucleate boiling data describe nonlinear power laws.

To determine (the relationship between heat transfer coefficient and temperature difference)*, the coefficient (h) . . . is plotted against ΔT . . . at constant boiling temperature. A log-log plot . . . results in a series of straight lines with a slope of 2.5. . . The data would therefore indicate that* (h {ΔT} is a power law of exponent 2.5—ie q{ΔT} is a power law of exponent 3.5.*)*

The digital methodology that results in highly nonlinear power laws is described in Cooper (1984). This methodology is also based on the *a priori* deduction or assumption that nucleate boiling data describe nonlinear power laws.

Correlations in the form of (power laws) are produced directly from raw data by a . . . least squares program. . . Here the fit is among log h, log q.

The problem with the a priori deduction or assumption that nucleate boiling data describe highly nonlinear power laws

Adiutori (1994) states that the problem with the *a priori* deduction or assumption that nucleate boiling data describe highly nonlinear power laws is that it results in induction methodology that is *not* rigorous. Adiutori (1994) states:

---

[1] A few nucleate boiling heat transfer studies, such as Mesler and Banchero (1958), correctly concluded that nucleate boiling data describe highly *linear* behavior. However, they are seldom cited.

Rigorous induction methodology is achieved by plotting data in linear *coordinates and fitting a curve through regions which contain closely spaced data.*

Induction should be based on data plotted on *linear* charts because functionality is readily apparent on linear charts, whereas functionality is distorted and *not* readily apparent on log log charts.

A nucleate boiling heat transfer correlation based on alternate methodology

In alternate methodology, nucleate boiling correlations are determined by *"plotting data in linear coordinates and fitting a curve through regions which contain closely spaced data".* This was in fact the methodology used by Nukiyama (1934).

Alternate methodology results in the conclusion that literature data indicate that nucleate boiling heat transfer data are *not* generally correlated by *nonlinear* power laws in the form of Eq. (17). As Nukiyama concluded, nucleate boiling heat transfer data are generally correlated by *linear* equations in the form of Eq. (15).

Adiutori (1994) states:

- *Examples of data originally judged to support the linear view are those of Nukiyama (1934) and Mesler and Banchero (1958).*
- *Examples of data originally judged to support the power law view, and later shown to be highly linear, are those of Perry (1948), Cichelli and Bonilla (1945), Corty (1951), Stock (1960), Aladiev (1960), and Berenson (1960 and 1962).*
- *Data cited by Rohsenow (1952) to validate his widely accepted power law correlation in fact exhibit linear behavior.*

The a priori deduction or assumption that transition boiling heat transfer data describe nonlinear power laws

Transition boiling data in heat transfer literature are generally plotted on logarithmic charts presumably because of the *a priori* deduction or assumption that transition boiling heat transfer data describe nonlinear power laws with negative exponent.

For example, Berenson (1960 and 1962) obtained data on 20 boiling curves using a vented pool boiler with a round, flat boiler plate which was steam heated on the lower surface. The boiling fluid was n-pentane, and the boiling surfaces tested were nickel, copper, and inconel. The data were plotted on log log charts, and straight lines drawn through transition boiling regions. Berenson (1962) concluded the following about the transition boiling region:

It was found, with the exception of some of the data presented in Fig. 5, that the transition boiling data lie along a straight line connecting the burnout point and the film-boiling minimum point on log log graph paper. This is also true of the transition boiling data

28

obtained by Braunlich (1941) and Kaulakis and Sherman (1938).

In summary, three experiments for doctoral theses performed at MIT over a period of more than 20 years independently concluded that "transition boiling data lie along a straight line connecting the burnout point and the film-boiling minimum point on log log graph paper".

The problem with the a priori deduction or assumption that transition boiling heat transfer data describe nonlinear power laws

Due to the vagaries of log log charts, it was not noticed that seventeen of Berenson's twenty boiling curves contain little or no data in the transition boiling region. Consequently straight lines were drawn through the transition region of seventeen boiling curves that have little or no data in the transition region.

Three of the boiling curves (Runs 7, 8, and 9) contain data throughout the transition boiling region. (Runs 7, 8, and 9 contain the data referred to in the phrase "with the exception of some of the data presented in Fig. 5".) The transition boiling region data from Runs 7, 8, and 9 lie on highly *curved* lines on log log charts.

$$q_{tb} = q_{max} - (q_{max} - q_{min})(\Delta T - \Delta T_{max\,q})/(\Delta T_{min\,q} - \Delta T_{max\,q}) \qquad \Delta T_{max\,q} \leq \Delta T \leq \Delta T_{min\,q} \qquad (18)$$

Hesse (1973) obtained transition boiling data using an apparatus in which boiling takes place on the outer surface of a thin wall tube made of nickel; the boiling fluids tested were R112, R113, and R114; tests were performed at pressures from 0.5 to 20 bars; the heat source was water pumped at high velocity through the tube. Boiling curve data were obtained, and the data plotted on log q vs log ΔT charts. In the transition boiling region, the data describe curved lines on log log charts, and straight lines on linear charts. (The linear charts are in Adiutori (1991).)

Ellion (1954) was the first to design and build an electrically heated, forced convection boiler that could operate stably in the transition boiling region. The boiler was a double tube heat exchanger in which the boiling interface was the outer surface of the inner tube. When Ellion's boiling data are plotted on linear coordinates, the data from three of the runs are highly linear in the transition region, and the data from one of the runs is curved in the transition region. (The linear charts are in Adiutori (1991).)

McDonough et al (1961) reported the first transition boiling experiment at high pressure. The boiler in the experiment was a double tube, counter flow heat exchanger in which boiling water flowed upward inside the inner tube. Linear equations were induced from transition region data.

Ragheb et al (1978) investigated transition region boiling. The results presented in Ragheb et al

The problem with the *a priori* assumption or deduction that transition boiling heat transfer data describe nonlinear power laws is that transition boiling heat transfer data do *not* describe nonlinear power laws, as evidenced by the fact that transition boiling heat transfer data do *not* describe straight lines on log log charts.

Using alternate methodology to determine correlations for transition boiling heat transfer

If alternate methodology is used, correlations for transition boiling heat transfer are determined by plotting data on *linear* charts, and determining functionality by inspecting the chart.

If Berenson's 20 boiling curves are plotted on linear charts, it is apparent that 17 curves have little or no data in the transition region, and curves for Runs 7, 8, and 9 have data throughout the transition region. On linear charts, data from Runs 7, 8, and 9 describe straight lines between the maximum and the minimum in the boiling curve, indicating that the relationship between heat flux and temperature difference in the transition boiling region is described by *linear* equations in the form of Eq. (18). (A linear chart of Runs 7, 8, and 9 is in Adiutori (1974).)

(1978) are reported in digital form in ANL reports. For example, boiling curve data for a mass flow rate of 203 kg/m²s and sub cooling values of 0, 13.9, and 27.8 C are reported in digital form in Cheng et al (1978). When these data are plotted on linear coordinates, the transition boiling data describe straight lines. (The linear chart is in Adiutori (1991).

In summary, the problem with the *a priori* assumption or deduction that transition boiling heat transfer data describe nonlinear power laws is that transition boiling heat transfer data in the literature generally describe *linear* equations in the form of Eq. (18).[2]

Conventional methodology used to determine the generic correlation for heat transfer to a turbulent, one phase Newtonian fluid

In conventional methodology, the generic correlation for heat transfer to a turbulent, one phase Newtonian fluid is based on the following *a priori* deduction:

- Deduce that h depends on D, G, k, $C_{p,\,and\,\mu}$.
- Deduce that the h correlation is in the form of Eq.

$$h = f\{D\}f\{G\}f\{k\}f\{C_P\}f\{\mu\} \qquad (19)$$

---

[2] If transition boiling data describe straight lines on log log charts rather than linear charts, dq/dΔT is much more negative in the upper end of the transition region. This has practical importance in analyses to determine fuel temperature transients following a loss of coolant flow in water cooled nuclear reactors.

- Deduce that each function in Eq. (19) is the parameter raised to an exponent, as in Eq. (20).

$$h = aD^b G^c k^d C_p^e \mu^f \qquad (20)$$

- Deduce that the values of the constants in Eq. (20) are the same for all Newtonian fluids.
- Deduce that Eq. (20) is dimensionally homogeneous.
- Use dimensional analysis to deduce that Eq. (20) can be replaced by Eq. (21).

$$Nu = aRe^b Pr^c \qquad (21a)$$

$$h = ak^{1-c} D^{b-1} G^b \mu^{c-b} C_p^c \qquad (21b)$$

The problem with the deduction that h equals the product of each correlating parameter raised to an exponent

The problem with the deduction that h equals the product of each correlating parameter raised to an exponent is that there is no basis for it. It is a deduction without foundation.

Recall that the film heating correlations by Wieghardt (1946) and by Hartnett, Birkebak, and Eckert (1961) are based on the deduction that η equals the product of each correlating parameter raised to an exponent, and both correlations violently *disagree* with much of the data. Also recall that the film heating correlation that resulted from applying the alternate methodology to the data by Hartnett, Birkebak, and Eckert does *not* state that η equals the product of each parameter raised to an exponent, and that correlation agrees with *all* of the data.

If alternate methodology is used, it is not *a priori* deduced that correlations are the product of each important parameter raised to an exponent. Correlation functionality is determined *a posteriori* by induction, and *all* functions are acceptable.

a) The problem with Equation (21)

The problem with Eq. (21) is that it has *nothing to do with data*. It is *entirely* the result of *a priori* deduction. Data are required merely to quantify a, b, and c in Eq. (21).

Note that the accuracy and validity of Eq. (21) are suspect because:

- There is no sound basis for the assumption that correlations are generally the product of important parameters raised to exponents.
- There is no sound basis for the assumption that a correlation that applies to *all* Newtonian fluids can be determined by a test program in which only one Newtonian fluid is tested.
- The relationship between μ and h is determined *without* measuring μ.
- The relationship between k and h is determined *without* measuring k.
- The relationship between C_p and h is determined *without* measuring Cp.

- It indicates that the exponents of D and G are both dependent on b, and therefore the D exponent can be determined without varying D.

Eq. (22a) is a generally accepted correlation determined primarily by the *a priori* deduction described above. Note that Eqs. (22a) and (22b) are identical, and that Eq. (22b) is in a much more useful form in that it *reveals* parameter functionality because parameters are *explicit*, whereas Eq. (22a) *conceals* parameter functionality because parameters are *implicit* in group parameters. Also note that Eq. (22a) *cannot* be used to determine h unless it is first transformed to Eq. (22b).

$$Nu = .023 Re^{.8} Pr^{.4} \qquad (22a)$$

$$h = .023 \, D^{-.2} G^{.8} k^{.6} \mu^{-.4} C_p^{.4} \qquad (22b)$$

b) "Scientific" correlations

The word "scientific" is generally considered synonymous with "rigorously correct". Parametric correlations are generally considered scientific if they are primarily the result of *a priori* deduction, and considered *un*scientific if they are primarily the result of *a posteriori* induction.

But the truth is just the opposite. As evidenced by the above film heating correlations and the boiling correlations, correlations that are primarily the result of rigorous *a posteriori* induction are likely to be much more correct—much more scientific—than correlations that are primarily the result of *a priori* deduction.

Engineering laws such as Hooke's law and Ohm's law are "scientific", but they are *not* primarily the result of *a priori* methodology. They are primarily the result of *a posteriori* induction.

Newton's view of the scientific method

In a letter to Father Pardies, Newton (1672) described his view of the scientific method in the following:

The best and safest method of philosophizing seems to be, first to enquire diligently into the properties of things, and to establish these properties by experiment, and then to proceed more slowly to hypothesis for the explanation of them. For hypotheses should be employed only in explaining the properties of things, but not assumed in determining them . . .

In other words, in Newton's view of the scientific method, parametric correlations should be determined by *a posteriori* induction rather than *a priori* deduction.

A priori deduction if alternate methodology is used to determine a fluid specific correlation for heat transfer to a turbulent, one phase Newtonian fluid

If alternate methodology is used to determine a *fluid specific* correlation for heat transfer to a turbulent, one phase Newtonian fluid, it is *a priori* deduced that a

correlation in the form of Eq. (23) will correlate the data. The functions in Eq. (23) are determined *a posteriori*, and *any* function that closely describes the data is acceptable.

$$h = af\{G\}f\{D\}f\{T_{fluid}\} \qquad (23)$$

If the data do not verify that Eq. (23) correlates the data, a different correlation form is deduced.

Fluid specific heat transfer correlations that result from alternate correlation methodology
If alternate methodology is used:

- The resultant correlation includes only parameters measured in the experiment.
- Parameters in fluid specific correlations are *explicit* rather than implicit in group parameters such as Re.
- Fluid specific correlations are desirable because:

  o They more accurately describe the heat transfer behavior of the specified fluid than fluid generic correlations.
  o They are more user friendly in that they do not require reference to property tables.
  o They more readily reveal functionality.

- Fluid specific correlations such as Eq. (23) *cannot* be dimensionally homogeneous because G is the only parameter that includes the dimension of mass. Correlations that are not dimensionally homogeneous must be in the form of "dimensional equations", a form widely used in mid-twentieth century.

In dimensional equations, parameter symbols represent numerical value but *not* dimension, and the dimension units that underlie parameter symbols are specified in an accompanying nomenclature. The following is an example of a "dimensional equation":

For the turbulent flow of gases in straight tubes, the following dimensional equation for forced convection is recommended for general use:

$$h = 16.6\, c_p(G')^{0.8}/(D_i')^{0.2}$$

where c_p is the specific heat of the gas at constant pressure, B.T.u./(lb.)(°F), G' is the mass velocity, expressed as lb. of gas/sec./sq. ft, . . . and D_i' is in inches. Perry (1950)

The design of an experimental study to determine a fluid specific correlation for heat transfer to a turbulent, one phase Newtonian fluid

The design of an experimental study to determine a fluid specific correlation for heat transfer to a turbulent, one phase Newtonian fluid is shown in Table 1. The numbers in the table represent the relative values

of the parameters. Table 1 indicates that each parameter is to be tested at 5 values while the other parameters are at their lowest value, and at the same 5 values while the other parameters are at their highest values.

Table 1: Experiment Design

G	T_{fluid}
1	1 to 5
5	1 to 5
1 to 5	1
1 to 5	5

Table 1 indicates that 20 data points are required for each diameter tested, 10 to determine $f\{G\}$ and $f\{T_{fluid}\}$, and 10 to verify that the effect of each parameter is independent of the value of the other parameters. Since Eq. (22b) indicates that q is a weak function of D, the experiment design would reasonably call for only three values of D, and the entire experiment would require 60 data points.

How a fluid generic correlation can be determined from a fluid specific correlation

A fluid generic correlation can be determined from a fluid specific correlation as follows:

- Assume that Eq. (24) applies. Note that $f\{T_{fluid\,x}\}$ is from a fluid specific correlation for fluid x, and k, C_p, and μ are functions of $T_{fluid\,x}$.

$$f\{T_{fluid\,x}\} = k^a C_p^{\,b} \mu^c \qquad (24)$$

- Use $f\{T_{fluid\,x}\}$ data to determine optimum values of a, b, and c in Eq. (24), or use the corresponding exponents in Eq. (22b).

In the fluid specific correlation, replace $f\{T_{fluid\,x}\}$ with the right side of Eq. (24), resulting in a fluid generic correlation. The generic correlation should be accompanied by a statement such as "This fluid generic correlation is based on a fluid specific correlation for fluid x, and the assumptions that:

  o $f\{D\}$ and $f\{G\}$ are the same for all Newtonian fluids.
  o The values of a, b, and c in Eq. (24) are the same for all Newtonian fluids. (Or "The values
  o of a, b, and c are from Eq. (22b))"

III. Conclusions

Methodology that is primarily *a posteriori* induction should be used to determine parametric correlations because, as the examples in the text demonstrate, it results in correlations that more closely agree with data than methodology that is primarily *a priori* deduction.

Symbols
a to f constants
C_p heat capacity

D   diameter
G   mass flow rate
h $q/\Delta T$ k thermal conductivity
m $G_{slot/Gms}$
n   constant
Nu   Nusselt number
Pr   Prandtl number
q   heat flux
Re   Reynolds number
s   slot height
T   temperature
w   slot width
W   flow rate
W′   flow rate per unit slot width
x   distance downstream of slot exit
μ   viscosity
η   film effectiveness

Subscripts

DNB   departure from nucleate boiling
Max   maximum in the boiling curve
Min   minimum in the boiling curve
Ms   main stream
Nb   nucleate boiling
Ofdnb   onset of fully developed nucleate boiling
Tb   transition boiling

References Références Referencias

1. Acharya, S. and Kanani, Y., 2017, Ch. 3, Advances in film cooling heat transfer, *Advances in Heat Transfer,* Sparrow, E.M. and Abraham, J.P.
2. Adiutori, E. F., 1974, *The New Heat Transfer*, Ventuno Press, pp 6-31 and 7-24
3. Adiutori, E. F., 1991, Thermal behavior in the transition region between nucleate and film boiling, presented at 3rd ASME-JSME Thermal Engineering Joint Conference, March, 1991, in Reno, NV. Printed in the Conference Proceedings, v 2, pp 51-58
4. Adiutori, E. F., 1994, A critical examination of the view that nucleate boiling heat transfer data exhibit power law behavior, *Japanese Society of Mechanical Engineers International Journal*, Series B, Vol. 37, No. 2, pp 394-402
5. Adiutori, E. F., 2017, *The New Engineering*, 3rd edition, Ventuno Press, pp 145-148
6. Aladiev, I. T., 1960, Experimental data on heat transfer with nucleate boiling of subcooled liquid in tubes, convective and radiant heat transfer, Izd-vo Akad. Nauk SSSr
7. Berenson, P. J., 1960, On transition boiling heat transfer from a horizontal surface, Thesis, MIT
8. Berenson, P. J., 1962, Experiments on pool-boiling heat transfer, *Int. J. Heat and Mass Transfer*, Vol. 5, pp 985-999 Braunlich, R. H., 1941, Heat transfer to boiling liquids, thesis, MIT
9. Bunker, R. S., 2006, Cooling design analysis, *The Gas Turbine Handbook*, pp 295-309, National Energy Technology Laboratory, US Dept. of Energy, Morgantown, W Va
10. Cheng, S. C., Ragheb, H., Ng, W. W. L., Heng, K. T., and Roy, S., 1978, Transition boiling heat transfer in forced vertical flow, Argonne National Laboratory Report ANL-78-75
11. Cichelli, M. T. and Bonilla, C. F., 1945, Heat transfer to boiling liquids under pressure, Trans. AIChE, Vol. 41, p. 755
12. Colban, W. F., Thole, K. A., and Bogard, D., 2011, A film cooling correlation for shaped holes on a flat plate surface, *J. Turbomach*, 133, 11002, https://doi.org/10.1115/1.3450526
13. Cooper, M. G., 1984, Heat flow rates in saturated nucleate pool boiling—A wide-ranging examination using reduced properties, *Advances in Heat Transfer*, J. P. Hartnett and T. V. Irvine, Vol. 16, p 157
14. Corty, C., 1951, Surface variables in boiling, Ph.D. Thesis, Univ Michigan
15. Cryder, D. S. and Finalbargo, A. C., 1937, Heat transmission from metal surfaces to boiling liquids: effect of temperature of the liquid on film coefficient, *AIChE*, Vol. 33, p. 346
16. Ellion, M. E., 1954, A study of the mechanism of boiling heat transfer, JPL Memo 20-88 (originally prepared as a PhD thesis, Cal Tech)
17. Hartnett, J. P., Birkebak, R. C., and Eckert, E. R. G., 1961, Velocity distributions, temperature distributions, effectiveness and heat transfer coefficients for air injected through a tangential slot into a turbulent boundary layer, pp 293-306, *ASME Journal of Heat Transfer*, pp 293-306, August
18. Hesse, G., 1973, Heat transfer in nucleate boiling, maximum heat flux and transition boiling, *Int Jour. Heat and Mass Transfer*, 16, pp 1611-1627
19. Kaulakis, E. G. and Sherman, L. M., 1938, thesis, MIT
20. Kays, W. M., 1966, *Convective Heat and Mass Transfer*, McGraw-Hill
21. McDonough, J. B., Milich, W., and King, E. C., 1961, An experimental study of partial film boiling region with water at elevated pressures in a round vertical tube, *Chem Eng Prog Symp Series*, v 57, No. 32, pp 197-208
22. Mesler, R. B. and Banchero, J. T., 1958, Effect of super-atmospheric pressures on nucleate boiling of organic liquids, *AIChE Journal*, Vol. 4 (1), p 102
23. Newton, I., 1672, Letter to Ignatius Pardies as quoted by William L. Harper in *Isaac Newton's Scientific Method: Turning Data Into Evidence about Gravity* and cosmology https://en.wikiquote.org/wiki/Isaac_Newton

24. Nukiyama, S., 1934, The maximum and minimum values of the heat Q transmitted from metal to boiling water under atmospheric pressure, J. Japan Soc. Mech. Engrs., vol. 37 p.207; English translation in Int. J. Heat Mass Transfer, 1966, vol. 9, p. 1419
25. Perry, C. W., 1948, Ph.D. Thesis, Johns Hopkins Univ, Baltimore
26. Perry, J. H., 1950, *Chemical Engineers' Handbook*, p. 467, McGraw-Hill
27. Ragheb, H. S., Cheng, S. C., and Groeneveld, D. C., 1978, Measurement of transition boiling boundaries in forced convection flow, Int Jour Heat Mass Transfer, v 21, pp 1621-1624
28. Rohsenow, W. M., 1952, A method of correlating heat transfer data for surface boiling of liquids, Trans ASME, p. 969
29. Stock, B. J., 1960, Observations on transition boiling heat transfer phenomena, ANL-6175
30. Wieghardt, K., 1946, AAF Translation No. F-TS-919-RE

This page is intentionally left blank

An Experimental Investigation of Performance of Composite Brake Pads

By S. K. Vignesh

Abstract- This project work on new material selection for friction pad. New pollution less brake pad, and also increases the performance, durability, weight reduction was developed using Glass fibre, Jute fibre, Basalt fibre. Disc brakes are used for reducing speed without losing braking stability, controllability and their ability to provide a wide ranging torques. The literature study found that the currently used material asbestos is harmful due to its carcinogenic nature. The experimentation involves the use of different samples of composite materials which is performed on pin on disc apparatus where friction reaction against load, speed, temperature and wear are studied and the improved result is discussed.

Keywords: glass fiber, basalt, laminate, brake.

GJRE-A Classification: FOR Code: 091399p

ANEXPERIMENTALINVESTIGATIONOFPERFORMANCEOFCOMPOSITEBRAKEPADS

Strictly as per the compliance and regulations of:

An Experimental Investigation of Performance of Composite Brake Pads

S. K. Vignesh

Abstract- This project work on new material selection for friction pad. New pollution less brake pad, and also increases the performance, durability, weight reduction was developed using Glass fibre, Jute fibre, Basalt fibre. Disc brakes are used for reducing speed without losing braking stability, controllability and their ability to provide a wide ranging torques. The literature study found that the currently used material asbestos is harmful due to its carcinogenic nature. The experimentation involves the use of different samples of composite materials which is performed on pin on disc apparatus where friction reaction against load, speed, temperature and wear are studied and the improved result is discussed.

Keywords: glass fiber, basalt, laminate, brake.

I. Introduction

Brake pad are made with materials like, graphite, brass and ceramics. This work aimed at obtaining a suitable friction material, taking cost, performance and environmental implication into consideration. For all categories of vehicles that are equipped with brake discs, brake pads form vital components. They are steel backing plates with friction material fasten to the surface facing the brake disc. There are two types of brakes are available they are drum brakes and disc brakes, usually drum brakes has shoes inside the drum and in the disc brake they contains the metal disc which would rotate inside the caliper.

II. Methadology
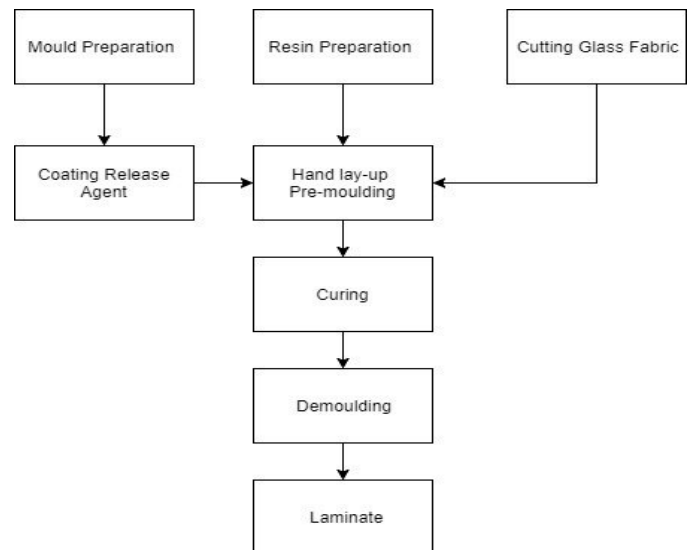
III. Materials

a) Glass Fibres

Glass fiber are modern materials that used in mechanical and production industries. They are been produced by the modern methods. They exhibit useful huge properties such as hardness, transparency, resistance to chemical attack, stability, and inertness, as well as desirable fibre properties such as strength, flexibility, and stiffness. Glass fibres are used in the manufacture of structural composites, printed circuit boards and a wide range of special purpose products.

Figure 1: Glass fiber

b) Basalt fibre

Basalt rock will be wont to create not solely volcanic rock bars however conjointly volcanic rock

Author: Assistant professor, Mechanical Department, VI Institute of technology. e-mail: Skvrajesh1995@gmail.com

materials, sliced volcanic rock fibre strands, continuous volcanic rock filament wires and volcanic rock mesh. a number of the potential applications of those volcanic rock composites are: plastic compound reinforcement, soil strengthening, bridges and highways, industrial floors, heat and sound barriers for residential and industrial buildings, bullet proof vests and retrofitting and rehabilitation of structures.

Figure 2: Basalt fiber

c) Jute fibre

Jute is a important natural fiber crop in India next to cotton. In trade and trade, jute and Mesta crop along called raw jute as their uses are nearly same. Raw jute plays a very important role within the country's economy. Raw jute was first used in planting and for the packing industry. however, it's currently emerged as a flexible material for numerous applications, such as, textile industries, paper industries, building and automotive industries, use as soil saver, use as ornamental and furnishing materials, etc. Raw jute being perishable and annually renewable supply, it's thought of as associate degree setting friendly crop and it helps within the maintenance of the setting and ecological balance. Jute as a natural fibre has some definite inherent blessings.

Figure 3: Jute fiber

d) Epoxy Resin and Hardner

Figure 4: Resin and Hardner

Properties of Resin (Ly556)
Aspect (visual) clear, pale yellow liquid
Colour (Gardner, ISO 4630) $\leq$ 2
Epoxy content 5.30 - 5.45 [eq/kg]
Viscosity at 25 °C 10000 - 12000 [MPa s]
Density at 25 °C 1.15 - 1.20 [g/cm3]
Flash point (ISO 2719) > 200 [°C]
Storage temperature (see expiry date on original container) 2 - 40 °C [°C]

Properties of Hardener (Hy906)
Aspect (visual) clear, pale yellow liquid
Colour (Gardner, ISO 4630) $\leq$ 2
Viscosity at 25 ° 175 - 350 [MPa s]
Density at 25 °C 1.20 - 1.25 [g/cm3]
Flash point > 135 [°C]
Storage temperature (see expiry date on original container) 2 - 40 °C [°C]

IV. FABRICATION

a) Lay-up process

Once all the materials square measure ready, the digital computer is prepared and therefore the mould preparation done; the scholars will begin with the lay-up method. the primary step is to combine the organic compound and therefore the hardener. The proportions square measure sometimes given by the provider and might be found on the containers of the hardener or organic compound. The parts will be either measured by weight for by volume however it's vital to follow these proportions specifically as this is often an entire reaction and every one element should react utterly for max strength of the matrix. it's best to live proportions victimization the degree methodology and a screw in pump that inserts into the cans of organic compound and hardener. These pumps will be purchased beside the containers of organic compound and hardener. make certain to stay the organic compound pump and instrumentation high break away the pump and instrumentation high of the hardener as a

result of any contamination can initiate the reaction and cause the ensuing mix to harden.

The admixture is performed within the mixing containers with the blending stick and may be done slowly therefore on not board any excess air bubbles within the organic compound. watch out to combine utterly and deliberately for a full 2 minutes before applying. it's best to use a "flat" stick- like tongue depressor; a spherical stick doesn't work well because it doesn't 'paddle' the mixture to mix it properly. Note: Plastic admixture containers could soften throughout the chemical reaction, therefore it's best to use containers that square measure specifically created for the aim of blending epoxy glue. These square measures usually accessible from the organic compound merchant. Next Associate in Nursing adequate amount of mixed organic compound & hardener is deposited within the mold and a brush or roller is employed to unfold it around all surface. it's vital to not add an excessive amount of organic compound, which can cause too thick of a layer, nor to feature but the required quantity, which can cause holes within the surface of the half once it's cured. Associate in Nursing estimate of the number of organic compounds required will be supported weight of glass fiber artefact. One will assume fifty-unit resin/50% unit fibre.
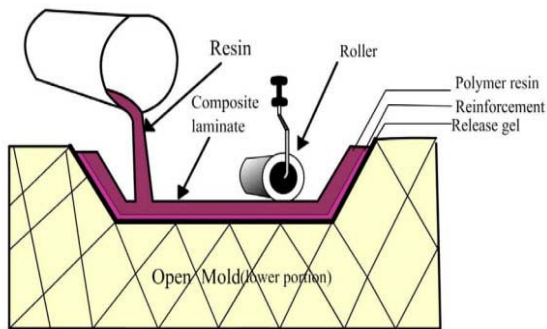
Figure 5: Hand lay-up method

Figure 6: Glass fiber-basalt and glass fiber-jute

V. Testing Methods

a) Hardness Test

The hardness test was performed with the aid of Brinell hardness tester. The specimen was indented for 10 seconds (dwell time), after which corresponding Brinell hardness numbers were calculated by using formula.

$$BHN = 2F/(\pi D(D - (D - d)^{\frac{1}{2}})$$

Where
F= Force in Kgf
D= Diameter of the indenter ball
d= Diameter of the indentation

Figure 7: Hardness test in Existing brake pad

Figure 8: Hardness test in composite material

Temperature Test

Temperature take a look at is employed to gauge the behaviour of the merchandise once exposed to varied temperature extremes. so as to accelerate the amendment in physical properties of a cloth or product, constant elevated temperature is employed.

Figure 9: Specimen prepared for temperature test
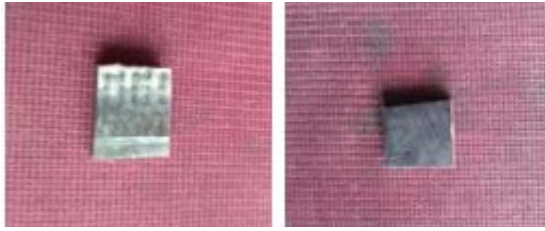
Figure 10: Specimen after temperature test

VI. Results

Table 1: Surface wear test

Material/ composition	W0 (g)	W1 (g)	Time min	Wear Rate (g/m)
Sample 1	6.12	6.02	20	0.005
Sample 2	5.192	5.150	20	0.0021
Sample 3	5.377	5.308	20	0.00345

Table 2: Water Absorption test

Material/ composition	Weight before immersion W0 (g)	Weight after immersion W1 (g)	Absorption %
Sample 1	33.7	41.52	23.2
Sample 2	30	34.23	14.1
Sample 3	32.4	38.64	19.2

Table 3: Temperature Test

Material/ composition	Temperature 1(^{0}c)	Temperature 2(^{0}c)	Temperature 3 (^{0}c)
Sample 1	150(colour changed)	200 (Edge burned)	320(fully burned)
Sample 2	150(No change)	200 (colour changed)	320 (Edge burned)
Sample 3	150(Edge colour changed)	200 (Colour turned into dark)	320 (Fully burned)

Table 4: Hardness Test

Material/ composition	Hardness number BHN	Hardness value MPa
Sample 1	4.83	13.6
Sample 2	14.43	47
Sample 3	8.12	27.2

Table 5: Tensile Test

Material/ composition	Tensile stress at break (N/mm2)
Sample 1	135.23
Sample 2	250.58
Sample 3	173.76

Table 6: Compressive Test

Material/ composition	Compressive stress (N/mm2)
Sample 1	135.23
Sample 2	250.58
Sample 3	173.76

VII. Conclusion

Fibers were used as filing material to provide composite brake pad. The new factory-made automobile brake pad was tested by decisive its mechanical and tribological properties. supported properties like temperature take a look at, hardness, lastingness, and compressive strength, wear strength the final result that get from the Glass and volcanic rock fibre based mostly restraint compared favourably with the prevailing one with amphibole material.

Specimen labeled specific gave superior performance over others. Temperature check, hardness, durability, and compressive strength, wear strength of the foremost effective composite specimen, are, severally. From investigation, the results of this work indicated that fibres that is Glass and volcanic rock fibres may be effectively used as a replacement for amphibole in friction lining/ brake pad materials. in contrast to amphibole primarily based brake pad and existing brake pad, the composite brake pad developed during this work is eco-friendly with none famed health implication. it's conjointly increase the lifetime of the brake pad. And conjointly can offer additional potency compared to existing brake pad, offer additional brake power.

References Références Referencias

1. Anon (2004). Automotive Brake Repairs Trends and Safety Issues.
2. Aigbodion, V. S., Akadike, U., Hassan, S. B., Asuke, F., Agunsoye, J. O. (2010).Development of Asbestos – free Brake Pad Using Bagasse. Tribology in industry, 32 (1), 45–50.

38

3. Bono, S. G., Dekyrger, W. J. (1990). Auto Technology, Theory and Service (2nd Ed.).DELMAR Publishers, New York, 45–48.
4. Aigbodion, V. S., Agunsoye, J. O. (2010). Bagasse (Sugarcane waste): Non-Asbestos Free Brake Pad Materials. LAP Lambert Academic Publishing, Germany, ISBN 978-3-8433-8194-9.
5. Dagwa, I. M., Ibhadode, A. O. A. (2006). Determination of Optimum Manufacturing Conditions for Asbestos-free Brake Pad Using Taguchi Method. Nigerian Journal of Engineering Research and Development. Basade Publishing Press Ondo, Nigeria, 5(4), pp. 1–8.
6. Sivarao, M., Amarnath, M. S., Rizal, A. K. (2009). an investigation toward development of economical brake lining wear alert system, IJENS, Vol: 9, No. 9, pp. 251-256.
7. Deepika, K., Bhaskar, Reddy C., Ramana, Reddy D. (2013). Fabrication and Performance Evaluation of a Composite Material for Wear Resistance Application. International Journal of Engineering Science and Innovative Technology (IJESIT) Volume 2, Issue 6, pp. 1-6.

This page is intentionally left blank

Logical Design Method and its Application in the Design of a Compressed Air Engine

By Ngang Tangie FRU, Na Esibe Clifford Nengang & Divine Kuhlon

Catholic University of Cameroon

Abstract- The logical design method developed in this paper stems from the first two phases and part of the third phase of the mechanical engineering design process. This research work had as research goal; developing a method that will facilitate the commencing of any design project in mechanical engineering. The approach used here is proven to be sustainable as it builds up constructively the design in question using theoretical tools and some demonstrative/figurative techniques that gradually highlight just the essential components necessary to the design in question. The first phase of the method is a mere identification of the problem which should be seen in the introductory chapter as the problem statement then elaborated in the literature review before being summarized under the subtitle of the identification of the need/problem in the body of the designing project proper.

Keywords: functional analysis, mechanical, logical design, compressed air, conceptual sketches, powered and lubricated.

GJRE-A Classification: FOR Code: 091399

LOGICALDESIGNMETHODANDITSAPPLICATIONINTHEDESIGNOFACOMPRESSEDAIRENGINE

Strictly as per the compliance and regulations of:

Logical Design Method and its Application in the Design of a Compressed Air Engine

Ngang Tangie FRU [α], Na Esibe Clifford Nengang [σ] & Divine Kuhlon [ρ]

Abstract- The logical design method developed in this paper stems from the first two phases and part of the third phase of the mechanical engineering design process. This research work had as research goal; developing a method that will facilitate the commencing of any design project in mechanical engineering. The approach used here is proven to be sustainable as it builds up constructively the design in question using theoretical tools and some demonstrative/figurative techniques that gradually highlight just the essential components necessary to the design in question. The first phase of the method is a mere identification of the problem which should be seen in the introductory chapter as the problem statement then elaborated in the literature review before being summarized under the subtitle of the identification of the need/problem in the body of the designing project proper. Though the lengthy introduction and literature review for the case study was not put on this paper, the summary of the identification of the need is what we see and the impact of that exercise to the steps that follow is eminent in the end results. The second phase; the definition of the problem, is studied in details on this paper with some tools applied for a better interpretation of the results. In the third phase, the synthesis; just the functional analysis, automation of the functioning of the design and conceptual sketches are elaborated in the application demonstration. The end result of the use of this method is the logical design of a compressed air engine. This clearly unveils the design of an engine that is powered and lubricated solely by compressed air.

Keywords: *functional analysis, mechanical, logical design, compressed air, conceptual sketches, powered and lubricated.*

I. Introduction

Many engineering creations happen to be results of accidental findings which put to question the very essence of the engineering activities which is obviously to create something useful. Working on the bases of the generalized mechanical design engineering process(Kovacevic), this research work has been able to put together a systemic method that will permit any engineer with a right sense of duty to develop a "Logical" design of whatever item he or she plans to create. This research work equally demonstrates the success of this approach as it presents how this unique method was used to realize a logical design of an engine powered and lubricated solely with compressed air. The paragraphs that follow consist of first the general method then the application example before the conclusion.

II. Method of Logical Design

Like every engineering project, activities start with the presentation of a problem or need. This method gives an approach on how this need can be fully developed to give solutions that are concrete and sustainable; through creating logical designs. This method is developed into three phases as can be seen below.

a) Identification of need (problem)

As this may sound, this phase involves the identification of the need of the design in question. Work for this phase normally starts in the introduction; as the problem statement is expressed; it then continuous in the literature review where the recent developments and limitations of such an undertaking are conveyed. Then all these are formally represented in a figurative identification of the need using a "Bull with Horn" representation (Granger).

b) Definition of problem

At this phase of the design process, the expected service functions of the solution to the above need will be spelt out under the identification of the service functions. This should be figuratively displayed using an "Octopus diagram"(AUDRY and TAILLARD). Closely followed should be a characterisation of these service functions and then establishment of a hierarchy of the service functions which is visualized on a "Bar chart". Until this level, the designing process should be done following strictly the simplest possible language as is recommended by the "Occam's Razor Principle" (Craig). It should be noted that even at this level of the work there might be some unidentified needs that might call for further modifications to be done in the first phase.

c) Synthesis

This phase initiates the detailing of the complexity of the design as is recommended by the Occam's Razor Principle (Craig). Here is studied the synthesis of the scheme, that is, connecting possible elements deemed essential to the design. This phase starts with a functional analysis systems technique (FAST)(Kaufman); which details the designer(s) choice,

Author α σ ρ: School of Engineering, Catholic University of Cameroon (CATUC) P.O. Box 782Bamenda, Cameroon.
e-mail: tf.ngang@catuc.org

41

or set of choices on how the major service functions will be executed, and this is displayed on a FAST diagram. This should be done bearing in mind the "Simplicity versus Complexity" and the "Independent functions" Principles of mechanical design (Craig). The interaction between the different elements identified in the lowest order function of the FAST diagram should be automated using the "GRAFCET" technique and then displayed using a "GRAFCET diagram". With the principle of functioning of the engine achieved, sketches of possible elements should be realised and this should be based on the designer(s) creative thoughts alongside some design principles like; "Saint-Venant's" principle, "Symmetry" Principle, "Triangulate for Stiffness" Principle, "Maxwell and Reciprocity" principle, "Stability" principle, "Avoid Bending Stresses" Principle, "Manage Friction" Principle, and "Self Principles"(Craig). The initial dimensions of these sketches should respect the Golden Rectangle Rule of (1.618:1). A sketched assembly should then be established permitting a visualization of the interaction of the various elements. This stage marks the end of the logical designing process.

III. Case Study of Compressed Air Engine

a) Identification of need

i. Raison-d'etre of the research work (design)

- A long lasting solution to the climate change, and other consequences of the excessive pollution of human activities of nowadays.

- A long lasting solution to the air pollution of the cities as a result of the ever increasing use of non-economic and highly polluting means of transport.
- A solution to global warming, particularly the cities.
- A solution to the non-economic use of the ever reducing stock of fossil fuels.
- The need for a more efficient engine for the cities.
- Need to design an efficient compressed air engine that is fully characterised and has clear power enhancement parameters.

ii. Design Purposes

- Zero CO_2 polluting engine.
- Zero Heart polluting engine.
- Engine powered and Lubricated solely by compressed air.
- Engine operating with almost no sound, very silent.
- Engine with very high mechanical efficiency.
- Engine with low parts count.

iii. Expression of Need

The expression of the need of this design is summarized in the "Bull with Horns" below.

Vehicles of the Urban transport sector   Compressed air
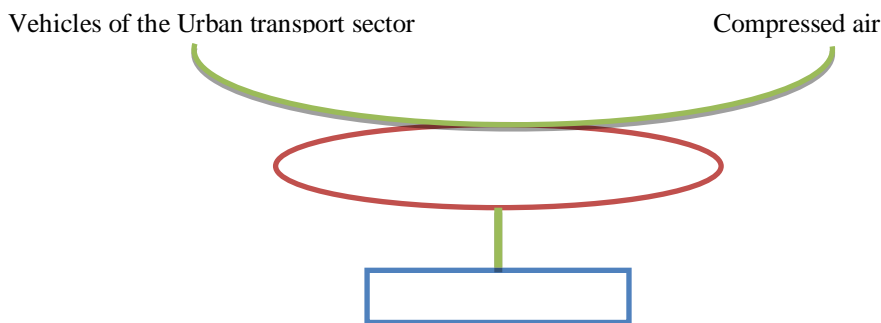
Fig. 1: Expression of the Design Need

b) Definition of problem

Under the definition of the problem, the need was further detailed out into some elementary service functions that contribute in one way or several ways to the accomplishment of the design purposes. Here the service functions were identified, characterised and then hierarchized.

i. Identification of the Service Functions

The identification of the service functions was facilitated by the construction of an octopus diagram. Here, the engine was placed in its environment of

functioning and all the players that are expected to have a principal or constraint influence to its functioning, related to it with respect to their functional contributions.
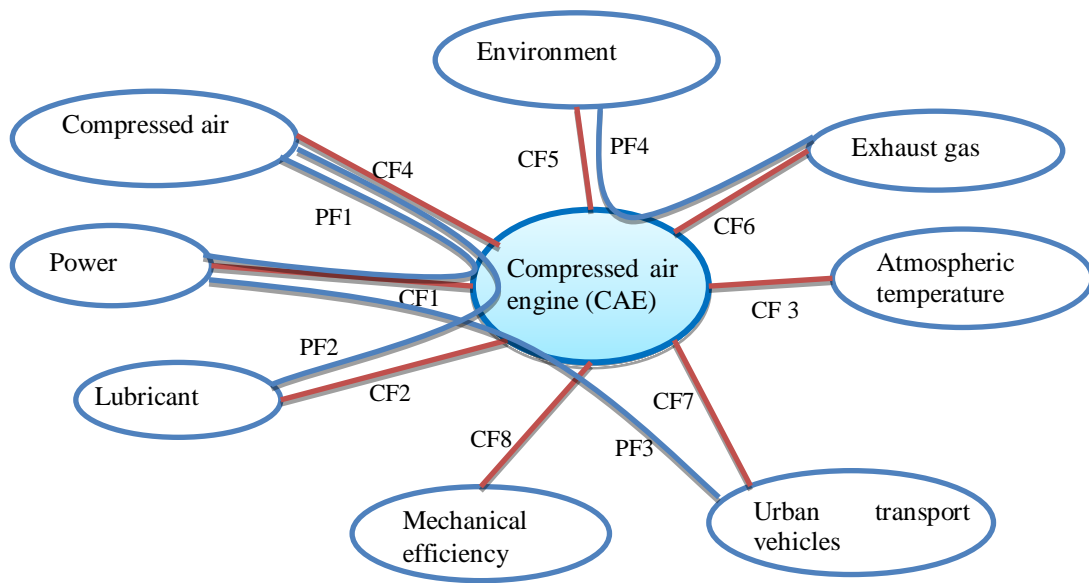
Fig. 2: Octopus diagram

Constraint functions (CF)

CF1: Need power to energize its moving parts
CF2: Use lubricant for low friction movement of parts
CF3: Operate at constant atmospheric temperature to guarantee isothermal expansion
CF4: Operate 100% with compressed air
CF5: Use environment as an energy sink for the Third Law of Thermodynamics
CF6: Exhaust gas is air at atmospheric temperature and pressure
CF7: Fit comfortably in urban transport vehicles
CF8: Operate at very high mechanical efficiency.

Principal functions (PF)

PF1: Potential energy stored in compressed air to be transformed to power, to run engine

PF2: Part of partially expanded compressed air to be used as lubricant
PF3: Power to be sufficient to run urban transport vehicles
PF4: Exhaust gas completely emitted to the environment.

ii. *Characterization of the Service Functions*

The characterization of the service functions was done according to the proportion of the injected air that is needed for a proper realization of each service function and the influence on a scale of 100%, of a service function on the overall design of the engine.

Table 1: Characterization of service functions

Service function	Injected air %	Influence %	Product
CF1	100	90	9000
CF2	10	40	400
CF3	100	10	1000
CF4	100	100	10000
CF5	100	100	10000
CF6	100	60	6000
CF7	100	20	2000
CF8	10	80	800
PF1	100	90	9000
PF2	10	90	900
PF3	100	50	5000
PF4	100	60	6000

These characteristics were then used to deduce the relative influence of the service functions at the level of hierarchi zing the service functions.

iii. *Hierarchi zing the Service Functions*

For a better appreciation of the service functions, the figures from the characterization of the service functions above was used with their product values rounded up to the closest 500s.

Table 2: Inter-service function appreciation masses

	CF2	CF3	CF4	CF5	CF6	CF7	CF8	PF1	PF2	PF3	PF4	Mass	%
CF 1	CF1/36	CF1/18	CF4/2.5	CF5/2.5	CF1/3	CF1/9	CF1/18	CF1/2	CF1/18	CF1/3.5	CF1/3	110.5	15.4
	CF2	CF3/4	CF4/40	CF5/40	CF6/24	CF7/8	CF8/4	PF1/36	PF2/4	PF3/20	PF4/24	0	0
		CF3	CF4/20	CF5/20	CF6/12	CF7/4	CF3/2	PF1/18	CF3/2	PF3/10	PF4/12	8	1.1
			CF4	CF4/2	CF4/3.5	CF4/10	CF4/20	CF4/2.5	CF4/20	CF4/4	CF4/3.5	128	17.9
				CF5	CF5/3.5	CF5/10	CF5/20	CF5/2.5	CF5/20	CF5/4	CF5/3.5	128	17.9
					CF6	CF6/6	CF6/12	PFI/3	CF6/12	CF6/2.5	CF6/2	70.5	9.8
						CF7	CF7/4	PF1/9	CF7/4	PF3/5	PF4/6	20	2.8
							CF8	PF1/18	CF3/2	PF3/10	PF4/12	8	1.1
								PF1	PF1/18	PF1/3.5	PF1/3	110.5	15.4
									PF2	PF3/10	PF4/12	8	1.1
										PF3	PF4/2.5	55	7.7
											PF4	70.5	9.8
											total	717	100

Table 3: Pareto table of the service functions

Nº	Functions	% of mass	Cumulated %
1	CF4	17.9	17.9
2	CF5	17.9	35.8
3	CF1	15.4	51.2
4	PF1	15.4	66.6
5	CF6	9.8	76.4
6	PF4	9.8	86.2
7	PF3	7.7	93.9
8	CF7	2.8	96.7
9	CF3	1.1	97.8
10	CF8	1.1	98.9
11	PF2	1.1	100
12	CF2	0	100

A histogram representation of this hierarchy was the drawn as is below.
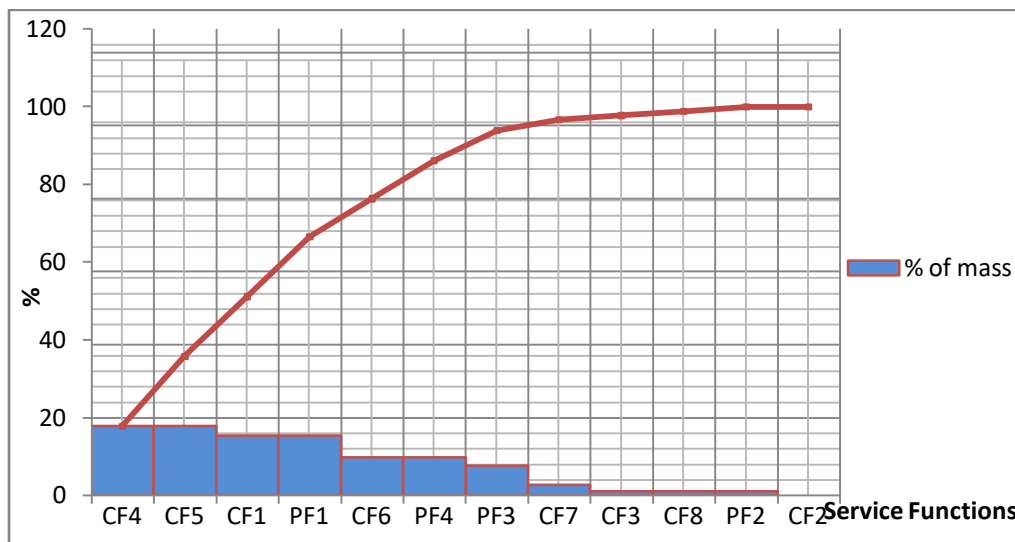
Fig. 3: Pareto display of the hierarchy

This Pareto display of the service functions was seen to highlight six service functions with over 80% of the design satisfactions, these included;

- CF4: Operate 100% with compressed air
- CF5: Use environment as an energy sink for the Third Law of Thermodynamics
- CF1:Need power to energize its moving parts
- PF1:Potential energy stored in compressed air to be transformed to power, to run engine
- CF6:Exhaust gas is air at atmospheric temperature and pressure
- PF4:Exhaust gas completely emitted to the environment
- The conclusion drawn from this was that these service functions have to be of utmost importance in the design process.

c) Design synthesis

The design synthesis phase included FAST, GRAFCET and then a figurative conception study.

i. *Functional analysis structure technique (FAST)*

Using the FAST method (Kaufman), a more complex functional analysis of a design model of the compressed air engine was done, as was recommended in the Occam's Razor Principle(Craig). A portray of the set of technical design choices for the accomplishment of the different principal service function was vividly represented on a FAST display, this was in accordance to the "Simplicity versus Complexity" principle.

The FAST display was seen as a logical representation of the way the designer chose to accomplish a compressed air engine with the ability to satisfy appropriately the different service functions.

The highest order function of the FAST display was "Power Urban Vehicle", and the next highest order function depended on the different service functions, starting with the principal ones. The lowest order functions were simplified representations of how much the design wished to render the design complex. It was done in accordance to the "independent function" principle.

From the FAST display, was extracted the following key components that play a major role in the functioning of the compressed air engine;

1. A reusable insulated compressed air storage cylinder (SC).
2. A multivariable transmitter for measurement (MT).
3. Throttle like valve (TV).
4. High pressure good heat conduction metallic pipe network (MP).
5. Adjustable metallic slot timer (ST) with inject slot (IS) and exhaust slot (ES).
6. Quasi fixed volume reception chamber (RC), equally called the pre expansion chamber; enclosed by the slot timer and a lid.
7. Enclosed poor heat conduction stator or casing, hexagonal cross section.
8. Poor conduction inlet manifold (IM) separate routes, some leading to EC (Primary Passages (PP)), while others the inner surface of the rotor (Secondary Passages (SP)).
9. Light metallic wings.
10. Dense metallic fixed axial rotor assembly.
11. The wings together with the inner walls of the stator and outer walls of the rotor enclose the expansion chamber (EC).
12. Exhaust manifold and stator lid (EM).
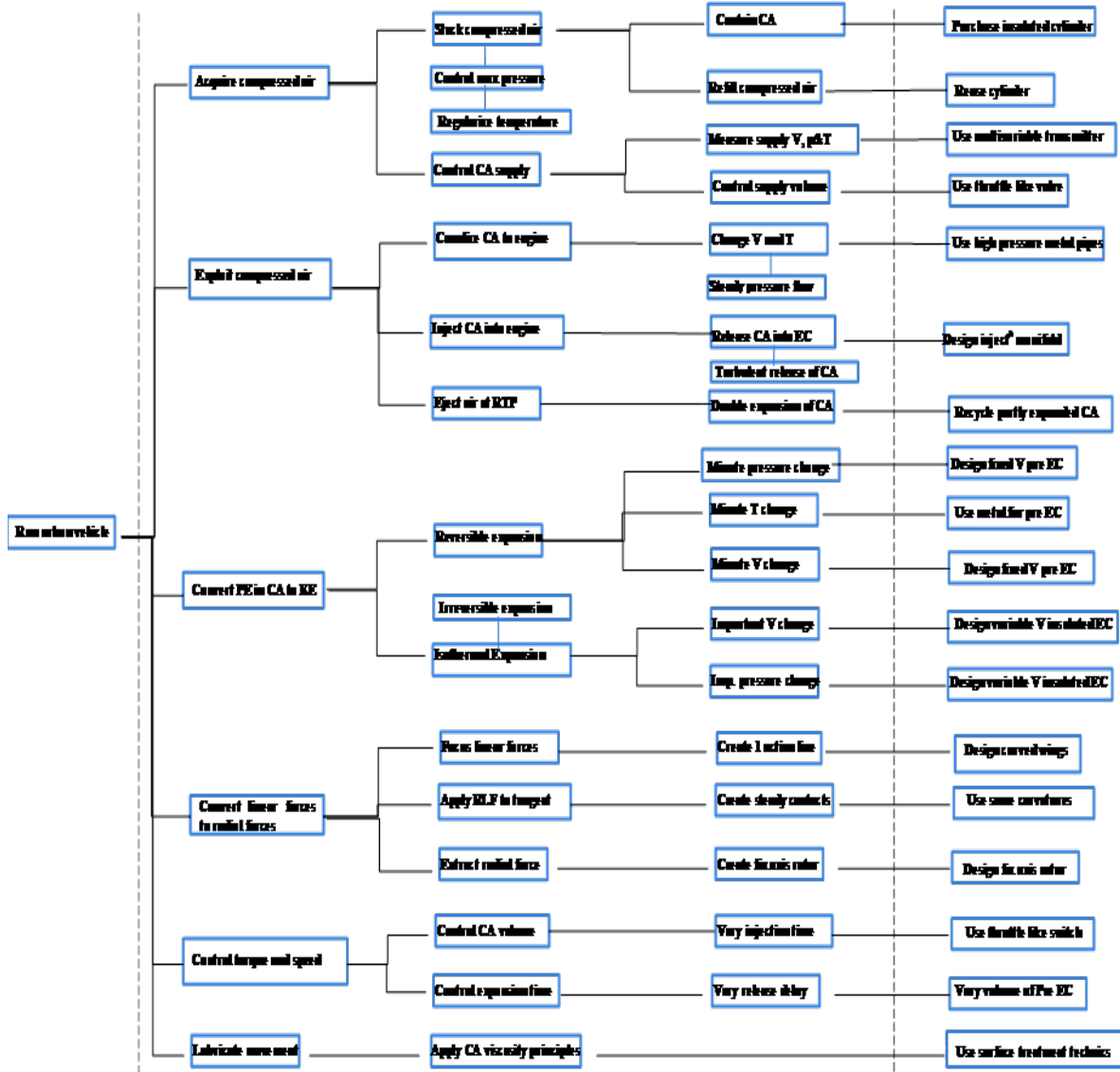
Fig. 4:   FAST Diagram of compressed air engine

ii. *Automation of compressed air engine operation*

| 01 | START | Open stop cup |

— enough CA in SC

| 02 | Throttle in CA | Use TV |

— appropriate quantity/speed desired

| 03 | Canalize CA to engine |

— arrival at RC

| 04 | Receive CA into RC | Change V&T reversibly |

— exposure of IS

| 11 | Adjust slot timer |

| 05 | Inject CA into PP available |

| 071 | Push wing open |

— passage into closed EC available

— Poor MT readings   Good MT readings

| 06 | Receive CA into closed EC |

| 072 | Move cylinder eccentrically |

— start expansion of CA

| 073 | Rotate wheels / Revolve wheels / Rotate rotor core |

| 07 | Displace wing of the EC | Rotate rotor |

— exposure of ES

| 08 | Displace wing | Rotate rotor |

| 081 | Exit air through ES |

— complete closure of EC

| 082 | Move cylinder eccentrically |

| 09 | Exhaust gas at RTP |

| 083 | Reinsert air into cylinder / Lubricate rotor components / Reinforce wheel revolution / Close wing EC |

— enough CA in SC   — not enough CA in SC

— engine stopped

| 10 | Close valve |

Fig. 5: GRAFCET diagram of compressed air engine

Bearing in mind the "independent function", "self", "Maxwell and Reciprocity" and "symmetry" principles of mechanical design; a model of automated process of the operation of this engine was derived using the GRAFCET technique.

Given this engine design was expected to operate mechanically and parts count reduced to a minimum, all the sensors were eliminated. The operation was expected to be continuous with momentary interventions done only by the operator.

The operation process of this engine was taken to be initiated with the opening of the stop-cup which was then followed by an iterative process of running and adjustment of the engine with operator intervention or not for an economic operation of the engine.

iii. *Structural conceptual sketches of the compressed air engine*

With a close appreciation of mechanical design principles like; ; "Saint-Venant's" principle, "Symmetry" Principle, "Triangulate for Stiffness" Principle, "Maxwell and Reciprocity" principle, "Stability" principle, "Avoid Bending Stresses" Principle, "Manage Friction" Principle, and "Self Principles"(Craig), an understanding of the functioning and automation of the engine, the next step involved conceptual structural sketches of the main component parts of the engine and their assembly.

iv. *Structural conceptual sketches of the component parts*

The Golden Rectangle Rule (1.618:1) ,discovered by Pythagoras was used in the realisation of sketch concepts so that they had greater chances of being realizable and with this understanding and the principles of symmetry, the design process of the component parts of the engine started from the outside working inwards. This made the stator of the engine the first component part sketched.

d) Engine stator

The stator constituted the foundation/framework of the compressed air engine, and from Occam Razor, this part being the first to be sketch was simply designed. As this part equally was the framework of the engine and from the self-principle which reinforces the use of the triangulate for stiffness principles, to render the engine ridged to withstand the reciprocating bombardment it has to support were applied to give a rigid framework for the engine. These principles alongside the Golden Triangle Rule and the principle of symmetry yielded the essential sketch of the stator.

e) Adjustable metallic slot timer

Made out of a good conductor material, the slot timer was designed to act as the 'camshaft' of this engine. It was made to initiate the injection and exhaust processes by conducting the compressed air in and out of the available expansion chamber. This part due to the goal of low parts count was designed compact. The designing of this part equally took into consideration the self-principle, the simplicity versus complexity principle and the St. Venant principle. The resulting adjustable slot timer was a conic structure that is assembled directly on the rotor arm by fixing and it had to fit perfectly in the inlet manifold such that it seals the slots exposing only one at a time to the reception chamber while connecting the inlet slot and exhaust slots of another.

f) Rotor arm

The rotor arm was a compact piece designed to fully execute the transmission task of converting momentary lateral translations into smooth uniaxial rotation. The rotor arm was seen to be unique in its design and was one of the pieces that defined the uniqueness of this engine. When assembled with the rotor wheels, an almost friction free rotor was expected produced.

g) Inlet manifold

The inlet manifold was a compact piece of work though stagnant it was seen to operate smoothly the transition from the inlet to the exhaust. Its compact nature assured a zero energy loss at for that operation and also reduced the part count not forgetting the limitation of moving parts thus it increased the sustainability of the engine.
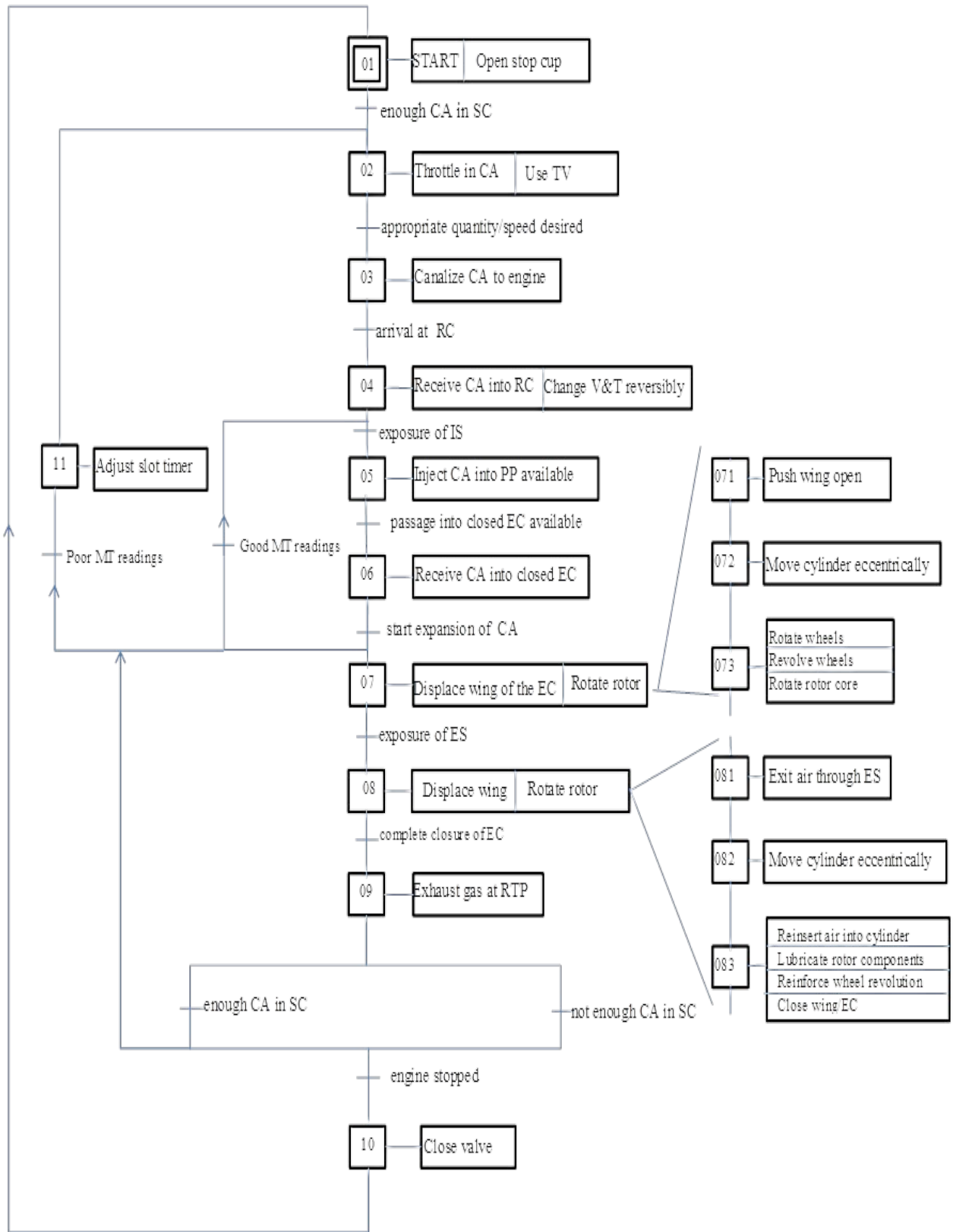
h) Exhaust manifold

The exhaust manifold was a simple piece design for two main purposes; seal the different chambers and assure a complete exhaust of the decompressed air.

i) Wings

The triangulate for stiffness principle, self-principle and the principle of symmetry result to concept that whenever a design consists of triangulated forces that are symmetrical with clearly identified lines of action, the stiffer and more sustainable it becomes. The wings were designed such that their contact with the rotor was a single line or a point when viewed as a cross section. This reduced loses due to friction and it also directed the radial forces to the centre of rotation and so assuring a self-annulment of the radial forces thus a better equilibrium of the engine in functioning contributing to the sustainability of the engine.

The design of the other parts of this engine were meant to assure the proper functioning of the above six principal parts. It should be noted that the dimensions of these parts were just tentative for these sketches were conceived solely on the bases of the functional understanding of the engine. These shapes were equally meant to assist in the mathematical conception as they were destined to be used to choose the coordinates best appropriate.

j) Structural conceptual sketch of the assembly

This assembly was established following strictly the concept represented on the GRAFCET diagram on how the engine was going to operate. The assembly was restricted only to the engine as the study had as interest to create first an ideal engine before the other elements could be added.

SECTION B-B
SCALE 1 : 3

SECTION A-A
SCALE 1 : 3
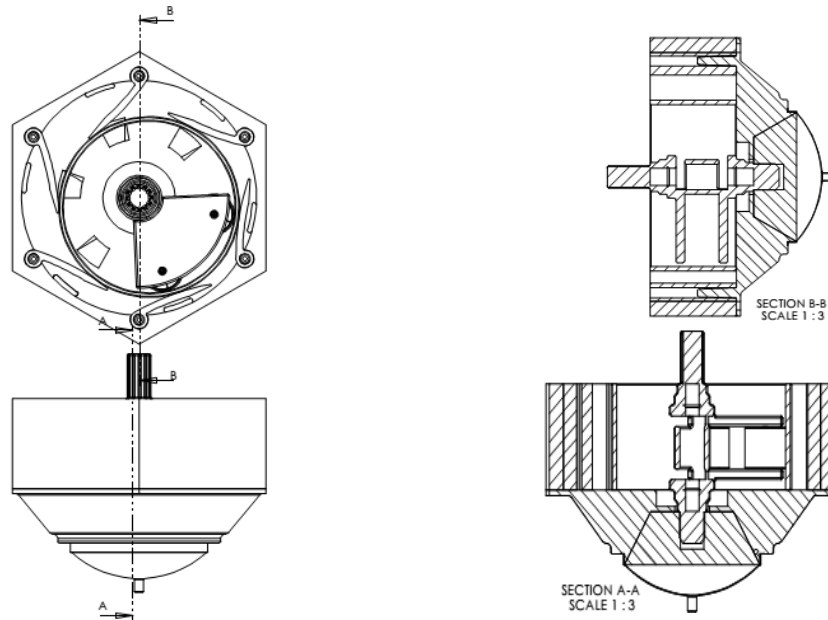
Fig. 6: Assembly sketch

IV. Conclusion

With the logical design of the engine set, the next step could be the kinematics studies closely followed by dynamic studies to complete the conceptual design of the compressed air engine in question. This method of realising logical design made sure none of the systems functions were left out and the end result was proven to be satisfactory.

Works Cited

1. AUDRY, F. and P. TAILLARD. La demarche d'analyse fonctionnelle. Versailles: academie Versailles, 2010.
2. Craig, K. "Fundamental Principles of Mechanical Designs." Mechanical Design Fundamentals. 2011.
3. Fru, Ngang Tangie. Design and Simulation of a compressed air Engine. Bambili, N.W, Cameroon: University of Bamenda, 2015.
4. Granger, Laurent. "Definir les Besoins avec L'Outil "Bete A Cornes" En Gestion de Project." 2019.
5. Kaufman, J. Jerry. Function Analysis Systems Technique – The Basics. Save international conference, 1997.
6. Kovacevic, Prof Ahmed. "Principles of Mechanical Design." School of Engineering and Mathematical Sciences. UK: Engineering Design Council, UK, 2009.
7. Psanis, Christodoulos. Modelling and Experimentation on Air Hybrid Engine Concepts for Automotive Applications. West London, United Kingdom: Brunel University, 2007.
8. Vinogradov, Oleg. Fundamentals of Kinematics and Dynamics of Machines and Mechanisms. Boca Raton, Florida: CRC Press LLC, 2000 N.W. Corporate Blvd, 2000.

This page is intentionally left blank

Refractory grade Bauxite: An Overview about the Effects of Different Bauxite Sources and Forming Processes on the Quality of the Material

By Vitor Guilherme de Oliveira, Luís Leonardo Horne Curimbaba Ferreira, Marcos Antônio dos Reis, Peter Miura Nakachima & André Luis Pereira

Abstract- Refractories have been very important for humankind development enabling the manufacturing of a wide range of materials. Primary industries demanding refractories include the manufacturing of steel, non-ferrous metals, glass, lime, cement, ceramics, petrochemicals and incineration. Refractory grade bauxites (RGBs) are high-alumina materials used as aggregates in shaped and unshaped refractory linings suitable to withstand high temperature heating and a corrosive environment. Despite the wide availability of bauxite ores in the world, few countries can supply a bauxite with refractory grades. Guyana, China and Brazil have emerged as suppliers for the refractory industry and the peculiarities of each bauxite from these countries impact directly on the refractory performance.

Keywords: refractory grade bauxite (RGB), high-alumina refractory, forming process.

GJRE-A Classification: FOR Code: 091399

Strictly as per the compliance and regulations of:

Refractory grade Bauxite: An Overview about the Effects of Different Bauxite Sources and Forming Processes on the Quality of the Material

Vitor Guilherme de Oliveira ᵃ, Luís Leonardo Horne Curimbaba Ferreira ᵟ, Marcos Antônio dos Reis ᵖ, Peter Miura Nakachima ⁿ & André Luis Pereira¥

Abstract- Refractories have been very important for humankind development enabling the manufacturing of a wide range of materials. Primary industries demanding refractories include the manufacturing of steel, non-ferrous metals, glass, lime, cement, ceramics, petrochemicals and incineration. Refractory grade bauxites (RGBs) are high-alumina materials used as aggregates in shaped and unshaped refractory linings suitable to withstand high temperature heating and a corrosive environment. Despite the wide availability of bauxite ores in the world, few countries can supply a bauxite with refractory grades. Guyana, China and Brazil have emerged as suppliers for the refractory industry and the peculiarities of each bauxite from these countries impact directly on the refractory performance. This work aims to study different sources of RGB and how the manufacturing process can impact the refractory properties. The Guyanese RGB presented the highest alumina content (~90% Al_2O_3). However, a Brazilian RGB with lower alumina content (~85% Al_2O_3) presented the highest hot modulus of rupture value (HMoR at 1200°C/5h = 5.12 MPa). As for the Chinese RGBs, these presented a higher heterogeneity, evidenced in variation on chemical composition resulting in worse thermo mechanical performance (HMoR< 4.10 MPa). Two different forming process for Brazilian RGBs showed that the briquetting operation produces angular-shaped grains (sphericity = 0.7), whereas the extrusion mechanism produces rounded grains (sphericity = 0.9) which induce better flowability in castables.

Keywords: refractory grade bauxite (RGB), high-alumina refractory, forming process.

I. Introduction

Ceramic industry is an important global segment of the economy with several applications. There are different properties in ceramic materials that characterize their use and one of them is the refractoriness. A refractory material has the property of resisting the heat, the mechanical stress and/or chemical attacks, it means, not abrupt changes in its chemical and physical properties in a wide temperature range and hostile environments, being a great raw material for applications in heat-processing industries as glass and metal industries [1].

The correct way of classifying a refractory must consider the sum of different factors. Regarding chemical composition, there are several names found in the refractory market: siliceous; silica-alumina; high-alumina; magnesian; chromitic-magnesian; chromic; graphite; zirconia-magnesia; and silicon carbide refractories; among several others. Formerly, the refractories are classified in acidic, basic, neutral or special by their chemical content and suitable environment of application, however it is not so useful nowadays due to the raw material combination in the refractory formulation. As for the shape, the refractory can be divided into shaped (bricks and cast shapes) and unshaped (monolithics), and it can still be classified as porous or dense according to the porosity level [2].

During the formulation of a refractory, close attention must be given to the selection of the refractory aggregate and the bonding system. Thus, refractories used in an iron-making process will differ from that of a steel-making process, since the nature of the metal and slag is different in these cases. In iron making, the metal and liquid slag are primarily neutral or slightly acidic in nature, whereas the slag is distinctively basic in the steel-making process. In summary, refractories chosen for iron making are based on alumina and silica, whereas magnesia-based refractories are the choice for steel making, because of their acidity and basicity, respectively [3][4].

Generally, the high-alumina refractories are marketed in terms of alumina content in intervals of 10%, ranging from 50% to higher than 90% [5]. According to the alumina content, Table 1 shows the possible raw materials and final predominant mineralogy of the refractory.

Author ᵃ ᵟ ᵖ ⁿ ¥: Mineração Curimbaba Ltda. Rodovia Poços de Caldas / Caldas, km 10, Poços de Caldas – MG, Brazil.
e-mail: vitor.oliveira@curimbaba.com.br
Author α: Universidade Federal de Alfenas – UNIFAL Rodovia José Aurélio Vilela, 11.999, Poços de Caldas - MG, Brazil
Author σ ⁿ ¥: Elfusa Geral de Eletrofusão Ltda. Rua Júlio Michelazzo, 501, São João da Boa Vista – SP, Brazil.
e-mail: andre.pereira@curimbaba.com.br

Table 1: Different classes of high-alumina refractories (Adapted from [4]).

Alumina content	Raw material	Mineralogy predominant of refractory
50%	Fireclay	Mullite, glass/free silica
50%-60%	Alumina minerals & fireclay; bauxite and clay	Mullite, glass and free silica
70%	Bauxitic clay; calcined bauxite and clay	Mullite, corundum and glass
80%-85%	Calcined bauxite	Corundum, mullite and glass.
Above 90%	Tabular or fused alumina aggregates	Corundum, mullite and glass.

For this class of refractories, the alumina-silica phase equilibrium diagram, shown in Figure 1, can explain much of the mineralogy of the final product after sintering [4]. However, some impurities such as iron oxide, titanium oxide and alkalis react in high temperatures and can form other phases not shown in this diagram, as tialite, rutile and hematite. These impurities come from the raw materials used to make the refractory and it is in accordance with the mineralogy of the resources [5].
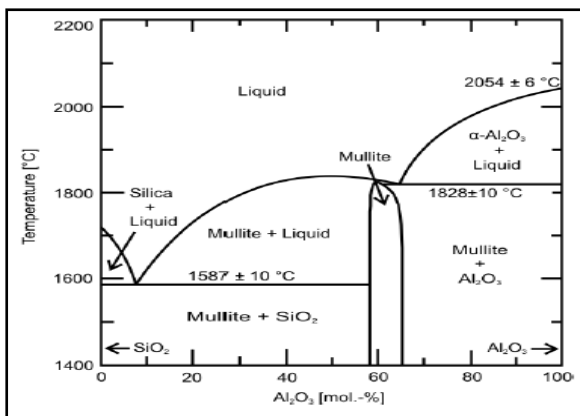
Figure 1: Silica-alumina phase-diagram.

As a note on phase equilibria diagram, refractories are usually not at thermo chemical equilibrium and the commercial refractories present some impurities. This means non-equilibrium phases may be present. An example might be a fireclay brick containing calcined bauxite aggregate (added for composition adjustment) with an overall composition of 50% Al_2O_3. This fired brick will contain corundum even though the phase diagram says it should not be present [4].

Globally, above 85% of the processed bauxite is destined to alumina production through Bayer Process and 94% of all this alumina is processed by Hall-Héroult process, to turn alumina to metal aluminum [2][6][7]. The remaining bauxite, or non-metallurgical bauxite, is destined for some other segments. Among them, it is inserted the refractory products, which iron and steelmakers consume more than 70% of the world production [6].

Guyana pioneered the manufacturing of RGB since 1940´s. China began supplying only in the 1970´s. Afterwards, Brazil started to produce some quantities [8]. According to the Ministry of Natural Resources of Guyana [6], 1.88 Mt of worldwide bauxite were directed to RGB production in 2015, being the main consumers China, Russia and India, existing only two significant worldwide suppliers: China and Guyana. According to the same source, Guyana was responsible for 6.6% of world´s RGB supply in 2015, while China takes the remainder. These numbers are close to the ones published by other sources, showing China currently with 95% of the world market share [9][10].

While bauxite ore from Brazil, Guyana and other areas with tropical climate tends to be gibbsitic ($Al(OH)_3$) whose aluminum hydroxide is trihydrate, Chinese one is mainly diasporic (α-AlO(OH)), a monohydrate [11]. In general, bauxite ores from these countries exhibit different mineralogy and physicochemical characteristics that promote different properties on the RGBs manufactured [12]. Traditionally, the mineralogy of RGB is composed by a combination among three or or more phases, hereinafter referred: corundum (1st phase), mullite (2nd phase), tialite, rutile and/or hematite. Table 2 shows some properties of each phase mentioned [13][14][15][16][17].

Table 2: Properties of RGB mineralogical phases

Phase	Corundum	Mullite	Tialite	Hematite	Rutile
Melting Temperature (°C)	2050	1828	1860	1595	1668
Density (g/cm³)	4.0	3.2	3.7	5.2	4.5

Thermal Conductivity (W/m.K)	33	3.9-6.3	1.5-2.5	7.85-9.03	7.4
Thermal Expansion (x 10^{-6} K^{-1})	4.6	α_a 3.1-4.1	α_a 11.8	11.8	8.5-9.5
		α_b 5.6-7.0	α_b 19.4		
		α_c 5.6-6.1	α_c (-2.6)		

Considering thermal process, the diaspore from raw bauxite is straightly converted to α-alumina during the firing, without metastable transition alumina [18], assuring the crystal growth and inhibiting the reaction with silica in the liquid phase to form mullite [12]. Furthermore, the higher grade of titanium oxide in Chinese bauxite favors the tialite formation (β-Al_2O_3.TiO_2) above 1350°C which can be an issue considering the mechanical strength due to its highly anisotropic thermal expansion (Table 2) and an eutectoid transformation during the cooling, decomposing it into its precursors, alumina and titania, in a wide range of intermediate temperature (750°C –1300°C) [14]. When gibbsite is the main mineral as per Brazilian and Guyanese bauxites, there are many phase transformations until corundum formation [18]. The slower grain growth facilitates the reaction between alumina and silica, increasing the mullite amount in the final product.

Recently, a Brazilian RGB produced with a gibbsitic bauxite was characterized and presented 19.4% (by weight) in mullite (acicular-shaped), while a Chinese RGB produced with a diasporic bauxite showed 15.4% in mullite (not acicular-shaped) and 4.4% in tialite (small crystallites). Bricks made with these RGBs using a conventional castable formulation showed the impact of those mineralogies in the thermo mechanical behavior, where the bricks made with Brazilian RGB withstood the hot load test (25 psi at 1600°C) and the bricks made with Chinese RGB failed under the same conditions [12].

Another work compared the difference between two processing ways of calcined bauxite: calcining from run of mine (ROM) bauxite, and calcining a bauxite after an ore processing, composed of size reduction, mixing and agglomeration. Processed bauxite showed the best results in the stress-strain test conducted under compression load in air. Moreover, the grains spatial distribution was remarkably more homogenous, demonstrating the importance of the processing in the final product properties and performance [19].

In a study which the aim was comparing four different forming processes (uniaxial pressing, extruding, lamination and slip casting) on sintered clay properties, the highest densification in the green body was obtained by pressing technique and it promoted larger quantity of mullite [20]. Japanese researchers studying forming processes of a porous ceramic (SiC) showed that compression molding (or uniaxial pressing) led to higher strength and homogeneity of the ceramic matrix, while extrusion led to lower strength and higher apparent porosity [21].

In an industrial scale, there are different technologies employed for the forming operations like briquetting or extrusion. Briquetting is a technique for agglomeration of fine particles under stresses like compression. The briquetting can be performed by a roller press (or briquette machine), in which a pressure is used to shape the material through its molds in the rolls surface. In this machine, the feedstock is forced to pass between two rolls that will produce the geometrical form of the material [22]. As for the industrial extruders, these can be manufactured with a single-screw, twin-screw or piston. The feed of this equipment needs to be done with a material having an optimum level of plasticity and flowability. The equipment, by screw rotation or piston pushing, will shape the product according its nozzle or die. Figure 2 shows a diagram for both equipment.
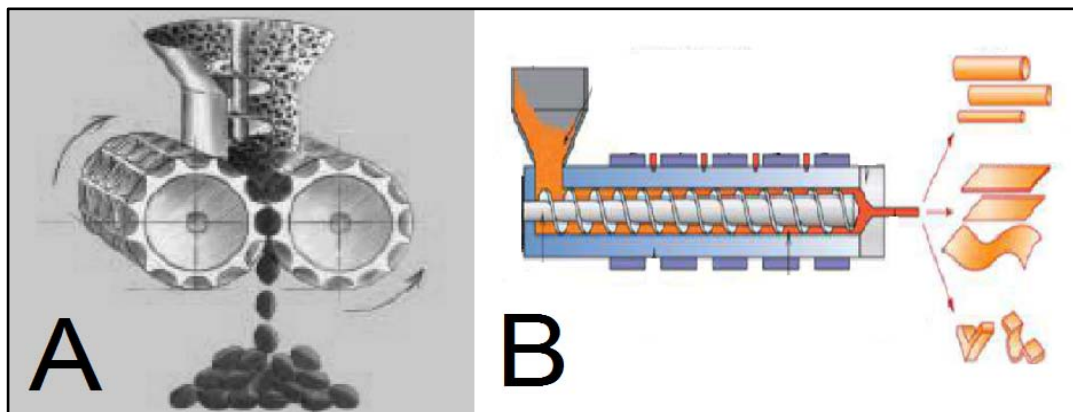
Figure 2: Diagram of forming machines: (A) briquette machine; (B) extruder (Adapted from [22] and [23]).

To improve the quality of briquettes, organic binders can be added to the raw materials before the forming process. Outstanding results were found by adding low percentages of corn starch or lignosulfonates into refractory grade bauxites, increasing the resistance of the green bodies formed [24].

In this work, the authors present a comparison between the technical properties of different refractory grade bauxites from China, Guyana and Brazil. For the case of Chinese RGBs, two classes were evaluated according to their alumina content (86% Al_2O_3 and 88%

Al_2O_3). For Brazilian RGBs, two forming process were taken into account (extrusion and briquetting).

II. Materials and Methods

Five samples of RGB in four size fractions as described in Table 3 were selected for this work: two Brazilian ones (MC A and MC B), one from Guyana (G) and two from China (CH86 and CH88). Figure 3 shows the samples and their size fractions.

Table 3: Description of the RGB fractions

Size Fractions	Description
-6.70|+2.36 mm	Particles predominantly smaller than 6.70 mm (opening diameter of a sieve = 0.265") and larger than 2.36 mm (8 mesh).
-2.36|+0.85 mm	Particles predominantly smaller than 2.36 mm (8 mesh) and larger than 0.85 mm (20 mesh).
-0.85 mm	Particles predominantly smaller than 0.85 mm (20 mesh).
-0.075 mm	Particles predominantly finer than 0.075 mm (200 mesh).

RGB	-6.70|+2.36 mm	-2.36|+0.85 mm	-0.85 mm	-0.075 mm
MC A (Brazilian)				
MC B (Brazilian)				
G (Guyanese)				
CH86 (Chinese)				
CH88 (Chinese)				

Figure 3: RGB samples and their size fractions

For Brazilian RGBs, the processing sequence began with a selection of bauxite ores as raw materials for an initial blending. The chemical composition for the crude bauxite blend was checked aiming to achieve an iron oxide (Fe_2O_3) content lower than 3.5% and a titanium oxide (TiO_2) content lower than 1.0%. Additionally, a special attention is taken to ensure the low alkaline oxides content. Such analysis result by X-Ray Fluorescence Spectrometry is shown in Table 4.

Afterwards, the right bauxite blend was dried and the material went through homogenization, milling and water addition for adjusting the moisture, until achieve an optimum plasticity to assure the forming processes.

Table 4: Chemical composition (%wt.) of the Brazilian bauxite blend (dry basis)

Al_2O_3	SiO_2	Fe_2O_3	TiO_2	K_2O	RO*	LOI**
59.0	5.03	3.29	0.75	0.06	0.09	31.5
RO = CaO + MgO						
**LOI = Loss on ignition at 1100°C/2h*						

Regarding the forming processes, two different routes were considered. MC A was produced using a single-screw-extruder and MC B was manufactured with a briquette machine. After conformation, MC B went through a lump crusher to reduce the size of the briquettes and, only after this crushing, the material was transferred to a rotary kiln for sintering. As for MC A route, the extruded material was straightly directed to a rotary kiln, eliminating the physical comminution step. Both materials were sintered over 1700 °C, and the run of kiln product was cooled through a rotary cooler and sized into the fractions "-6.70|+2.36 mm", "-2.36|+0.85 mm" and "-0.85 mm" by vibratory screening. Lastly, the fraction "-0.075 mm" was obtained by ball milling. Figure 4 presents a concise flowchart of the Brazilian RGB with its two forming processing routes.
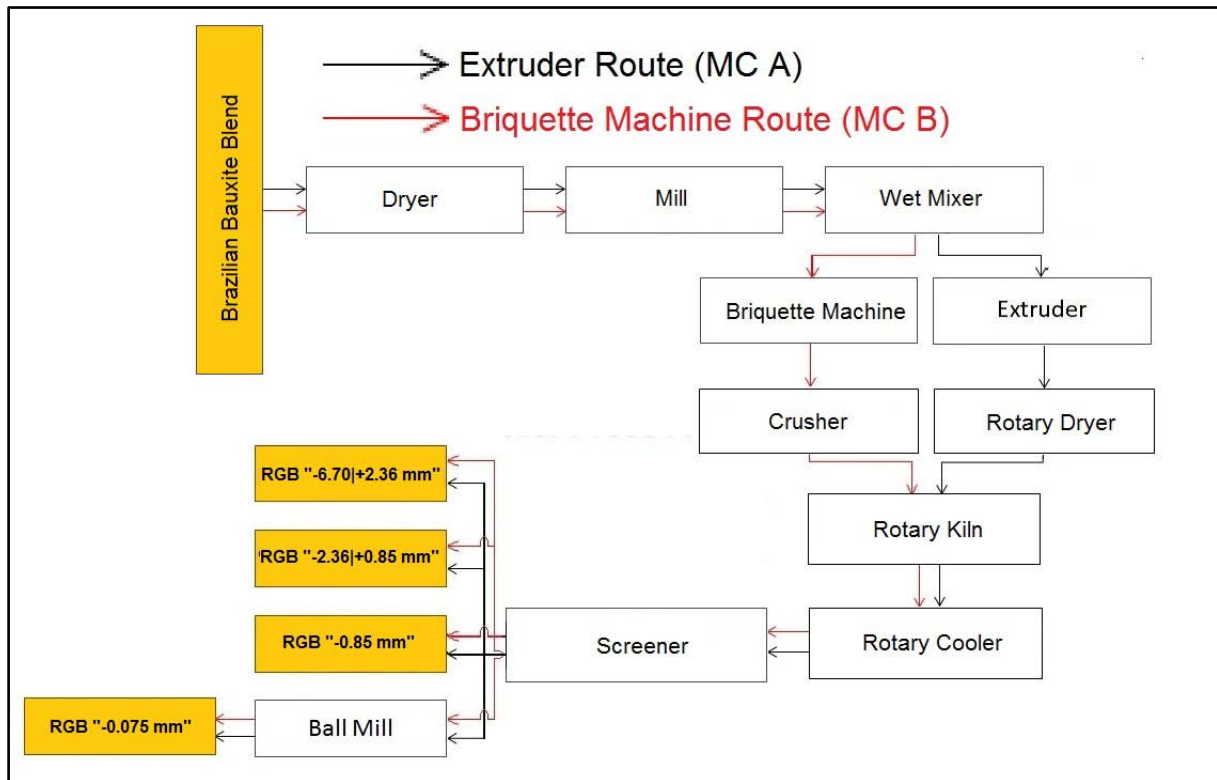
Figure 4: Flowchart for Brazilian RGB production using a single-screw-extruder or a roller press (briquette machine)

All RGBs were analyzed for particle-size distribution (PSD) in terms of retained weight on ASTM Standard sieves, and the "-6.70|+2.36 mm", "-2.36|+0.85 mm" and "-0.85 mm" size range shad also their particles shape evaluated in terms of sphericity. The sieves used for each size range are listed in Table 5 and the pattern for visual estimation of sphericity based on Krumbein Index is presented in Figure 5. Particularly for the fraction "-0.075 mm", due to their fineness, the PSD of the samples in terms of volume were obtained by laser diffraction (Malvern Mastersizer 2000).

Table 5: Sieves used for the particle-size analysis.

Size Range	Sieves ASTM Standard Number (and opening diameter in millimeter)				
-6.70|+2.36 mm	0.265" (6.70)	#4 (4.75)	#6 (3.35)	#8 (2.36)	#10 (2.00)
-2.36|+0.85 mm	#6 (3.35)	#10 (2.00)		#18 (1.00)	#20 (0.85)
-0.85 mm	#16 (1.18)	#18 (1.00)		#20 (0.85)	#30 (0.60)
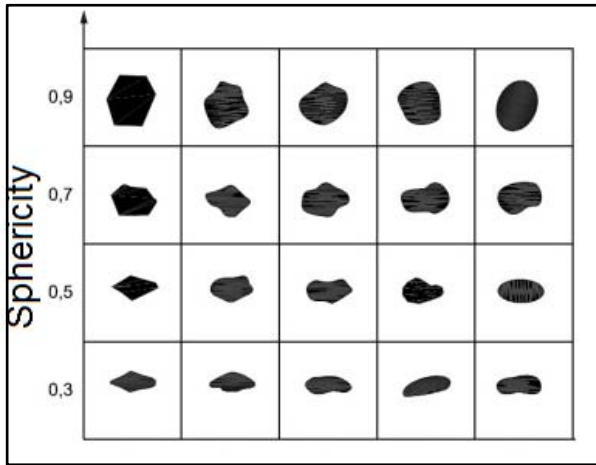
Figure 5: Chart for visual reference of particle sphericity (adapted from [25]).

Figure 6: Particle size distribution of the HP-CAC

Table 6: Chemical composition (%wt.) of the HP-CAC

Al_2O_3	CaO	SiO_2	Fe_2O_3	TiO_2	K_2O	Na_2O
69.5	24.3	3.23	2.31	0.24	0.16	0.04

All the samples were chemically analyzed by X ray fluorescence technique in a sequential wavelength dispersive spectrometer (XRF 1800, Shimadzu) after sample preparation by fusion method in a high frequency induction machine (HA-HF 16/2, Herzog).

The RGB mineralogy for the "-6.70|+2.36 mm" size range was evaluated by X-ray diffractometry in a vertical θ-2θ diffractometer (XRD 6000, Shimadzu), operating with a source of CuKα radiation (power = 40 kV, 30 mA) in a step scan mode (step = 0.02° 2θ, time = 2 s, scan range = 15 to 80° 2θ). After mineralogical phases identification, the Rietveld method was applied for quantitative phases analysis [26][27].

The apparent porosity, water absorption and specific gravity of the solid fraction for "-6.70|+2.36 mm" samples were evaluated through the Archimedes Principle by hot water intrusion pycnometry [28]. For the remaining fractions, the specific gravity was obtained as real density by helium gas intrusion pycnomety.

Performance tests were conducted in a convention castable formulation with 82% aggregates (RGBs) and 18% high-purity calcium aluminate cement (HP-CAC). For this test, a pre-mix of different sizes of RGB was prepared according to the following composition: 30%wt. "-6.70|+2.36 mm"; 30%wt. "-2.36|+0.85 mm"; 30%wt. "-0.85 mm"; 10%wt. "-0.075 mm". The PSD and the chemical composition of the HP-CAC are presented in Figure 6 and Table 6, respectively.

The castables were prepared with a water to concrete ratio in 9%wt. After 24 hours of curing time at room temperature, the castables were dried in a stove for 24 hours/110°C. The determination of the hot modulus of rupture (HMoR) was performed at 1200°C after five-hour of soaking time using the three-point bending technique [29]. The workability of the castables was also evaluated, and the phase identifications for the fired concretes were performed by X-ray diffractometry, aiming to evaluate the new phases formation under firing.

Flowability tests [30] were performed for the castables with Brazilian RGBs as aggregate (MC A and MC B), aiming to evaluate the morphology effect on it. In this special case, the aggregates fraction used was the "-6.70|+2.36 mm" size only.

III. RESULTS AND DISCUSSION

The chemical composition for each RGB size is presented in Table 7. The RGB G samples presented the highest aluminum oxide content on average (~90%), followed by CH88 (~87%), CH86 (~86%), MC A (~85%) and MC B (85%). The impurities varied with the samples, where Brazilian RGBs showed a considerable content of iron oxide (4-5%) and a low content of titanium, the Guyanese and Chinese RGBs showed a high content of titanium oxide (3-4%). These impurities can promote the formation of deleterious phases for refractories, specially tialite formation due to titanium presence.

Table 7: Chemical composition (%wt.)for the fractions of RGBs

RGB	Size Range	Al_2O_3	SiO_2	Fe_2O_3	TiO_2	K_2O	RO*
MC A	-6.70|+2.36 mm	85.2	8.18	4.80	1.20	0.15	0.17
	-2.36|+0.85 mm	85.4	8.04	4.81	1.20	0.13	0.14
	-0.85 mm	85.2	8.26	4.67	1.27	0.13	0.13
	-0.075 mm	84.5	8.22	5.20	1.33	0.08	0.30
MC B	-6.70|+2.36 mm	86.1	7.37	4.70	1.19	0.12	0.18
	-2.36|+0.85 mm	85.0	8.06	5.06	1.26	0.10	0.16
	-0.85 mm	83.5	10.1	4.60	1.06	0.14	0.27
	-0.075 mm	85.1	7.81	5.15	1.28	0.08	0.24
G	-6.70|+2.36 mm	89.2	6.02	1.24	2.97	0.00	0.10
	-2.36|+0.85 mm	90.3	5.17	1.26	2.81	0.00	0.04
	-0.85 mm	90.0	5.17	1.33	3.04	0.00	0.02
	-0.075 mm	89.4	5.48	1.67	2.93	0.00	0.04
CH86	-6.70|+2.36 mm	86.9	7.05	1.37	3.49	0.14	0.44
	-2.36|+0.85 mm	87.9	6.05	1.27	3.33	0.26	0.59
	-0.85 mm	84.9	8.39	1.97	3.27	0.17	0.70
	-0.075 mm	85.5	8.11	1.50	3.28	0.33	0.61
CH88	-6.70|+2.36 mm	88.3	5.77	1.22	3.32	0.25	0.49
	-2.36|+0.85 mm	89.0	5.27	1.10	3.27	0.27	0.48
	-0.85 mm	85.8	8.19	1.36	3.48	0.19	0.36
	-0.075 mm	85.2	8.31	1.39	3.67	0.15	0.62

RO: CaO + MgO.

The silica content decreased with the increasing of the particle size for Chinese RGBs. For instance, in the RGB CH88, silica content was 8.31% in the fraction "-0.075 mm", whereas for the fraction "-2.36|+0.85 mm", the lowest result was encountered (5.27%).

The higher content of alkalis and earth-alkaline oxides (K_2O and RO in Table 7) can configure another source of concerns for Chinese RGBs, because these oxides are related to the lowering of the softening point of the material.

Table 8 shows a statistic treatment considering the variation on chemical composition of the RGBs. The highest standard deviations were also encountered for the Chinese RGBs, mainly for the silica content. RGB MC A has the most homogeneous chemical composition. For MC A route, the feeding of the extruder demands a finer milling, ensuring a more effective mixture and preventing a chemical segregation during the process. The processes of milling, mixing and agglomerating work against the natural heterogeneity of the mineral resources of bauxite. Heterogeneity is connected with the aspect of the aggregate, in which the Chinese ones are colorful (i.e. singular grains in black, grey and brown), denoting a chemical and mineralogical heterogeneity.

Table 8: Standard deviation (%wt.) of main oxides of each RGB

RGB	Al_2O_3	SiO_2	Fe_2O_3	TiO_2	K_2O	RO*	Sum
MC A	0.39	0.10	0.23	0.06	0.03	0.08	0.89
MC B	1.07	1.21	0.27	0.10	0.03	0.05	2.73
G	0.51	0.40	0.20	0.10	0.00	0.03	1.24
CH86	1.36	1.07	0.31	0.10	0.09	0.11	3.03
CH88	1.86	1.59	0.13	0.18	0.06	0.11	3.92

RO: CaO + MgO.

The diffractogram and mineralogical composition of the RGBs are presented in Figure 7 and Table 9, respectively. Chinese RGBs presented the highest content of corundum, while the Brazilian ones the lowest. Corundum is the major phase of the calcined bauxites, and the most refractory phase in high-alumina refractories (Table 2).

Brazilian RGBs contain hematite in a low content, what can reduce the refractoriness of the system (Table 2). Both Guyanese and Chinese RGBs

presented tialite, but only the Chinese RGBs showed a small quantity of rutile, due to a eutectoid reaction of decomposition of tialite and/or lack of energy, temperature or homogenization for the reaction of all the titanium oxide with the aluminum oxide. The tialite phase brings some concerns because its formation is not irreversible and the refractory integrity can be impaired due to its highly anisotropic thermal expansion (Table 2).

Mullite is the secondary phase for all RGBs, having the greatest amounts for RGB MC A (20%) and RGB G (19%). The highest alumina content in RGB G ($\sim$89%) suggests a mullite richer in alumina ($3Al_2O_3.2SiO_2$ to $2Al_2O_3.1SiO_2$, Fig. 1). This higher grade of alumina in the stoichiometry of the mullite is caused by a substitution of a Si^{4+} cation and a removal of an oxygen ion from a $(Al,Si)O_4$ tetrahedron in its crystal structure, enriching the alumina content [13].
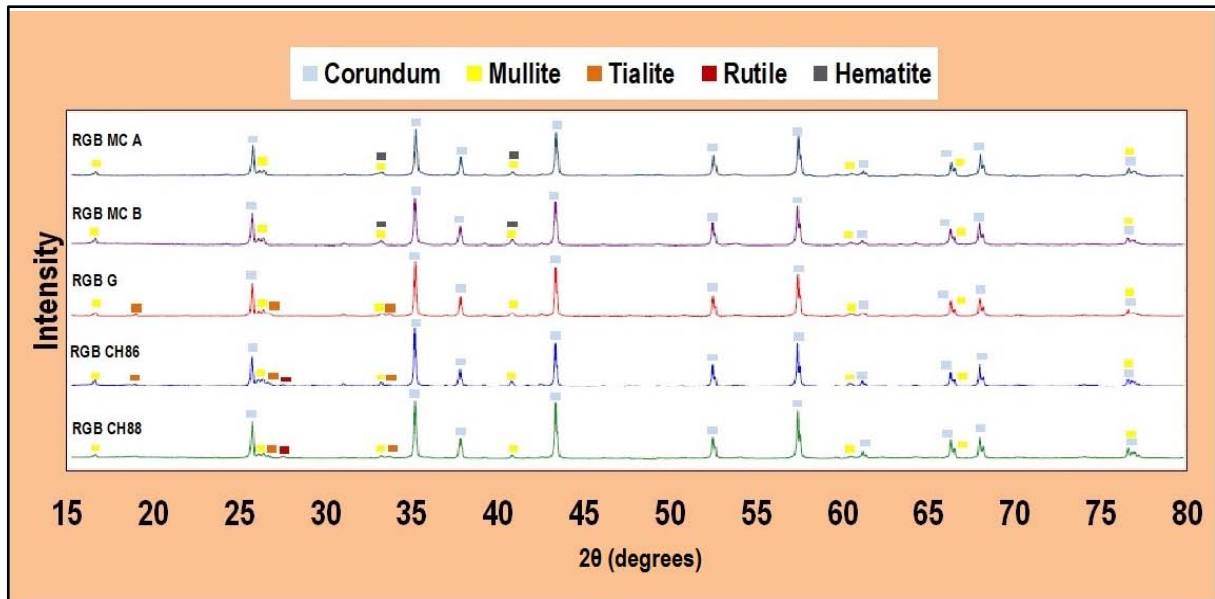
Figure 7: X-ray diffractograms for RGBs in the "-6.70|+2.36" mm fractions

Table 9: Mineralogical Composition (%wt.) for RGBs in the "-6.70|+2.36" mm fractions

Phase	Chemical Formula	MC A	MC B	G	CH86	CH88
Corundum	Al_2O_3	76.4	80.5	75.7	76.6	90.0
Mullite	$Al_{4+2x}Si_{2-2x}O_{10-x}$	20.0	16.6	19.0	16.9	5.20
Tialite	Al_2TiO_5	-	-	5.30	5.70	4.20
Rutile	TiO_2	-	-	-	0.80	0.60
Hematite	Fe_2O_3	3.60	2.90	-	-	-

Figure 8 shows the particle size distribution (PSD) for all the RGBs studied in this work. In general, the samples were within the size range specified (at least 80%wt. of the particles between the reference screens). Regarding the fraction "-6.70|+2.36 mm", Brazilian RGBs diverged from the other bauxites, presenting a higher quantity for finer particles, and a wider curve with maximum retention on sieve 2.36 mm. Chinese and Guyanese RGBs had a narrower distribution and the maximum retention on sieve 3.35 mm. For fraction "-2.36|+0.85 mm" the opposite occurred, the Brazilian RGBs had a narrower distribution, but continuing finer than the other bauxites.

Comparing the forming processes (MC A x MC B), Brazilian RGBs presented the same behavior about the size distribution for all fractions, except for "-0.85 mm" samples, where MC A sample had 70%wt. of retention on 0.60 mm opening screen, in comparison with the other samples which had more than 70%wt. of the particles passing by that same screen. It´s remarkable the influence of the forming process on the particle size, being the extrusion method responsible for the generation of a "-0.85mm" fraction with the most part of the particles distributed in -0.85 mm|+0.60 mm screens.

For "-0.075 mm" fractions analyzed by laser diffraction, the Brazilian RGBs showed the same behavior and intensity due to the ball milling operation, common for all samples.
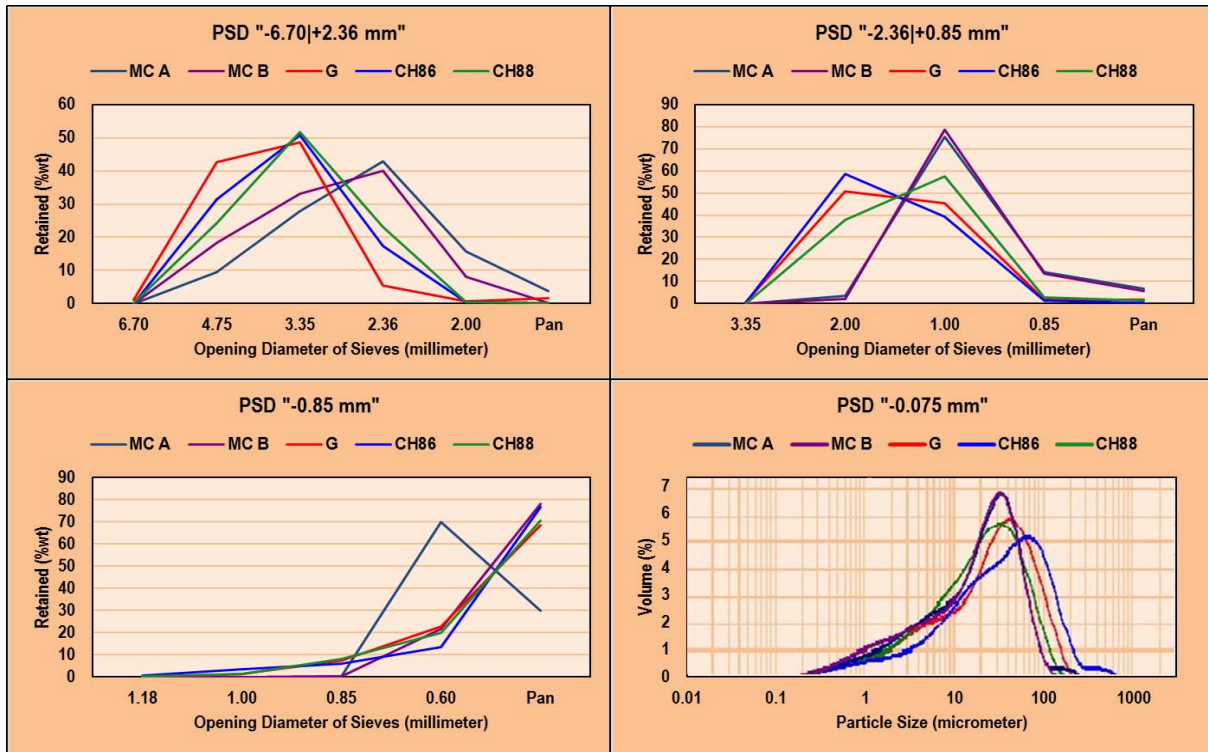
Figure 8: Particle size distributions of the RGB fractions

The sphericity of the three coarser fractions for all the RGB samples is presented by Table 10. The products from the extruder were rounded granules, while the briquette machine formed irregular-shaped particles, setting the main physical difference among those samples. Depending on the type of application, rounded grains can facilitate pumping operations and reduce the power employed to transport the material. Likewise, spherical grains play in favor of self-flow.

Table 10: Sphericity of the RGBs in different size fractions: "-6.70|+2.36 mm"; "-2.36|+0.85 mm"; "-0.85 mm"

RGB	Sphericity			
	-6.70|+2.36 mm	-2.36|+0.85 mm	-0.85 mm	Average
MC A	0.8	0.9	0.9	0.9
MC B	0.6	0.7	0.7	0.7
G	0.5	0.6	0.6	0.6
CH86	0.6	0.5	0.6	0.6
CH88	0.6	0.5	0.6	0.6

Regarding the apparent porosity and water absorption, results for all RGBs are presented in Figure 9. Apparent porosity of the Chinese RGBs are the lowest, whereas for the Guyanese RGB is the highest. Despite the Guyanese RGB chemical composition is the richest in aluminum oxide, its high porosity can be detrimental to the mechanical performance of the refractory. The Brazilian RGBs have a high apparent porosity, however the RGB MC B is lower than RGB MC A due to a higher compression in the briquette machine, if compared with an extruder. Water absorption is directly proportional to apparent porosity.
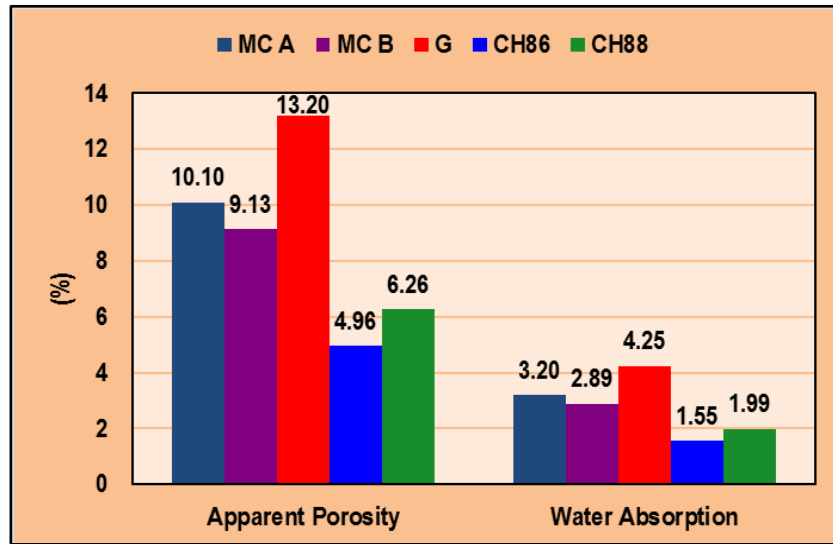
Figure 9: Physical indexes of RGBs in the "-6.70|+2.36" mm fraction

The specific gravities of all samples are presented in Figure 10. In general, the specific gravities increase with the decreasing of the particle sizes. It shows that, the reduction on number of closed pores in the particles, is proportional to the decreasing of the size of particles. That is, coarser particles have a higher number of closed pores, resulting in a lower weight per volume of material. The Guyanese RGB has the highest values in this property, what is good for a refractory because specific gravity relates with mechanical performance. The Brazilian RGBs have a specific gravity higher than the Chinese ones for the "-6.70|+2.36 mm" fraction, but lower for the "-0.85 mm" one. It can be related to the firing conditions, since the materials are sintered during the same run of kiln.
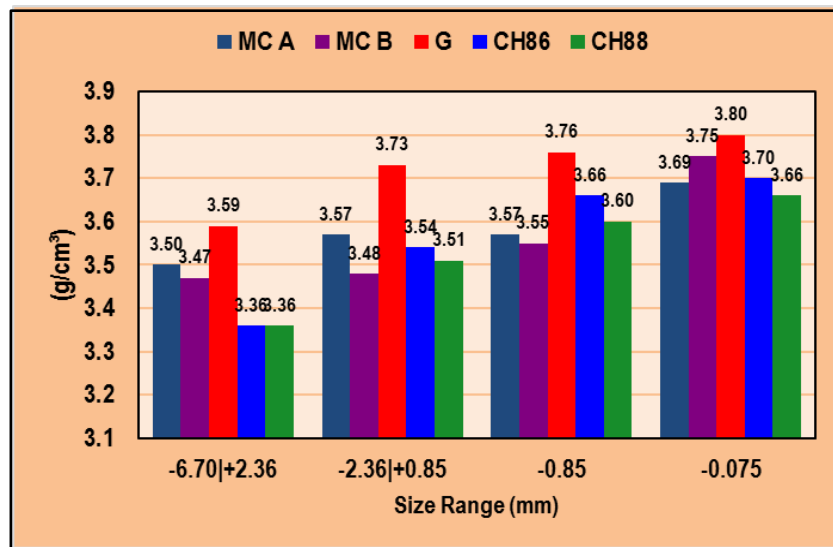
Figure 10: Specific gravity of the particles of RGB in each size range

The hot modulus of rupture (HMoR) at 1200°C of the castables measured through the three-point bending technique and the sum of the standard deviation on chemical composition (SDoCC) of the RGBs are shown in Figure 11. This performance test contemplates the effect of all properties discussed. In statistical terms, the results are in a same magnitude, being possible to infer that the crack propagation occurred through the cement matrix, and not throughout the aggregate grains (Figure 12). However, there is a noticeable correlation between the HMoR and the SDoCC of RGBs. The lower the chemical variability (deviation sum), the higher the mechanical strength (HMoR).In absolute terms, RGB MC A presented the best flexure strength (5.12 MPa) and RGB G the second one (5.04 MPa). In spite of having 90% of corundum (Table 9), the heterogeneity of RGB CH88 aggregates may have been a decisive factor of its worst thermo

mechanical performance. Isolated grains rich in phases as tialite or poorer in alumina can be harmful for refractory resistance. However, all the castables presented a good workability and the working time achieved for each castable is shown in Figure 13.
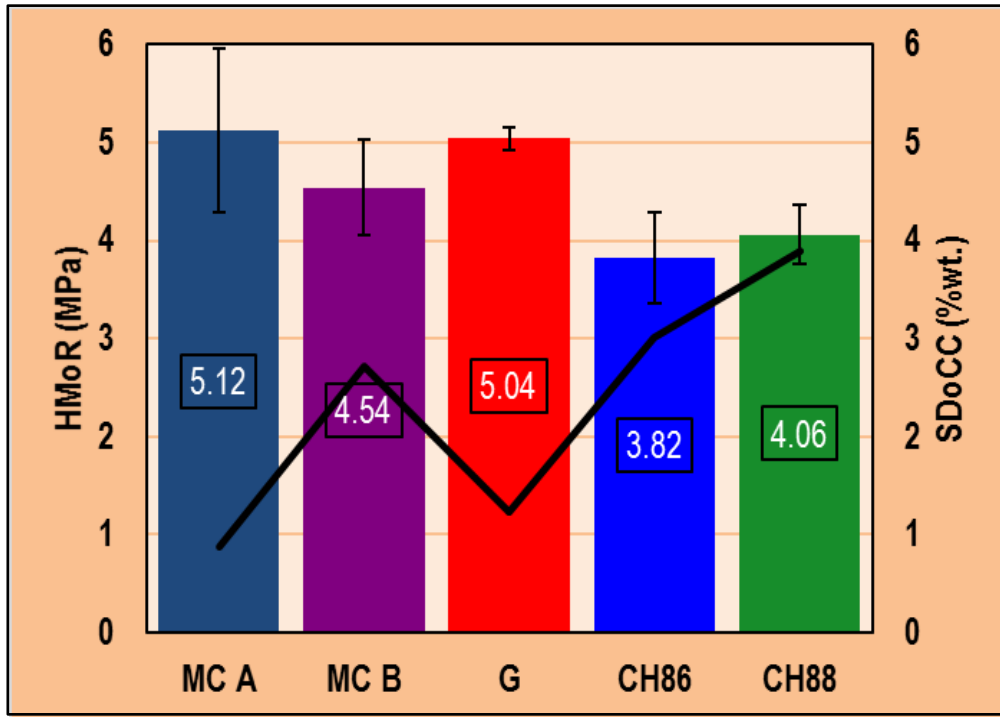
Figure 11: Hot modulus of rupture of castables produced with different RGB sources (column graph) and standard deviation on chemical composition of RGBs (line graph)
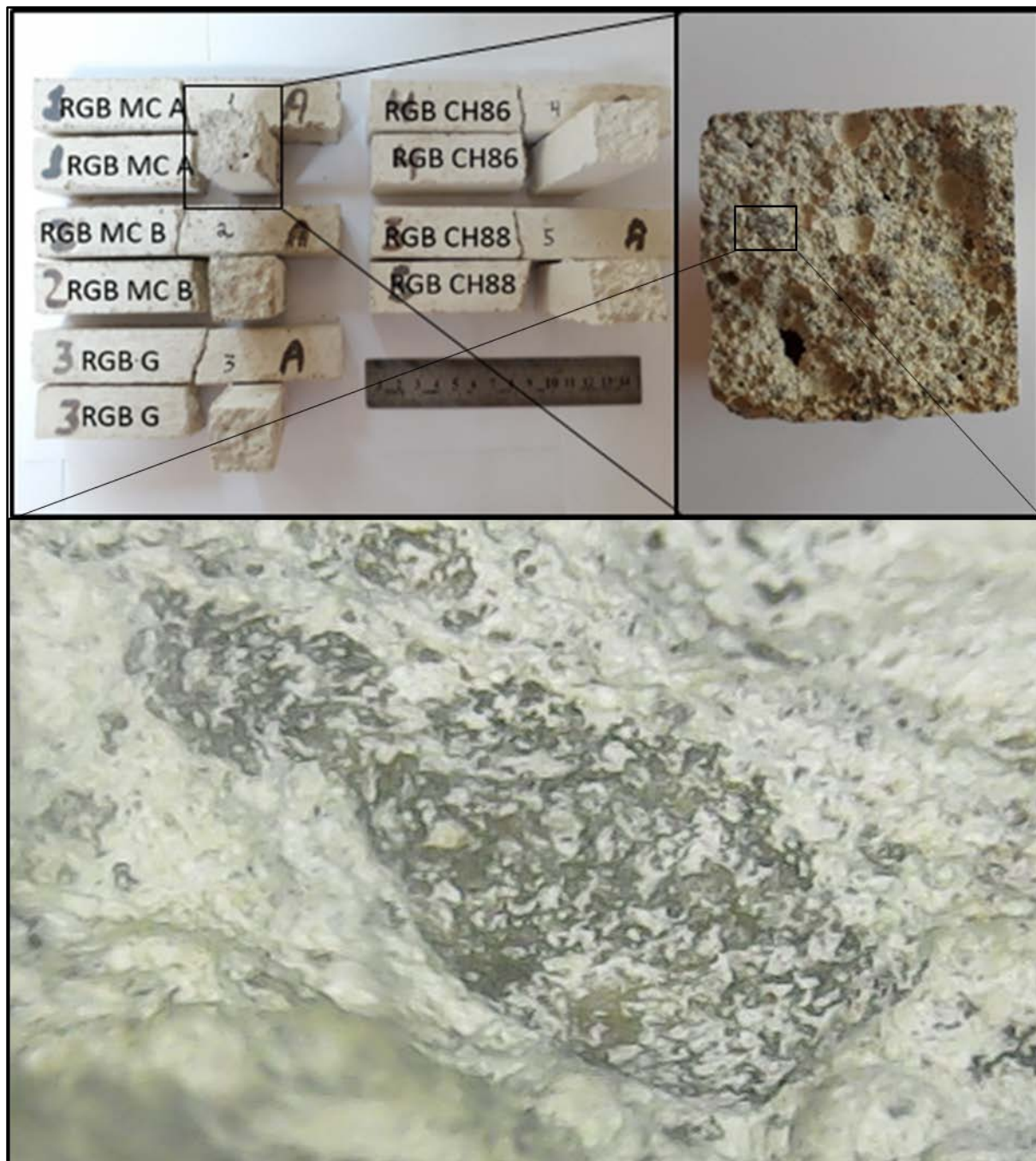
Figure 12: Specimens after hot modulus of rupture test, highlighting a good interaction between the RGB grain (sample MC A) and the cement matrix
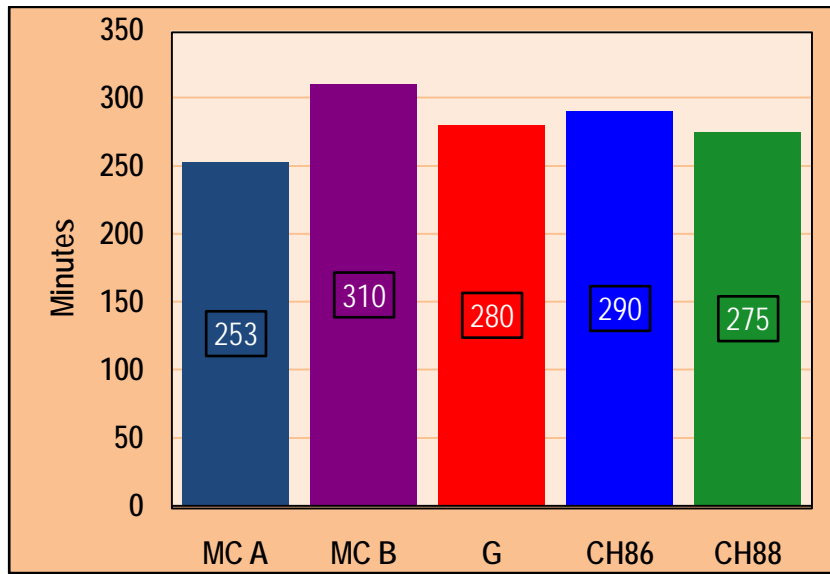
Figure 13: Workability of castables with RGBs as aggregate

Figure 14 shows the diffractograms of the castables after HMoR test, and the Table 11 lists the phases identified for each one, pointing them out in colored blocks. In addition to RGB phases, CAC phases such as grossite, gehlenite and hibonite were found.

Anorthite was found in all castables, result of a thermal reaction between the CAC binder and the RGB matrix. Especially for RGB G, a cristobalite peak was found, what can be related to silica crystallization from liquid phase cooling.
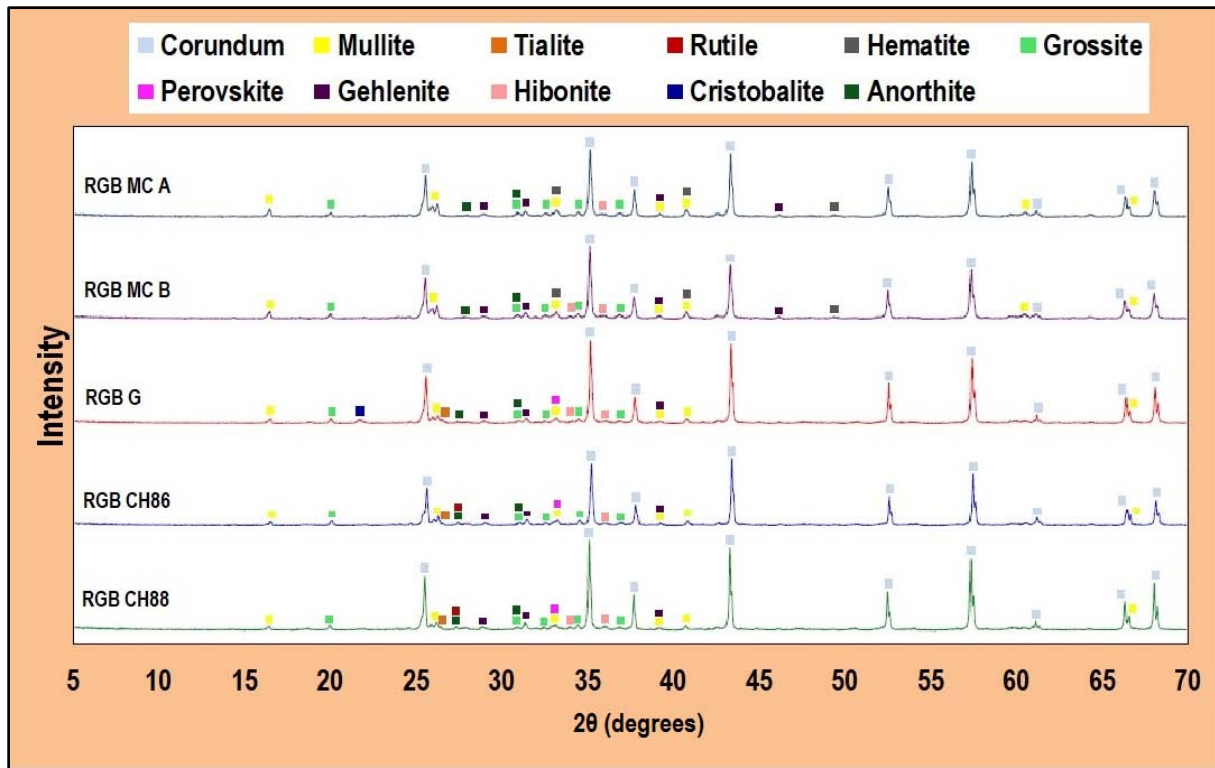
Figure 14: X-ray diffractograms of castables produced with different RGB sources and fired at 1200°C/5h

Table 11: Mineralogy of the castables after HMoR

Phase	MC A	MC B	G	CH86	CH88
Corundum (Al_2O_3)	■	■	■	■	■
Mullite ($Al_6Si_2O_{13}$)	■	■	■	■	■
Tialite(Al_2TiO_5)	Not	Not	■	■	■
Rutile(TiO_2)	Not	Not	Not	■	■
Hematite(Fe_2O_3)	■	■	Not	Not	Not
Grossite ($CaAl_4O_7$)	■	■	■	■	■
Perovskite ($CaTiO_3$)	Not	Not	■	■	■
Gehlenite($Ca_2Al_2SiO_7$)	■	■	■	■	■
Hibonite ($CaAl_{12}O_{19}$)	■	■	■	■	■
Cristobalite (SiO_2)	Not	Not	■	Not	Not
Anorthite ($CaAl_2Si_2O_8$)	■	■	■	■	■

The flowability test of the castable varying the type of forming process for Brazilian RGBs showed the influence of particle morphology. The results are shown in Figure 15. The higher the displacement, the higher the flowability. The castable with RGB MC A as aggregate presented a higher flowability when compared to the one with RGB MC B. Hence, being the particles rearrangement a function of the beats on the flow table, the more spherical-shaped particles in RGB MC A proportionated the higher displacement of the castable by rolling of those thick particles.
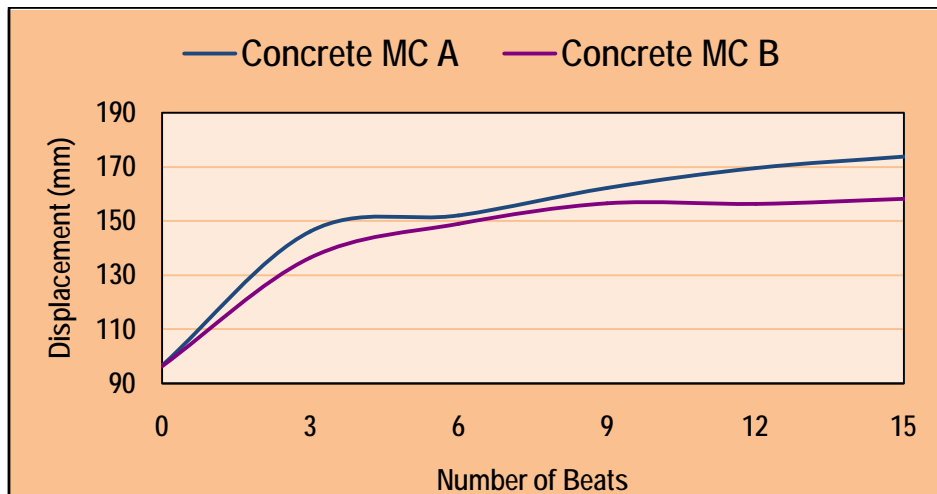
Figure 15: The impact of the forming process of RGBs on concretes flowability

IV. CONCLUSIONS

Refractory properties are a correlation between characteristics of raw material and the processing employed. Mineralogy, chemical composition, firing temperature, particle size, forming process and porosity index will define the performance of the refractory. Thermo mechanical tests presented a relationship with the variability of the chemical composition among the size fractions for the same RGB. The Brazilian RGB processed in an extruder (MC A), with the lowest standard variation on chemical composition (SDoCC = 0.88%) and tialite absence in its composition, promoted a castable with the highest hot modulus of rupture value (HMoR at 1200°C = 5.12 MPa). Guyanese RGB also got a great result (HMoR = 5.04 MPa), whereas the Chinese RGBs were the least resistant (HMoR: CH86 = 3.82 MPa; CH88 = 4.06 MPa), in accordance with their higher heterogeneity represented by the standard deviation on chemical composition (SDoCC: CH86 = 3.03%; CH88 = 3.92%).

All the refractory grade bauxites presented a high aluminum oxide content (> 83%), corundum and mullite as main phases, and a suitable working time (over 250 minutes) in a conventional castable formulation.

Despite of the highest alumina content (~90% Al_2O_3) of the Guyanese RGB, it has exhibited the lowest corundum content (75.7%), what can be related to a formation of a mullite richer in alumina (19.0%). The Chinese sample "RGB CH88" presented the highest corundum content (90%), however their impurities

enabled tialite formation (4.20%) which may have impaired the high temperature strength. Brazilian RGBs (MC A and MC B) presented high mullite content (20.0% and 16.6%) and low hematite content (3.60% and 2.90%), in a good balance with corundum (76.4% and 80.5%), promoting highly homogeneous grains and proper physical indexes for refractory applications as dense granulated materials.

The size and the morphology of the RGBs is affected by the processing route, and the shape of the grains impacted the flowability. Two different forming process for Brazilian RGBs showed that the briquetting operation produced angular-shaped grains (MC B: sphericity = 0.7) due to a briquettes fragmentation, whereas the extrusion mechanism produced rounded grains (MC A: sphericity = 0.9) which induced the flowability of the castables, comparing the displacement of both castables (MC A x MC B) on a flow table.

References Références Referencias

1. M. Allaby, Dictionary of Earth Sciences, New York: Oxford University Press Inc., 2008.
2. M. Victoria, "Argilas e Minerais Refratários," Companhia de Desenvolvimento de Minas Gerais, Belo Horizonte, 2018.
3. S. Banerjee, "Properties of Refractories," in Refractories Handbook, Boca Raton, Taylor & Francis Group, 2004.
4. D. A. Brosnan, "Alumina-Silica Brick," in Refractories Handbook, Boca Raton, Taylor & Francis Group, 2004.
5. Harbison-Walker Refractories Company, Handbook of Refractory Practice, Moon Township, 2005.
6. MRNG, "Bauxite Polite Briefs - Final Drafts," 10 July 2019. [Online]. Available: https://nre.gov.gy/2019/07/18/bauxite-policy-briefs-final-drafts/. [Accessed 19 September 2019].
7. USGS, "Bauxite and Alumina Statistics and Information,"2019.[Online].Available:https://minerals.usgs.gov/minerals/pubs/commodity/bauxite/.[Accessed 19 September 2019].
8. S. Hinds, "Refractory Bauxites," IM Refractories Supplement, 1983.
9. R. Flook, "Refractory evolution - implications for bauxite & alumina," in 3rd Asian Bauxite & Alumina Conference, 2013.
10. M. O' Driscoll, "The New World of China's Refractory Mineral Supply," in 61st International Colloquium on Refractories, Aachen, 2018.
11. C. Pascoal and V. C. Pandolfelli, "Bauxitas refratárias: Composição química, fases e propriedades - Parte I," Cerâmica, vol. 46, no. 298, pp. 76-89, 2000.
12. A. L. Pereira, M. A. Reis, L. L. H. C. Ferreira and P. M. Nakachima, "Brazilian refractory grade bauxite: a new alternative to refractories makers and users," Cerâmica, pp. 40-46, 2019.
13. J. Anggono, "Mullite Ceramics: Its Properties, Structure, and Synthesis," Journal Teknik Mesin, vol. 7, no. 1, pp. 1-10, 2005.
14. G. L. Lopes, "Processamento e Caracterização de Tialita a partir da Moagem de Alta Energia," Federal University of Alfenas, 2016.
15. G. R. Beardsmore and J. P. Cull, Crustal Heat Flow - A Guide to Measurement and Modelling, New York, 2001.
16. W. M. Haynes, CRC Handbook of Chemistry and Physics, Boca Raton: Taylor & Francis Group, 2017.
17. T. Huotari and I. Kukkonen, Thermal Expansion of Rocks: Literature Survey and Estimation of Thermal Expansion Coefficient for Olkiluoto Mica Gneiss, Posiva Oy, 2004.
18. K. Wefers, "Nomenclature, Preparation, and Properties of Aluminum Oxides, Oxide Hydroxides, and Trihydroxides," in Alumina Chemicals: science and technology handbook, 1990, pp. 13-22.
19. A. Caballero, J. Requena and S. Aza, "Refractory bauxites. How processing can improve high temperature mechanical properties," Ceramics International, vol. 12, no. 3, pp. 155-160, 1986.
20. C. I. Torres, N. M. Rendtorff, M. Cipollone, E. F. Aglietti and G. Suárez, "Comparative evaluation of properties of a clay based ceramic shaped via four techniques," Cerâmica, vol. 64, no. 370, pp. 176-182, 2018.
21. J. Eom, Y. Kim, C. B. Park and C. Wang, "Effect of forming methods on porosity and compressive strength of polysiloxane-derived porous silicon carbide ceramics," Journal of the Ceramic Society of Japan, vol. 120, no. 5, pp. 199-203, 2012.
22. A. B. Luz, J. A. Sampaio and S. C. A. França, Tratamento de Minérios, Rio de Janeiro: CETEM/MCT, 2010.
23. P. A. P. Martinez and W. F. J. Amorim, "Design of an Labaratory Polymer processing Extruder," 2019.
24. V. G. Oliveira, P. M. Nakachima, R. V. Fernandes, M. A. Reis, A. L. Pereira and L. L. H. C. Ferreira, "Improvement of the mechanical properties of green body bauxite briquettes through the addition of organic binders and methodologies for their evaluation," 63º Congresso Brasileiro de Cerâmica, 2019.
25. ISO 13503-2, Petroleum and natural gas industries - Completion fluids and materials — Part 2: Measurement of properties of proppants used in hydraulic fracturing and gravel-packing operations, 2006.
26. A. C. Larson and R. B. V. Dreele, General Structure Analysis System (GSAS), Los Alamos National Laboratory Report LAUR 86-748, 2004, p. 224.

27. B. H. Toby, "A Graphical user interface for GSAS," Journal of Applied Crystallography, pp. 210-221, 2001.
28. ABNT NBR 8592, "Graning dense refractory materials - Determination of bulk density - Method of test," Associação Brasileira de Normas Técnicas, 2012.
29. ABNT NBR 9642, "Refractory materials — Determination of hot modulus of rupture," Associação Brasileira de Normas Técnicas, 2012.
30. ABNT NBR 13320, "Refractory Materials - Determination of Fluifity of Conventional Castable and Castable of Free Flow," Associação Brasileira de Normas Técnicas, 2012.

This page is intentionally left blank

Study of Radioactive Waste Management of Nuclear Power Plant: Prospect of Rooppur Nuclear Power Plant

By Iftekhar Ahmed, Hriday Dhar Joni & Hridita Nowrin Pranti

University of Chittagong

Abstract- The nuclear power plant is required to supply a substantial amount of electricity for a densely populated country like Bangladesh. The government of Bangladesh has attached to a commitment to implement the Rooppur Nuclear Power Plant, and so Bangladesh will be the 33rd nuclear power-producing country after the successful construction of this plant. Bangladesh has planned to construct two power units (Rooppur-1 & Rooppur-2) with a capacity of 1200 MW, each of and is expected to go into operation in 2023. Russian Rosatom State Atomic Energy Corporation is constructing this nuclear power plant, which is the generation-3+ VVER-1200 model. But the main concern is how a third world country like Bangladesh can handle the tons of radioactive waste of RNNP. Radioactive waste i.e., a variety of solids, liquids, and gases which are produced during the generation of nuclear energy in a nuclear reactor. Depending on activity content, solid and liquid waste are disposed of in near-surface or deep geological facilities, and gaseous waste is dissolved by following some filtering process. If not properly disposed of or recycled, irradiation from radioactive waste will cause major problems for the environment. Various stages should be required for the removal of a tremendous amount of radioactive waste in a cost-effective way. This paper mainly delineates the proximate of radioactive waste management of RNNP and gives an account of (1) Radioactivity and radiation level, (2) Classification, (3) Treatment of solid, liquid and gaseous radioactive waste, (4) Reprocessing and packaging, (5) Storage and (6) Disposal.

Keywords: radioactive waste, waste management, LLW, ILW, HLW, process, storage, disposal.

GJRE-A Classification: FOR Code: 091399

STUDYOFRADIOACTIVEWASTEMANAGEMENTOFNUCLEARPOWERPLANTPROSPECTOFROOPPURNUCLEARPOWERPLANT

Strictly as per the compliance and regulations of:

Study of Radioactive Waste Management of Nuclear Power Plant: Prospect of Rooppur Nuclear Power Plant

Iftekhar Ahmed [α], Hriday Dhar Joni [σ] & Hridita Nowrin Pranti [ρ]

Abstract- The nuclear power plant is required to supply a substantial amount of electricity for a densely populated country like Bangladesh. The government of Bangladesh has attached to a commitment to implement the Rooppur Nuclear Power Plant, and so Bangladesh will be the 33rd nuclear power-producing country after the successful construction of this plant. Bangladesh has planned to construct two power units (Rooppur-1 & Rooppur-2) with a capacity of 1200 MW, each of and is expected to go into operation in 2023. Russian Rosatom State Atomic Energy Corporation is constructing this nuclear power plant, which is the generation-3+ VVER-1200 model. But the main concern is how a third world country like Bangladesh can handle the tons of radioactive waste of RNNP. Radioactive waste i.e., a variety of solids, liquids, and gases which are produced during the generation of nuclear energy in a nuclear reactor. Depending on activity content, solid and liquid waste are disposed of in near-surface or deep geological facilities, and gaseous waste is dissolved by following some filtering process. If not properly disposed of or recycled, irradiation from radioactive waste will cause major problems for the environment. Various stages should be required for the removal of a tremendous amount of radioactive waste in a cost-effective way. This paper mainly delineates the proximate of radioactive waste management of RNNP and gives an account of (1) Radioactivity and radiation level, (2) Classification, (3) Treatment of solid, liquid and gaseous radioactive waste, (4) Reprocessing and packaging, (5) Storage and (6) Disposal.

Keywords: radioactive waste, waste management, LLW, ILW, HLW, process, storage, disposal.

I. Introduction

The created radioactive by-product while producing nuclear power is called radioactive waste. The importance of researching radioactive waste has a significant research area all over the world. But the waste management of radioactive waste is a cause of public concern. Safe and economic radioactive waste management is the first and foremost requirement to implement a nuclear power plant. Spent fuel referees to as high-level waste, and no country yet has a complete long-term solution for storing this waste. The amount of high-level waste is currently increasing by around 12,000 metric tons each year in the world. According to IAEA, a nuclear power plant of 1000 megawatts produce approximately 27 tons of high-level waste each year.

And the two power units of RNPP generating 2.4 GWe is expected to go into operation in 2023 and 2024. So, according to the expectation, RNPP will produce about 50-60 tons of high-level waste every year. High-level waste requires both cooling and shielding during handling and transport. Remaining low-level waste contains a small amount of short-lived radioactivity that requires no special shielding. Most countries in the world are efficient at handling and managing low-level waste. But radioactive waste from nuclear reactors can be hazardous for the environment, and inhaling ionizing radiation at high dose levels can increase the risk of cancer. Hence, therefore, radioactive waste needs proper management from production to disposal. Russia has ensured that they will take back the high-level wastes of the Rooppur nuclear power plant. But today or tomorrow, Bangladesh has to be self-standing in the management of all kinds of radioactive waste arising during the operation of this nuclear power plant.

II. Radiation

When the emission or transmission of energy comes in the form of a wave from a source and travels through space is called radiation, and that is part of our everyday environment. Alpha, beta, and gamma radiation are three primary types of radiation that have different penetrating power in the matter. Alpha radiation passes through 5 cm air only and is a few cms of air can absorb it, beta radiation passes through air and paper and a thin sheet of paper can absorb it and gamma radiation passes through most things except thick lead and concrete and very thick wall of concrete can absorb it. Alpha radiation has maximum ionizing power, but beta radiation ionizing power is less than alpha radiation ionizing power, whereas gamma radiation has minimum ionizing power among them.

Author α σ ρ: Department of Physics, University of Chittagong.
e-mail: iftekharahmed0168@gmail.com
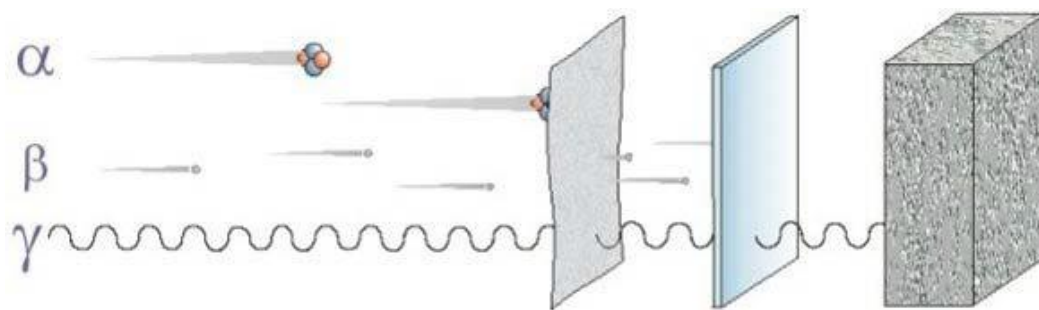
Fig. 1: Alpha, beta, and gamma have specific penetrating power in matter.

III. Radioactivity and Radiation Levels of rnnp Site

Typical radionuclide levels ^{238}U, ^{232}Th, and ^{40}K in the earthbound of the nuclear power plant site remain global midpoints, and ^{137}Cs of dirt and water tainting levels are below the detection level. The Bangladesh Atomic Energy Commission (BAEC) has implemented a robust radiation monitoring system at the RNPP site. The world average (1-4) radioactivity levels of ^{40}K, ^{232}Th, and ^{238}U are recorded as 400, 30 and 35 Bq.kg–1 on a complete basis, while the standard NPP values at Rooppur recorded as 379.6, 26.6 and 17.9 Bq.kg–1 on a stand-alone basis are in world esteem. Average annual viable estimates are 0.96 mSv.y-1 (96 mrem. y–1) considering indoor and outdoor inhabitance factors respectively 0.8 and 0.2. In 2015, J. Ferdous researched soil radioactivity at the proposed RNPP site and had an average of 30.85 Bqkg-1Ra-236, 40.88 Bqkg-1Th-232, and 390.10 Bqkg-1 K-40. A comparison of the number of radioactive particles of RNPP with other locations of the world is given below.

Table-1: Comparison of RNPP with other locations of the world.

Location	Activity in Bqkg-1		
	Ra-236	Th-232	K-40
Dhaka, Bangladesh	37.8	58.2	790.8
Chittagong, Bangladesh	34.6	60	438
Jessore, Bangladesh	48	53	481
Nine Southern Districts, Bangladesh	42	81	833
Eastern Sichuan Province, China	26	49	440
Peshwar, Pakistan	65	84	646
Nigeria	8.3	34.3	684
Louisiana, USA	43-95	50-190	43-729
Worldwide average	40(15-50)	40(7-50)	580(100-700)
RNPP Site	29.55	42.07	393.60

IV. Classification of Radioactive Waste

There are six categories of radioactive waste according to the International Atomic Energy Agency (IAEA) they are as follows:
➔ Exempt waste (EU).
➔ Very short-lived waste (VSLW).
➔ Very low-level waste (VLLW).
➔ Low-level waste (LLW).
➔ Intermediate-level waste (ILW).
➔ High-level waste (HLW).

• Exempt waste

Exempt waste is a kind of waste that contains radioactive materials at a certain level, which no longer requires further any treatment to control. It consists of small concentrations of radionuclides that once regulatory authority cleans this, it won't be regarded as baneful for the environment.

• Very short-lived waste

This type of waste has very short half-life radionuclide that can be stored for some time up to a few years until its radioactive content diminished by radioactive decay (radioactive decay is the process by which an unstable atomic nucleus loses energy by electromagnetic radiation) and so it is baneful for certain period. This waste is stored for a certain period so that the activity falls to the level of exempt waste. Very short-lived waste is usually using for medical and research purposes.

• Very low-level waste

The radioactivity of very low-level waste is close to natural radioactivity, and its activity is less than 100 kBq/kg. It is compatible with the regulation in near-surface landfill type facilities with limited regulatory control. This type of radioactivity falls to natural radioactivity after a few decades, and disposing of this

waste is not a serious issue. It consists of rubble and scrap metals produced during the operation of nuclear power sites.

- Low-level waste

Low-level waste contains mostly limited amounts of long-lived radionuclides that have high radioactivity. It requires appeasement for a few hundred years and can be deposited near the surface level. So, there is no requirement of any further shielding during transport or handling. This type of waste can be disposed of at varying depths from the surface down to (25-30) meters.

- Intermediate-level waste

Though intermediate-level waste, contains high amounts of radionuclide compare to low-level waste it requires no cooling but shielding. Usually, it is solidified in bitumen before storage. It contains long-lived

radionuclides that it's not that much easy to deposit near surface level like 30-meter depth. So, it requires disposal at greater depth up to a hundred meters.

- High-level waste

The high-level waste consists of 3% of the volume, which is produced from reprocessing of spent fuel of the world's radioactive waste. High-level radioactive waste is the highly radioactive material produced as a byproduct of the reactions that occur inside nuclear reactors. This waste requires both cooling and shielding. It is the most detrimental among all the waste because these materials are highly radioactive. Reprocessing or recycling spent nuclear fuel is not a proper solution because it still causes a quantity of waste. So, dispose of this type of material in the deep inside geologically is the right and safest solution.
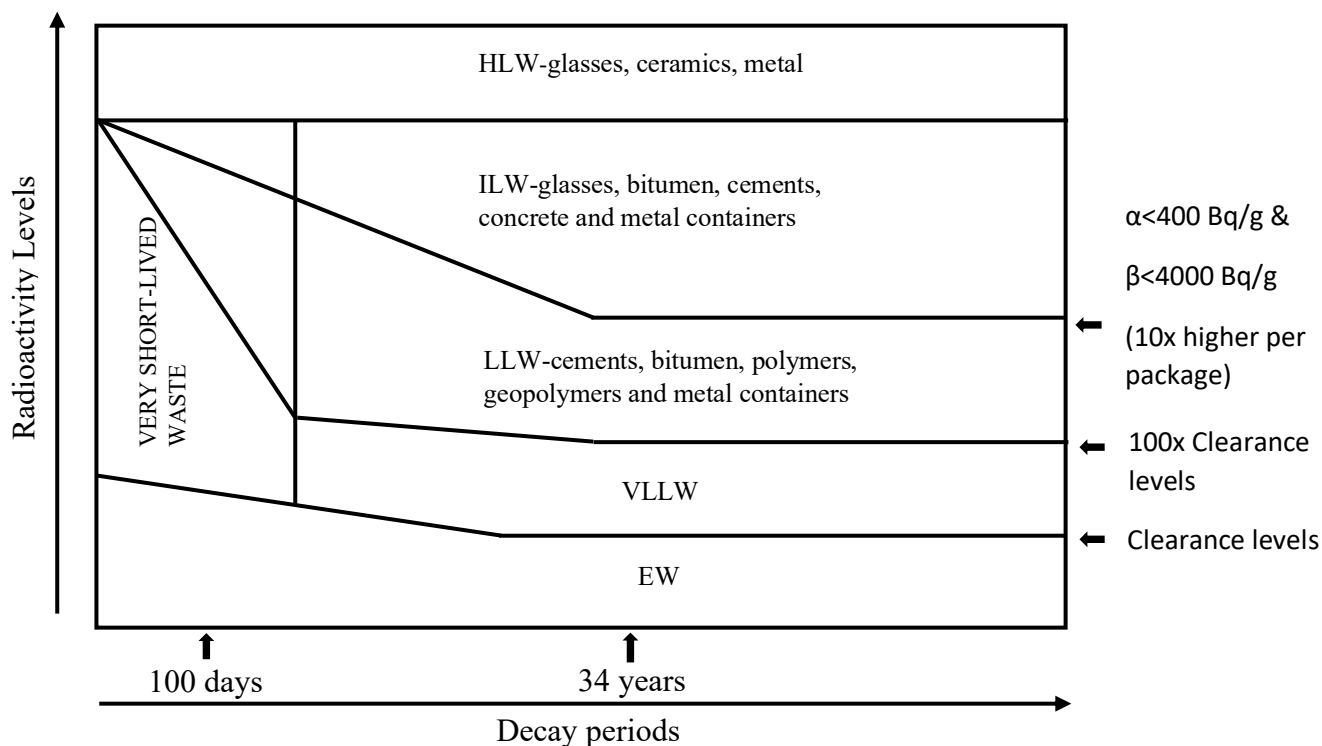
Fig. 2: Schematic of IAEA radioactive waste classification.

V. Basic Steps in Radioactive Waste Management

Bangladesh Atomic Energy Commission (BAEC) has established the Central Radioactive Waste Processing and Storage Facility (CWPS) on the campus of AERE, Savar under the Government Annual Development Project, and the IAEA Technical Co-operation Project. The function of this facility is to handle the low and intermediate level of radioactive waste except for high-level radioactive waste during the production of electricity in the nuclear power plant. Bangladesh and Russia together came to a decision

that Russia will take back the high-level radioactive waste. So, various stages should be required to perform the function of this facility. They can be categorized into the following steps:

a) Characterization

The characterization of radioactive waste is the first and foremost thing because it is necessary to determine whether it is in physical or chemical states. It is an essential parameter to enable dissociation of radioactive waste for demobilization, recycle, and transfer or disposal. Low-level waste can be disposed of near-surface level, but high-level waste will require the deep geological facility.

b) Reduction

Generation-3+ VVER-1200 model is modern technology, which would be helpful to reduce the amount of radioactive waste just because of its easy maintenance.

c) Reprocessing and packaging

During the production of electricity, radioactive waste emerges in the form of liquid, solid, and gaseous. By super compacting, low-level solid waste and intermediate-level solid waste can turn into much smaller volumes, but the main issue is liquid waste can't be disposed of. Filtration and ion exchange are vital to remove radioactive material from liquid and then transform it into solid. Typical immobilization methods include solidification of low and intermediate-level radioactive waste in cement or polymer and vitrification of high-level liquid waste in a glass matrix. After applying this method, low-level waste and intermediate-level waste can be packaged in the steel containers.

d) Storage

It is a vital part of the processing of waste management to avoid further any chance of radiation, which can devastate the environment. Radioactive isotopes disintegrate from few minutes to hundreds of years depends entirely on its half-life. As an example, strontium-90 and cesium-137 have half-lives of 30 years, whereas plutonium-239 has a half-life of 24,000years. Most nuclear-spent fuel, which has not been reprocessed, is safely stored in a specially designed pool at the reactor site. After some years it can be stored in some steel containers.

e) Disposal

It is the most challenging task of waste management yet all over the world. A deep and stable geologic location is the appropriate selection to store radioactive waste for the long-term. In this method, at first, the appropriate geologic place needs to be selected appropriately and excavate to form long tunnels under the surface using traditional mining technology. Then radioactive wastes need to be placed there safely far from the human population. But the technique is still under observation. If any geological changing occurs like an earthquake, then it would be a massive disaster because the stored nuclear waste has the potential to leak into the environment. Recently Germany is working on this, and they are expecting to place radioactive waste in a long tunnel from 2027. According to this plan, the path of the concrete tunnel will be closed completely by cement barrage so that radioactive isotopes can disintegrate. Another kind of geologic disposal is storing radioactive waste under the deep ocean. But this method is even riskier because it would be difficult to monitor for leakage of radioactive waste and the management of the whole procedure. Disposal of radioactive waste is still under investigation, and it won't be a simple task for a third world country like Bangladesh.

The waste management of RNPP can be sorted out according to these steps:
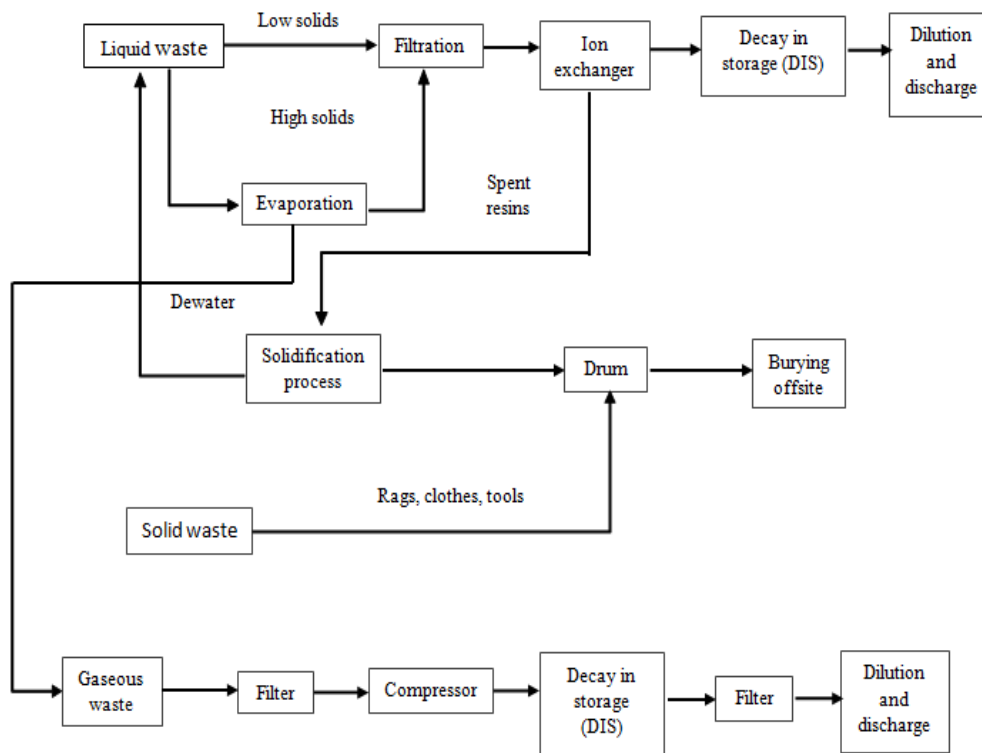
Fig. 3: Block diagram of radioactive waste handling system.

VI. TREATMENT OF LIQUID RADIOACTIVE WASTE

Different radioactive waste streams arise (usually contains soluble and insoluble radioactive components) during the generation of electricity in a nuclear power plant. This steam is different, depend on the amount of liquid waste generated and the activity content as well. The main sources of liquid radioactive waste are water from the fuel storage pools and the primary coolant in water-cooled reactors. According to the reactor type, the formation of the liquid radioactive waste varies, which contains boric acid or organic substance that need individual disposition. The essential treatment and conditioning of liquid radioactive waste are ion sorption, chemical precipitation, evaporation, cementation, membrane process, polymerization, bituminization.

The schematic representation of liquid radioactive waste management operations is given below:
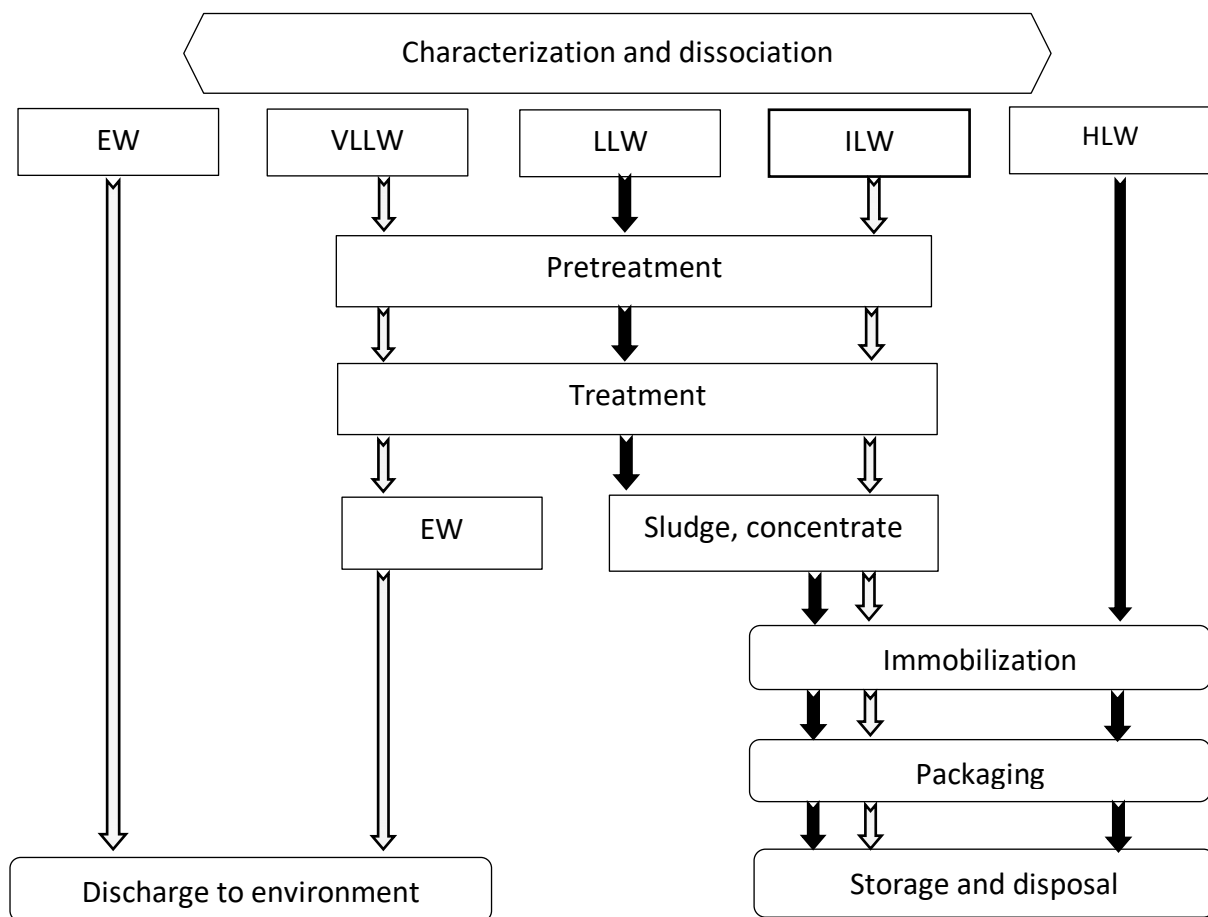
Fig. 4: Schematic representation of liquid radioactive waste management operations.

- Chemical precipitation process

One of the primary methods of radioactive waste management is to dispel radioactive materials from liquid waste. Chemical treatment or precipitation is one of the removal processes by which the majority of liquid waste could be reprocessed and dismiss to the surrounding without any risk. This method is mainly used in the VVER-1200 model nuclear power plant, which is based on the coagulation-flocculation segregation principle. It is generally used to treat high volume, low-level liquid waste streams. Most radionuclides can be precipitated by calcium or iron phosphate, barium sulfate, sodium sulfate, copper sulfate, cobalt sulfide, calcium carbonate, sodium borohydride, etc. Those precipitated chemicals treat the low-levels liquid waste (37-3.7×10^6 Bq/L) containing activity Strontium-90 and cesium-137 as the prime radionuclides. The resulting sludge from a combination of clarification and flocculation is concentrated by transfusion, filtration, and separating substances of

different densities by centrifuge. Mainly a chemical precipitation process comprises four stages:

➔ Addition of reagents, adjustment of pH to form the precipitate.

➔ Coagulation-flocculation
➔ Alluviation
➔ Solid-liquid segregation.

Table-2: Typical chemical reagents used in precipitation processes-

Radionuclide	Process agent	pH	Decontamination factor
Pu, Am	Hydroxides	7-12	>10^3
	Oxalates	1	>10^3
Cr	Ferrous hydroxide	≥8.5	>10^2
Mn	Manganese hydroxide	≥8.5	>10^2
	Manganese dioxide	≥8.5	>10^2
Co, Fe	Ferrous or ferric hydroxides	≥8.5	>10^2
Sr	Calcium or iron phosphate	>11	>10^2
	Calcium carbonate	10.5	>10^2
	Barium sulphate	≥8.5	>10^2
Zr, Nb, Ce	Hydroxides	>8.5	10^2-10^3
Sb	Ferrous hydroxides	5-8.5	5-10
	Titanium hydroxide	5-8.5	10-10^2
	Diuranate	8.5-10.5	20-30
Ru	Copper + ferrous hydroxide	8.5	10-25
	Cobalt sulfide	1-8.5	30-150
	Sodium borohydride	8.5	50
Cs	Ferrocyanide	6-10	>10^2
	Zeolite	7-11	10
	Tetraphenylborate	1-13	10^2-10^3
	Phosphotungstic acid	1	>10^2

- Ion exchange process

Ion exchange is standardized and has a widespread application in the treatment methods for the management of liquid radioactive waste at nuclear power plants. It is so efficient at transferring the radioactive content of a large volume of liquid into a small volume of solid. Vermiculite is the natural minerals that are widely used for decontamination of cesium-137 in effluents in spent fuel storage pool water. Ion exchangers carry exchangeable ions which can be interchanged by an equal number of positive or negative ions when the ion exchanger is in contact with a liquid that contains ions and conducts electricity easily. The positively charged functional groups involve anions, and similarly, when they negatively charged, they involve cations. According to the following equation:

$$R – H + Cs+ \leftrightarrow R – Cs + H+$$
.
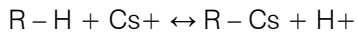
Where R is the insoluble matrix of the ion exchange resin, hydrogen releases its hydrogen ion into the solution and takes cesium ion from this solution. Here electroneutrality is maintained because every $Cs+$ dispelled from solution is replaced by an $H+$.

To remove radioactive metals from liquid radioisotopes are concentrated onto the $Fe(OH)3$. The resulting sludge should be placed in a metal drum before being mixed with cement to form a solid waste. Ion exchange properties of zeolite are the possible solution for low-level and intermediate-level liquid waste treatment. The ion exchange with the sodium ions of zeolite can dispel the cationic radioisotopes.

Table-3: pK values for the most common functional groups of organic ion exchangers

Cation Exchangers		Anion Exchangers	
Functional group	pK	Functional group	pK
-SO3H (strong acidic)	1-2	≡N+ (strong basic)	1-2
–PO3H2	2-5	=N	4-6
–COOH	4-6	=NH	6-8
–OH (weak acidic)	9-10	–NH2 (weak basic)	8-10

- Evaporation process

When liquid radioactive waste has a high concentration of radionuclides as well as high decontamination factor (e.g. 10^4-10^6), it is convenient to concentrate the liquid waste by using vaporization. This process is widely using in the nuclear power plant, which is entirely based on the thermosiphon system to minimize maintenance problems. Two-stage evaporation is inevitable to perform this process, one stage is decontamination, and the other is concentration. The first stage can be applied when the required decontamination factor is lower. While evaporating distilled water (high purity), non-volatile components such as radionuclides and salts remain. The presence of stabilized components such as ruthenium, iodine, high concentration of HNO3 reduces the high decontamination factor clearly. Though evaporation is a common practice all over the world; it has some disadvantageous too. The large size of apparatus, high maintenance costs, requires exposure of enormous surfaces of liquid, temperature enhanced rapidly are the main disadvantages of evaporation.

- Cementation process

This method has been practiced for immobilization of low-level radioactive waste concentrates on the nuclear power plant for more than 40 years. The cementation process has some advantages due to the availability of cement, inexpensive raw material, low volume reduction, operational simplicity, thermal stability, provide better radiation resistance, and based on traditional technology. Cementation is one of the conventional processes of converting liquid radioactive waste into a solid for long term storage or disposal. Some common types of cement such as pozzolanic cement, high alumina cement, ordinary Portland cement, blast furnace slag cement is used in power plants all over the world. The application of some cement is listed below for further study.

Table-4: Application of cement types

Cement type	Application
Ordinary Portland cement	very high chloride and sulfate resistant, organic ion exchange materials, inorganic ion exchange materials and secondary process waste (dry and wet)
Pozzolanic cement	hydraulic structures-dams, retaining walls, lower permeability, increased strength
High alumina cement	Rapid hardening and strength, marine construction and sewer infrastructure, increased resistance to sulfate and acid attack
Blast furnace slag cement	good resistance towards sulphate and chloride attack, greater durability and reduced permeability due to fineness

Ordinary Portland cement is the conventional type of cement that has been using in the nuclear power plant due to its high mechanical strength. In the cementation process, the waste, water, and additives are dosed from a tank into the fiber-reinforced concrete container or drum. Then cement is added to the waste loaded drum and mix with the waste carefully. The ratio of water and cement is generally 0.4 for an ideal mixer coating, which provides for better cleaning. Radioactive waste becomes half, and due to the volume increase by the cementation process. Through this process, low and intermediate level liquid waste can be processed conveniently without risk.

- Bituminization process

Bituminization is a common process for the treatment of low and intermediate-level waste. It is a hot process where radioactive concentrates are mixed with bitumen such as direct distilled, oxidized, emulsion at high temperatures. Insolubility in water, chemical inertness, high incorporation capacity, and reasonable cost are some advantages of the bituminization process. Batch bituminization and continuous bituminization processes are the two types of bituminization process.

Batch bituminization is the conventional process where liquid waste mixed with bitumen at about 200°C. If any water present, volatilization continues until reaching the required waste composition. After cooling, the mixture becomes solid and is then discharged into steel containers.

Though it has many disadvantageous over advantageous such as lower stability against radiation than cement, reacts with sodium nitrate, it decreases in viscosity at 70°C and few more made this process obsolete.

- Membrane process

Various membrane processes like ultra-filtration, dialysis, pervaporation, and reverse osmosis have been developed for the treatment of low-level (37–3.7×106 Bq/L) liquid waste. The removal of radioactive substances in membrane processes is convenient so that the nuclear industry adopts this process. Reverse osmosis is asymmetric 'skin type' membrane, which follows the diffusion mechanism method. Ultra-filtration is an asymmetric microporous type membrane that follows sieving mechanism method. Ultra-filtration processes can operate as highly efficient "sieves," capable of fractionating particle species according to size. Some advantages of this process are efficacious at low temperatures, lower energy requirement, simple to scale up, and most of all, no phase changes involved.

VII. TREATMENT OF SOLID RADIOACTIVE WASTE

Radioactive solid wastes producing from the nuclear power plant are segregated into compressible or non-compressible and combustible or noncombustible. Compressible waste, e.g., paper, clothing, plastics undergo low-pressure compaction and non-compressible waste, e.g., scrap metal, rubble, and mineral insulating material undergo high-pressure compaction and are packed in suitable containers.

These wastes are classified depending on the concentration of the wastes and half-life of the radioactivity. 95% of the total solid waste has low activity and convenient to handle rather than high activity. Some treatment and conditioning of solid radioactive waste are low force compaction, super force compaction, incineration, pyrolysis, plasma, metal melting, molten salt oxidation, thermochemical, etc. The schematic representation of solid radioactive waste management operations is given below:
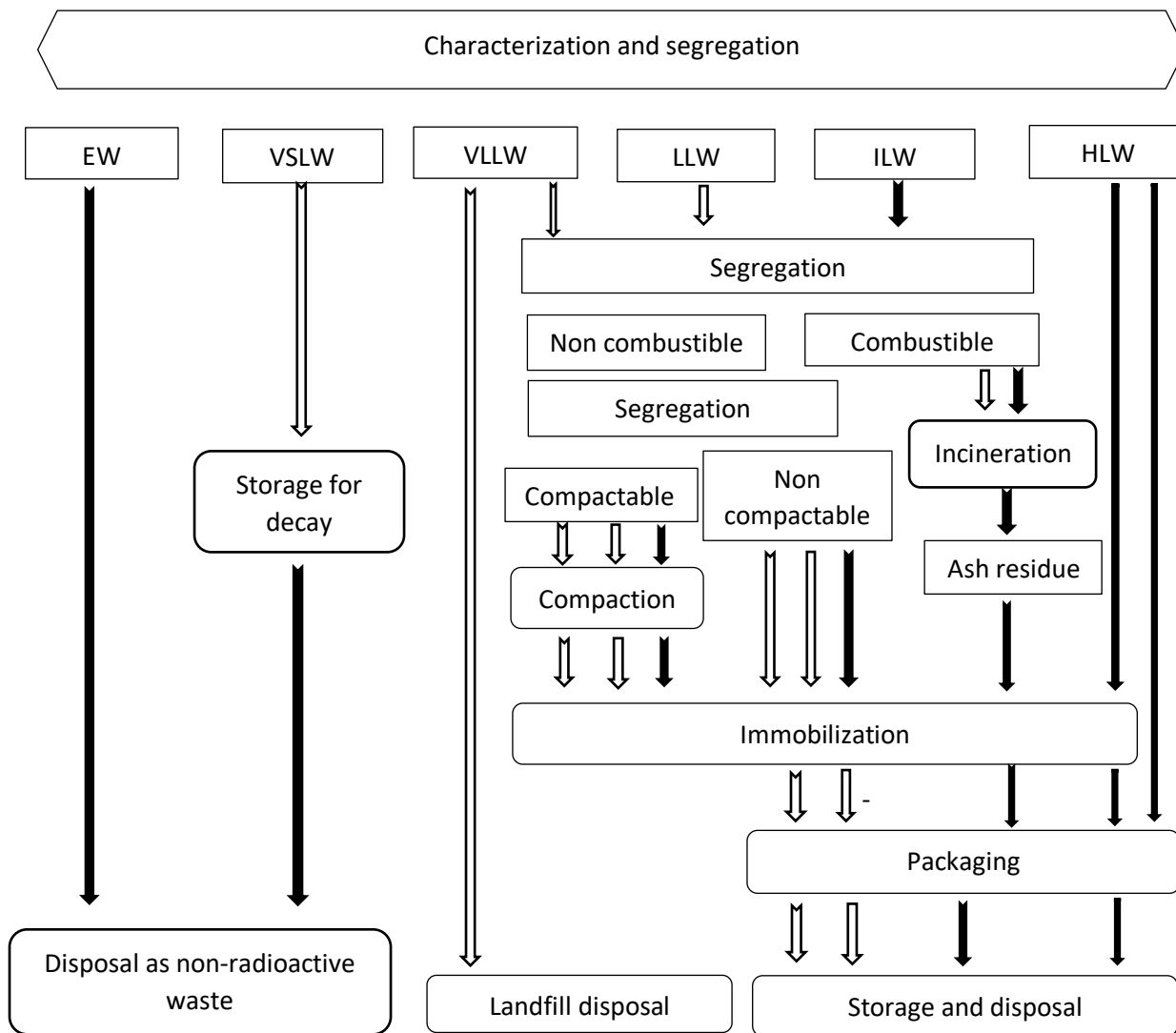
Fig. 5: Schematic representation of solid radioactive waste management operations.

- Low and super force compaction

Compaction reduces the total volume of LIL solid waste without changing physical and chemical properties and becomes economical for transporting. Low and super force are two types of compaction. Low force compaction is a renowned method for compactible low-level solid waste, and the compaction force is up to 50 tones. Radioactive solid waste can be compacted up to several levels by this method and the waste is collected in suitable containers. A volume reduction factor of low force compaction is (3-5), entirely depends on the volume and nature of the waste material. Though this process is facile to operate and relatively lucrative, its volume reduction factor is limited by spring back. Super force compaction is used for previously compacted waste as well as for incinerator

ash, air filters, small metal pieces, soft plastics, thermal insulation materials. It has a high-volume reduction factor (5-10), and the compaction force is up to 2000 tons. Generally, this method is not lucrative for small amounts of waste because of its high equipment and maintenance cost.

- Incineration

Incineration is the well-proven technology, and combustible solids from nuclear power plants are reduced by this method. This provides a very high-volume reduction factor for combustible waste such as plastics, fabrics, paper, etc. and can be used for both solid and liquid wastes as well as for biohazardous and medical waste. Relatively high capital cost for investment, need to meet the environmental requirements for discharges, requiring a special regime for the treatment of alpha bearing waste are the main disadvantages of incineration method.

- Pyrolysis

Pyrolysis is a common way to process the high organic content waste such as charcoal, resins, plastic, etc. It is an irreversible process which occurs at temperatures above 800°F in the absence of oxygen and under pressure. Retention of radioactivity in the pyrolyzer residue is > 99.99% and has low gas flow rates compared to incineration. So that, this process easily manages the end product. The processes can be heated externally, thus minimizing gas flows, which would otherwise require radiological control. Slow, flash, and fast pyrolysis are the three types of the pyrolysis process. Slow pyrolysis occurs at a slow heating rate; low temperatures range from 32.18 to 35.6°F per second. Flash pyrolysis occurs at a high heating rate; high temperatures compared to slow pyrolysis ranges from 752 and 1112°F per second. When the amount of radioactive waste is excessive fast pyrolysis process is effective. Fast pyrolysis occurs at an extremely high heating rate, and high temperatures range from 1202 to 1832°F.

- Plasma

The plasma process temperature is up to 1800°C, which allows the melting of LIL radioactive waste. This process is suitable for long term storage and disposal. The final waste form is robust and free of organic material. Volume reduction factors of this process can range from 6:1 to 10:1 for metallic waste, while for other combustibles, the volume reduction factor (VRF) can rise as high as 100:1. But the process is a bit expensive to construct and not that easy to operate.

- Molten salt oxidation

Molten salt oxidation is an emerging technology that is an alternative to traditional incineration of organic waste. This process can be used for the destruction of organic content. Low temperature is required to operate this process. But it requires specialized techniques for adequate conditioning of the salt product. Limitation to small and medium solid waste programs and not capable of handling high-level waste materials are the major disadvantages.

VIII. Treatment of Gaseous Radioactive Waste

Noble gases (^{41}Ar, ^{85}Kr, ^{133}Xe), halogens, tritium, the radioiodines-129, and -131 and carbon-14 are the most principal volatile radionuclides as a form of radioactive gaseous waste is generated in the nuclear power plant. The amount of gaseous waste production entirely depends on the reactor type. Among the noble gases, ^{133}Xe, with its short half-life, is less dangerous and can be dissolved easily. The gaseous radioactive waste should be treated rightly before discharge to the surroundings. Because external exposure can cause severe damage to human tissue and can create other skin diseases. Ventilation and air cleaning system is the first and foremost process to remove most of the radioactive components before discharging. By this process, almost all radioactive particles remove (about 99.9%). The cryogenic segregation method is becoming popular nowadays for the removal of ^{85}Kr and ^{133}Xe. The procedure of charcoal or adsorption can also remove the radioactive iodine. Oxidization is the convenient removal process for tritium to remove from waste effluents and converting the tritium to T_2O. Caustic scrubbing is used to remove carbon-14 from the gaseous effluents, and high-efficiency filtration techniques can be applied for the removal of radioactive particulate matter. After completing those tasks, the gas is contained into gas tanks and should be sealed for storage up to 60 days (depends on their radioactivity). Then release to the atmosphere properly through the ventilation system.

IX. Storage Facilities

Storage facilities for radioactive waste material are the crucial consideration of RNNP. Radioactive wastes are stored to make surrounding harmless and to avoid any subtle risk. Tons of radioactive waste are produced per month per nuclear reactor all over the world. So, it is assuming that tons of radioactive materials from RNNP needs temporary storage facilities. After storing high-level radioactive wastes, Russia will take back those waste for reprocessing. These days, different types of storage policies are taken all over the world. Discussion on some suitable storage facilities for RNPP are given below:

- Storage ponds

Centralized facilities such as CLAB in Sweden are using this type of storage system. This pond is generally 7-12 meters deep, and initial radioactive waste is kept under the water to conserve radioactive materials cool. The storage pond is specially situated at the

reactor site and designed for the cooling of the fuel rods. Such ponds are robust constructions made of thick reinforced concrete with steel liners. This pond provides protection shielding from radiation, can storage fuel 10 to 20 years easily, and then send for disposal or reprocessing.

- Dry cask storage

Dry cask storage has been using in one-third of the overall nuclear power plant in America. It is a well-known method of storing high-level radioactive materials using certain shielded transfer casks. It is designed as a safer solution to store radioactive waste that is better than storage ponds. This method is very functional for storage as well as transportation. Spent nuclear fuel that has already been cooled in ponds for at least five years can easily be stored in dry cask storage. Currently, the USA, Canada, Germany, Bulgaria, Lithuania, Russia, Ukraine are adopting this storing facility for high-level radioactive waste.

- Interim surface storage

Specially designed interim surface storage facilities are currently using to store 7000-8000 tons of spent fuel all over the world. It is one of the best temporary solutions to ensure the safe storage of IHLW for long-term disposal and convenient to monitor continuously. This storage facility not only allows spent fuel to cool but also uses as a final destination for reprocessing waste. The most radioactive waste is currently stored in France by this surface storage facility.

X. Disposal Options

Disposal of radioactive waste is the most challenging task for Bangladesh. Bangladesh relies on Russia that they will take back high-level radioactive waste from RNNP. Disposal of low and intermediate-level waste is quite simple to handle in terms of high-level waste. Almost 97% of radioactive waste is LILW, and the remaining 3% is difficult to store and dispose of. Disposal is the last and crucial part of the radioactive waste management process. When there is no intention to reprocess radioactive waste, the best option is disposal. It is mandatory to choose a disposal site suitably so that no natural disaster can cause a catastrophe. Based on sub-soil investigation and analysis on the natural disaster of Bangladesh, RNPP and its surrounding area of above 0.20g to 0.25g should withstand 7.5 to 9.5 Mw earthquakes easily. Finland, Sweden, France have made the most progress on final disposal. Recently Germany is working on a high-level radioactive waste disposal system, and they are expecting to place radioactive waste in a long tunnel from 2027. Some commonly accepted disposal options that Bangladesh can implement in the near future are given below:

- Near-surface disposal

Near-surface disposal facilities at ground level are on or below the earth's surface where the protective covering is of the order of a few meters thick (at depths of tens of meters). These facilities are suitable for handling low-level and intermediate-level waste types with limited amounts of short-lived activity. Generally, each nuclear facility has its near-surface disposal facility. Waste containers are stored in installed vaults and backfilled when the vaults are filled. Many countries, including Finland, the Netherlands, Sweden, Spain, France, the UK, and the USA has implemented this facility for LLW and ILW.

- Deep geological disposal

Deep and stable geologic location (at depths between 250m and 1000m for mined or somewhat more than 1000m) is the appropriate selection to store long-lived ILW and HLW for the long-term. Most countries have researched deep geological disposal, and now it is an official policy in several countries. In this process, a suitable geological site must first be chosen and excavated to form long concrete tunnels under the ground using conventional mining technology. And the concrete tunnel route will be perfectly closed by a cement bridge so that radioactive isotopes can disintegrate. Deep geological disposal system is implemented in the USA and the preferred sites selected in several countries, including Belgium, Canada, Finland, France, Japan, Russia, Spain, Sweden, the Czech Republic, Argentina, Australia, and the United Kingdom.

XI. Results and Discussions

Rooppur Nuclear Power Plant is based on the generation-3+ VVER-1200 model that has modern safety management. It is anticipating that RNPP can add up 2,400MW of electricity to the national grid by 2023, and that is needful to supply an adequate amount of electricity for Bangladesh. This research paper is based on a theoretical framework, and the objective is to demonstrate what would be the treatment of radioactive waste of forthcoming RNPP. RNPP will produce tons of radioactive waste, which is hazardous for humankind and the surroundings. Perfect reprocessing, packaging, storage and disposal is required to ensure the safety of the surroundings. LLW doesn't require shielding during handling, and so its disposal system is quite easy. But the remaining ILW and HLW waste require both indefectible storage and disposal facilities to avoid further any chance of radiation, which can devastate the environment. And inhaling ionizing radiation at high dose levels can increase the risk of cancer. Russia has agreed to take back the high-level radioactive waste from RNPP. However, Russia may charge Bangladesh the cost of transportation and reprocess of HLW. Though handling, storage, and disposal of LLW and ILW

pose no serious problem, Bangladesh will manage those radioactive waste. Bangladesh can also be self-standing in the management of HLW by doing the above procedures efficiently.

XII. Conclusion

The government of Bangladesh expressed its firm commitment to build a nuclear plant to reduce its dependence on conventional resources and provide a great amount of electricity. Radioactive waste is a byproduct of a nuclear power plant, and radioactive waste management is the biggest concern for Bangladesh. Bangladesh would certainly face up some limitations, such as costing a lot of money to transport radioactive waste; the waste might emerge even if put into geological respiratory and radiation risk to workers, etc. Bangladesh's government should take the necessary steps to overcome those limitations and ensure safety. So, the government, BAEC, and nuclear industry should work together to deliver perfect reprocessing, packaging, storage and disposal facilities, and ensure the safety of surroundings.

References Références Referencias

1. N. Khelurkar, S. Shah, and H. Jeswani, "A review of radioactive waste management," no. September, 2016.
2. K. Raj, K. K. Prasad, and N. K. Bansal, "Radioactive waste management practices in India," *Nucl. Eng. Des.*, vol. 236, no. 7–8, pp. 914–930, 2006.
3. R.O. Abdel Rahman, H. A. Ibrahium, and Y. T. Hung, "Liquid radioactive wastes treatment: A review," *Water (Switzerland)*, vol. 3, no. 2, pp. 551–565, 2011.
4. M. Montazer and D. Montazer, "Radioactive waste management of nuclear power plants," *Trans. Am. Nucl. Soc.*, vol. 100, no. 7, p. 175, 2009.
5. P. Plant, "Feasibility and Safety Study of Nuclear Power in Bangladesh: Perspective to Rooppur Nuclear," pp. 121–125.
6. J. Ferdous, A. Begum, and A. Islam, "Radioactivity of soil at proposed Rooppur Nuclear Power Plant site in Bangladesh," *Int. J. Radiat. Res.*, vol. 13, no. 2, pp. 135–142, 2015.
7. V. M. Efremenkov, "Radioactive waste management of nuclear power plants," *Trans. Am. Nucl. Soc.*, vol. 100, p. 175, 2009.
8. International Atomic Energy Agency, "Radioactive Waste Management Objectives," *IAEA Nucl. Energy Ser.*, vol. 18, no. 5, p. 32, 2011.
9. M. I. Ojovan, *Radioactive waste characterization and selection of processing technologies*. Woodhead Publishing Limited, 2011.
10. International Atomic Energy Agency, "Application of Ion Exchange Processes for the Treatment of Radioactive Waste and Management of Spent Ion Exchangers," *Tech. reports Ser. No.408*, no. 408, p. 115, 2002.
11. S. Kumar, S.S. Ali, M. Chander, N.K. Bansal, and K. Balu, "Integrated Radioactive Waste Management from NPP, Research Reactor and Back End of Nuclear Fuel Cycle- An Indian Experience," vol. 17, no. 17 2, pp. 1–8.
12. "Disposal of Nuclear Waste: Methods and Concerns." [Online]. Available: http://large.stanford.edu/courses/2013/ph241/xie2/. [Accessed: 18-Dec-2019].
13. "Bangladesh 2018." [Online]. Available: https://www-pub.iaea.org/MTCD/Publications/PDF/cnpp2018/countryprofiles/Bangladesh/Bangladesh.htm. [Accessed: 18-Dec-2019].
14. "Chemical Precipitation - an overview | Science Direct Topics." [Online]. Available: https://www.sciencedirect.com/topics/engineering/chemical-precipitation. [Accessed: 18-Dec-2019].
15. "Solid Radioactive Waste - an overview | ScienceDirect Topics." [Online]. Available: https://www.sciencedirect.com/topics/chemistry/solid-radioactive-waste. [Accessed: 18-Dec-2019].
16. "Liquid Radioactive Waste - an overview | ScienceDirect Topics." [Online]. Available: https://www.sciencedirect.com/topics/engineering/liquid-radioactive-waste. [Accessed: 18-Dec-2019].
17. "Radioactive waste - Wikipedia." [Online]. Available: https://en.wikipedia.org/wiki/Radioactive_waste.
18. "Rooppur Nuclear Power Plant - Wikipedia." [Online]. Available: https://en.wikipedia.org/wiki/Rooppur_Nuclear_Power_Plant.

GLOBAL JOURNALS GUIDELINES HANDBOOK 2019

WWW.GLOBALJOURNALS.ORG

Fellows

FELLOW OF ASSOCIATION OF RESEARCH SOCIETY IN ENGINEERING (FARSE)

Global Journals Incorporate (USA) is accredited by Open Association of Research Society (OARS), U.S.A and in turn, awards "FARSE" title to individuals. The 'FARSE' title is accorded to a selected professional after the approval of the Editor-in-Chief /Editorial Board Members/Dean.

> The "FARSE" is a dignified title which is accorded to a person's name viz. Dr. John E. Hall, Ph.D., FARSE or William Walldroff, M.S., FARSE.

FARSE accrediting is an honor. It authenticates your research activities. After recognition as FARSE, you can add 'FARSE' title with your name as you use this recognition as additional suffix to your status. This will definitely enhance and add more value and repute to your name. You may use it on your professional Counseling Materials such as CV, Resume, and Visiting Card etc.

The following benefits can be availed by you only for next three years from the date of certification:

FARSE designated members are entitled to avail a 40% discount while publishing their research papers (of a single author) with Global Journals Incorporation (USA), if the same is accepted by Editorial Board/Peer Reviewers. If you are a main author or co-author in case of multiple authors, you will be entitled to avail discount of 10%.

Once FARSE title is accorded, the Fellow is authorized to organize a symposium/seminar/conference on behalf of Global Journal Incorporation (USA).The Fellow can also participate in conference/seminar/symposium organized by another institution as representative of Global Journal. In both the cases, it is mandatory for him to discuss with us and obtain our consent.

You may join as member of the Editorial Board of Global Journals Incorporation (USA) after successful completion of three years as Fellow and as Peer Reviewer. In addition, it is also desirable that you should organize seminar/symposium/conference at least once.

We shall provide you intimation regarding launching of e-version of journal of your stream time to time.This may be utilized in your library for the enrichment of knowledge of your students as well as it can also be helpful for the concerned faculty members.

The FARSE can go through standards of OARS. You can also play vital role if you have any suggestions so that proper amendment can take place to improve the same for the benefit of entire research community.

As FARSE, you will be given a renowned, secure and free professional email address with 100 GB of space e.g. johnhall@globaljournals.org. This will include Webmail, Spam Assassin, Email Forwarders,Auto-Responders, Email Delivery Route tracing, etc.
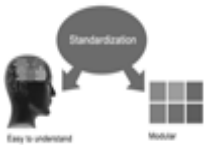
The FARSE will be eligible for a free application of standardization of their researches. Standardization of research will be subject to acceptability within stipulated norms as the next step after publishing in a journal. We shall depute a team of specialized research professionals who will render their services for elevating your researches to next higher level, which is worldwide open standardization.

The FARSE member can apply for grading and certification of standards of their educational and Institutional Degrees to Open Association of Research, Society U.S.A. Once you are designated as FARSE, you may send us a scanned copy of all of your credentials. OARS will verify, grade and certify them. This will be based on your academic records, quality of research papers published by you, and some more criteria. After certification of all your credentials by OARS, they will be published on your Fellow Profile link on website https://associationofresearch.org which will be helpful to upgrade the dignity.

The FARSE members can avail the benefits of free research podcasting in Global Research Radio with their research documents. After publishing the work, (including published elsewhere worldwide with proper authorization) you can upload your research paper with your recorded voice or you can utilize chargeable services of our professional RJs to record your paper in their voice on request.

The FARSE member also entitled to get the benefits of free research podcasting of their research documents through video clips. We can also streamline your conference videos and display your slides/ online slides and online research video clips at reasonable charges, on request.

The FARSE is eligible to earn from sales proceeds of his/her researches/reference/review Books or literature, while publishing with Global Journals. The FARSE can decide whether he/she would like to publish his/her research in a closed manner. In this case, whenever readers purchase that individual research paper for reading, maximum 60% of its profit earned as royalty by Global Journals, will be credited to his/her bank account. The entire entitled amount will be credited to his/her bank account exceeding limit of minimum fixed balance. There is no minimum time limit for collection. The FARSE member can decide its price and we can help in making the right decision.

The FARSE member is eligible to join as a paid peer reviewer at Global Journals Incorporation (USA) and can get remuneration of 15% of author fees, taken from the author of a respective paper. After reviewing 5 or more papers you can request to transfer the amount to your bank account.

MEMBER OF ASSOCIATION OF RESEARCH SOCIETY IN ENGINEERING (MARSE)

The 'MARSE ' title is accorded to a selected professional after the approval of the Editor-in-Chief / Editorial Board Members/Dean.

The "MARSE" is a dignified ornament which is accorded to a person's name viz. Dr. John E. Hall, Ph.D., MARSE or William Walldroff, M.S., MARSE.

MARSE accrediting is an honor. It authenticates your research activities. After becoming MARSE, you can add 'MARSE' title with your name as you use this recognition as additional suffix to your status. This will definitely enhance and add more value and repute to your name. You may use it on your professional Counseling Materials such as CV, Resume, Visiting Card and Name Plate etc.

The following benefitscan be availed by you only for next three years from the date of certification.

MARSE designated members are entitled to avail a 25% discount while publishing their research papers (of a single author) in Global Journals Inc., if the same is accepted by our Editorial Board and Peer Reviewers. If you are a main author or co-author of a group of authors, you will get discount of 10%.

As MARSE, you will be given a renowned, secure and free professional email address with 30 GB of space e.g. johnhall@globaljournals.org. This will include Webmail, Spam Assassin, Email Forwarders,Auto-Responders, Email Delivery Route tracing, etc.

We shall provide you intimation regarding launching of e-version of journal of your stream time to time.This may be utilized in your library for the enrichment of knowledge of your students as well as it can also be helpful for the concerned faculty members.

The MARSE member can apply for approval, grading and certification of standards of their educational and Institutional Degrees to Open Association of Research, Society U.S.A.

Once you are designated as MARSE, you may send us a scanned copy of all of your credentials. OARS will verify, grade and certify them. This will be based on your academic records, quality of research papers published by you, and some more criteria.

It is mandatory to read all terms and conditions carefully.

Auxiliary Memberships

Institutional Fellow of Open Association of Research Society (USA)-OARS (USA)

Global Journals Incorporation (USA) is accredited by Open Association of Research Society, U.S.A (OARS) and in turn, affiliates research institutions as "Institutional Fellow of Open Association of Research Society" (IFOARS).

The "FARSC" is a dignified title which is accorded to a person's name viz. Dr. John E. Hall, Ph.D., FARSC or William Walldroff, M.S., FARSC.

The IFOARS institution is entitled to form a Board comprised of one Chairperson and three to five board members preferably from different streams. The Board will be recognized as "Institutional Board of Open Association of Research Society"-(IBOARS).

The Institute will be entitled to following benefits:

The IBOARS can initially review research papers of their institute and recommend them to publish with respective journal of Global Journals. It can also review the papers of other institutions after obtaining our consent. The second review will be done by peer reviewer of Global Journals Incorporation (USA) The Board is at liberty to appoint a peer reviewer with the approval of chairperson after consulting us.

The author fees of such paper may be waived off up to 40%.

The Global Journals Incorporation (USA) at its discretion can also refer double blind peer reviewed paper at their end to the board for the verification and to get recommendation for final stage of acceptance of publication.

The IBOARS can organize symposium/seminar/conference in their country on behalf of Global Journals Incorporation (USA)-OARS (USA). The terms and conditions can be discussed separately.

The Board can also play vital role by exploring and giving valuable suggestions regarding the Standards of "Open Association of Research Society, U.S.A (OARS)" so that proper amendment can take place for the benefit of entire research community. We shall provide details of particular standard only on receipt of request from the Board.

The board members can also join us as Individual Fellow with 40% discount on total fees applicable to Individual Fellow. They will be entitled to avail all the benefits as declared. Please visit Individual Fellow-sub menu of GlobalJournals.org to have more relevant details.

We shall provide you intimation regarding launching of e-version of journal of your stream time to time. This may be utilized in your library for the enrichment of knowledge of your students as well as it can also be helpful for the concerned faculty members.

After nomination of your institution as "Institutional Fellow" and constantly functioning successfully for one year, we can consider giving recognition to your institute to function as Regional/Zonal office on our behalf.
The board can also take up the additional allied activities for betterment after our consultation.

The following entitlements are applicable to individual Fellows:

Open Association of Research Society, U.S.A (OARS) By-laws states that an individual Fellow may use the designations as applicable, or the corresponding initials. The Credentials of individual Fellow and Associate designations signify that the individual has gained knowledge of the fundamental concepts. One is magnanimous and proficient in an expertise course covering the professional code of conduct, and follows recognized standards of practice.

Open Association of Research Society (US)/ Global Journals Incorporation (USA), as described in Corporate Statements, are educational, research publishing and professional membership organizations. Achieving our individual Fellow or Associate status is based mainly on meeting stated educational research requirements.

Disbursement of 40% Royalty earned through Global Journals : Researcher = 50%, Peer Reviewer = 37.50%, Institution = 12.50% E.g. Out of 40%, the 20% benefit should be passed on to researcher, 15 % benefit towards remuneration should be given to a reviewer and remaining 5% is to be retained by the institution.

We shall provide print version of 12 issues of any three journals [as per your requirement] out of our 38 journals worth $ 2376 USD.

Other:

The individual Fellow and Associate designations accredited by Open Association of Research Society (US) credentials signify guarantees following achievements:

➢ The professional accredited with Fellow honor, is entitled to various benefits viz. name, fame, honor, regular flow of income, secured bright future, social status etc.

- In addition to above, if one is single author, then entitled to 40% discount on publishing research paper and can get 10%discount if one is co-author or main author among group of authors.
- The Fellow can organize symposium/seminar/conference on behalf of Global Journals Incorporation (USA) and he/she can also attend the same organized by other institutes on behalf of Global Journals.
- The Fellow can become member of Editorial Board Member after completing 3yrs.
- The Fellow can earn 60% of sales proceeds from the sale of reference/review books/literature/publishing of research paper.
- Fellow can also join as paid peer reviewer and earn 15% remuneration of author charges and can also get an opportunity to join as member of the Editorial Board of Global Journals Incorporation (USA)
- • This individual has learned the basic methods of applying those concepts and techniques to common challenging situations. This individual has further demonstrated an in–depth understanding of the application of suitable techniques to a particular area of research practice.

Note :

"
- In future, if the board feels the necessity to change any board member, the same can be done with the consent of the chairperson along with anyone board member without our approval.

- In case, the chairperson needs to be replaced then consent of 2/3rd board members are required and they are also required to jointly pass the resolution copy of which should be sent to us. In such case, it will be compulsory to obtain our approval before replacement.

- In case of "Difference of Opinion [if any]" among the Board members, our decision will be final and binding to everyone.
"

Preferred Author Guidelines

We accept the manuscript submissions in any standard (generic) format.

We typeset manuscripts using advanced typesetting tools like Adobe In Design, CorelDraw, TeXnicCenter, and TeXStudio. We usually recommend authors submit their research using any standard format they are comfortable with, and let Global Journals do the rest.

Alternatively, you can download our basic template from https://globaljournals.org/Template.zip

Authors should submit their complete paper/article, including text illustrations, graphics, conclusions, artwork, and tables. Authors who are not able to submit manuscript using the form above can email the manuscript department at submit@globaljournals.org or get in touch with chiefeditor@globaljournals.org if they wish to send the abstract before submission.

Before and during Submission

Authors must ensure the information provided during the submission of a paper is authentic. Please go through the following checklist before submitting:

1. Authors must go through the complete author guideline and understand and *agree to Global Journals' ethics and code of conduct,* along with author responsibilities.
2. Authors must accept the privacy policy, terms, and conditions of Global Journals.
3. Ensure corresponding author's email address and postal address are accurate and reachable.
4. Manuscript to be submitted must include keywords, an abstract, a paper title, co-author(s') names and details (email address, name, phone number, and institution), figures and illustrations in vector format including appropriate captions, tables, including titles and footnotes, a conclusion, results, acknowledgments and references.
5. Authors should submit paper in a ZIP archive if any supplementary files are required along with the paper.
6. Proper permissions must be acquired for the use of any copyrighted material.
7. Manuscript submitted *must not have been submitted or published elsewhere* and all authors must be aware of the submission.

Declaration of Conflicts of Interest

It is required for authors to declare all financial, institutional, and personal relationships with other individuals and organizations that could influence (bias) their research.

Policy on Plagiarism

Plagiarism is not acceptable in Global Journals submissions at all.

Plagiarized content will not be considered for publication. We reserve the right to inform authors' institutions about plagiarism detected either before or after publication. If plagiarism is identified, we will follow COPE guidelines:

Authors are solely responsible for all the plagiarism that is found. The author must not fabricate, falsify or plagiarize existing research data. The following, if copied, will be considered plagiarism:

- Words (language)
- Ideas
- Findings
- Writings
- Diagrams
- Graphs
- Illustrations
- Lectures

- Printed material
- Graphic representations
- Computer programs
- Electronic material
- Any other original work

AUTHORSHIP POLICIES

Global Journals follows the definition of authorship set up by the Open Association of Research Society, USA. According to its guidelines, authorship criteria must be based on:

1. Substantial contributions to the conception and acquisition of data, analysis, and interpretation of findings.
2. Drafting the paper and revising it critically regarding important academic content.
3. Final approval of the version of the paper to be published.

Changes in Authorship

The corresponding author should mention the name and complete details of all co-authors during submission and in manuscript. We support addition, rearrangement, manipulation, and deletions in authors list till the early view publication of the journal. We expect that corresponding author will notify all co-authors of submission. We follow COPE guidelines for changes in authorship.

Copyright

During submission of the manuscript, the author is confirming an exclusive license agreement with Global Journals which gives Global Journals the authority to reproduce, reuse, and republish authors' research. We also believe in flexible copyright terms where copyright may remain with authors/employers/institutions as well. Contact your editor after acceptance to choose your copyright policy. You may follow this form for copyright transfers.

Appealing Decisions

Unless specified in the notification, the Editorial Board's decision on publication of the paper is final and cannot be appealed before making the major change in the manuscript.

Acknowledgments

Contributors to the research other than authors credited should be mentioned in Acknowledgments. The source of funding for the research can be included. Suppliers of resources may be mentioned along with their addresses.

Declaration of funding sources

Global Journals is in partnership with various universities, laboratories, and other institutions worldwide in the research domain. Authors are requested to disclose their source of funding during every stage of their research, such as making analysis, performing laboratory operations, computing data, and using institutional resources, from writing an article to its submission. This will also help authors to get reimbursements by requesting an open access publication letter from Global Journals and submitting to the respective funding source.

PREPARING YOUR MANUSCRIPT

Authors can submit papers and articles in an acceptable file format: MS Word (doc, docx), LaTeX (.tex, .zip or .rar including all of your files), Adobe PDF (.pdf), rich text format (.rtf), simple text document (.txt), Open Document Text (.odt), and Apple Pages (.pages). Our professional layout editors will format the entire paper according to our official guidelines. This is one of the highlights of publishing with Global Journals—authors should not be concerned about the formatting of their paper. Global Journals accepts articles and manuscripts in every major language, be it Spanish, Chinese, Japanese, Portuguese, Russian, French, German, Dutch, Italian, Greek, or any other national language, but the title, subtitle, and abstract should be in English. This will facilitate indexing and the pre-peer review process.

The following is the official style and template developed for publication of a research paper. Authors are not required to follow this style during the submission of the paper. It is just for reference purposes.

Manuscript Style Instruction (Optional)

- Microsoft Word Document Setting Instructions.
- Font type of all text should be Swis721 Lt BT.
- Page size: 8.27" x 11'", left margin: 0.65, right margin: 0.65, bottom margin: 0.75.
- Paper title should be in one column of font size 24.
- Author name in font size of 11 in one column.
- Abstract: font size 9 with the word "Abstract" in bold italics.
- Main text: font size 10 with two justified columns.
- Two columns with equal column width of 3.38 and spacing of 0.2.
- First character must be three lines drop-capped.
- The paragraph before spacing of 1 pt and after of 0 pt.
- Line spacing of 1 pt.
- Large images must be in one column.
- The names of first main headings (Heading 1) must be in Roman font, capital letters, and font size of 10.
- The names of second main headings (Heading 2) must not include numbers and must be in italics with a font size of 10.

Structure and Format of Manuscript

The recommended size of an original research paper is under 15,000 words and review papers under 7,000 words. Research articles should be less than 10,000 words. Research papers are usually longer than review papers. Review papers are reports of significant research (typically less than 7,000 words, including tables, figures, and references)

A research paper must include:

a) A title which should be relevant to the theme of the paper.
b) A summary, known as an abstract (less than 150 words), containing the major results and conclusions.
c) Up to 10 keywords that precisely identify the paper's subject, purpose, and focus.
d) An introduction, giving fundamental background objectives.
e) Resources and techniques with sufficient complete experimental details (wherever possible by reference) to permit repetition, sources of information must be given, and numerical methods must be specified by reference.
f) Results which should be presented concisely by well-designed tables and figures.
g) Suitable statistical data should also be given.
h) All data must have been gathered with attention to numerical detail in the planning stage.

Design has been recognized to be essential to experiments for a considerable time, and the editor has decided that any paper that appears not to have adequate numerical treatments of the data will be returned unrefereed.

i) Discussion should cover implications and consequences and not just recapitulate the results; conclusions should also be summarized.
j) There should be brief acknowledgments.
k) There ought to be references in the conventional format. Global Journals recommends APA format.

Authors should carefully consider the preparation of papers to ensure that they communicate effectively. Papers are much more likely to be accepted if they are carefully designed and laid out, contain few or no errors, are summarizing, and follow instructions. They will also be published with much fewer delays than those that require much technical and editorial correction.

The Editorial Board reserves the right to make literary corrections and suggestions to improve brevity.

FORMAT STRUCTURE

It is necessary that authors take care in submitting a manuscript that is written in simple language and adheres to published guidelines.

All manuscripts submitted to Global Journals should include:

Title

The title page must carry an informative title that reflects the content, a running title (less than 45 characters together with spaces), names of the authors and co-authors, and the place(s) where the work was carried out.

Author details

The full postal address of any related author(s) must be specified.

Abstract

The abstract is the foundation of the research paper. It should be clear and concise and must contain the objective of the paper and inferences drawn. It is advised to not include big mathematical equations or complicated jargon.

Many researchers searching for information online will use search engines such as Google, Yahoo or others. By optimizing your paper for search engines, you will amplify the chance of someone finding it. In turn, this will make it more likely to be viewed and cited in further works. Global Journals has compiled these guidelines to facilitate you to maximize the web-friendliness of the most public part of your paper.

Keywords

A major lynchpin of research work for the writing of research papers is the keyword search, which one will employ to find both library and internet resources. Up to eleven keywords or very brief phrases have to be given to help data retrieval, mining, and indexing.

One must be persistent and creative in using keywords. An effective keyword search requires a strategy: planning of a list of possible keywords and phrases to try.

Choice of the main keywords is the first tool of writing a research paper. Research paper writing is an art. Keyword search should be as strategic as possible.

One should start brainstorming lists of potential keywords before even beginning searching. Think about the most important concepts related to research work. Ask, "What words would a source have to include to be truly valuable in a research paper?" Then consider synonyms for the important words.

It may take the discovery of only one important paper to steer in the right keyword direction because, in most databases, the keywords under which a research paper is abstracted are listed with the paper.

Numerical Methods

Numerical methods used should be transparent and, where appropriate, supported by references.

Abbreviations

Authors must list all the abbreviations used in the paper at the end of the paper or in a separate table before using them.

Formulas and equations

Authors are advised to submit any mathematical equation using either MathJax, KaTeX, or LaTeX, or in a very high-quality image.

Tables, Figures, and Figure Legends

Tables: Tables should be cautiously designed, uncrowned, and include only essential data. Each must have an Arabic number, e.g., Table 4, a self-explanatory caption, and be on a separate sheet. Authors must submit tables in an editable format and not as images. References to these tables (if any) must be mentioned accurately.

Figures

Figures are supposed to be submitted as separate files. Always include a citation in the text for each figure using Arabic numbers, e.g., Fig. 4. Artwork must be submitted online in vector electronic form or by emailing it.

PREPARATION OF ELETRONIC FIGURES FOR PUBLICATION

Although low-quality images are sufficient for review purposes, print publication requires high-quality images to prevent the final product being blurred or fuzzy. Submit (possibly by e-mail) EPS (line art) or TIFF (halftone/ photographs) files only. MS PowerPoint and Word Graphics are unsuitable for printed pictures. Avoid using pixel-oriented software. Scans (TIFF only) should have a resolution of at least 350 dpi (halftone) or 700 to 1100 dpi (line drawings). Please give the data for figures in black and white or submit a Color Work Agreement form. EPS files must be saved with fonts embedded (and with a TIFF preview, if possible).

For scanned images, the scanning resolution at final image size ought to be as follows to ensure good reproduction: line art: >650 dpi; halftones (including gel photographs): >350 dpi; figures containing both halftone and line images: >650 dpi.

Color charges: Authors are advised to pay the full cost for the reproduction of their color artwork. Hence, please note that if there is color artwork in your manuscript when it is accepted for publication, we would require you to complete and return a Color Work Agreement form before your paper can be published. Also, you can email your editor to remove the color fee after acceptance of the paper.

TIPS FOR WRITING A GOOD QUALITY ENGINEERING RESEARCH PAPER

Techniques for writing a good quality engineering research paper:

1. Choosing the topic: In most cases, the topic is selected by the interests of the author, but it can also be suggested by the guides. You can have several topics, and then judge which you are most comfortable with. This may be done by asking several questions of yourself, like "Will I be able to carry out a search in this area? Will I find all necessary resources to accomplish the search? Will I be able to find all information in this field area?" If the answer to this type of question is "yes," then you ought to choose that topic. In most cases, you may have to conduct surveys and visit several places. Also, you might have to do a lot of work to find all the rises and falls of the various data on that subject. Sometimes, detailed information plays a vital role, instead of short information. Evaluators are human: The first thing to remember is that evaluators are also human beings. They are not only meant for rejecting a paper. They are here to evaluate your paper. So present your best aspect.

2. Think like evaluators: If you are in confusion or getting demotivated because your paper may not be accepted by the evaluators, then think, and try to evaluate your paper like an evaluator. Try to understand what an evaluator wants in your research paper, and you will automatically have your answer. Make blueprints of paper: The outline is the plan or framework that will help you to arrange your thoughts. It will make your paper logical. But remember that all points of your outline must be related to the topic you have chosen.

3. Ask your guides: If you are having any difficulty with your research, then do not hesitate to share your difficulty with your guide (if you have one). They will surely help you out and resolve your doubts. If you can't clarify what exactly you require for your work, then ask your supervisor to help you with an alternative. He or she might also provide you with a list of essential readings.

4. Use of computer is recommended: As you are doing research in the field of research engineering then this point is quite obvious. Use right software: Always use good quality software packages. If you are not capable of judging good software, then you can lose the quality of your paper unknowingly. There are various programs available to help you which you can get through the internet.

5. Use the internet for help: An excellent start for your paper is using Google. It is a wondrous search engine, where you can have your doubts resolved. You may also read some answers for the frequent question of how to write your research paper or find a model research paper. You can download books from the internet. If you have all the required books, place importance on reading, selecting, and analyzing the specified information. Then sketch out your research paper. Use big pictures: You may use encyclopedias like Wikipedia to get pictures with the best resolution. At Global Journals, you should strictly follow here.

6. Bookmarks are useful: When you read any book or magazine, you generally use bookmarks, right? It is a good habit which helps to not lose your continuity. You should always use bookmarks while searching on the internet also, which will make your search easier.

7. Revise what you wrote: When you write anything, always read it, summarize it, and then finalize it.

8. Make every effort: Make every effort to mention what you are going to write in your paper. That means always have a good start. Try to mention everything in the introduction—what is the need for a particular research paper. Polish your work with good writing skills and always give an evaluator what he wants. Make backups: When you are going to do any important thing like making a research paper, you should always have backup copies of it either on your computer or on paper. This protects you from losing any portion of your important data.

9. Produce good diagrams of your own: Always try to include good charts or diagrams in your paper to improve quality. Using several unnecessary diagrams will degrade the quality of your paper by creating a hodgepodge. So always try to include diagrams which were made by you to improve the readability of your paper. Use of direct quotes: When you do research relevant to literature, history, or current affairs, then use of quotes becomes essential, but if the study is relevant to science, use of quotes is not preferable.

10. Use proper verb tense: Use proper verb tenses in your paper. Use past tense to present those events that have happened. Use present tense to indicate events that are going on. Use future tense to indicate events that will happen in the future. Use of wrong tenses will confuse the evaluator. Avoid sentences that are incomplete.

11. Pick a good study spot: Always try to pick a spot for your research which is quiet. Not every spot is good for studying.

12. Know what you know: Always try to know what you know by making objectives, otherwise you will be confused and unable to achieve your target.

13. Use good grammar: Always use good grammar and words that will have a positive impact on the evaluator; use of good vocabulary does not mean using tough words which the evaluator has to find in a dictionary. Do not fragment sentences. Eliminate one-word sentences. Do not ever use a big word when a smaller one would suffice.

Verbs have to be in agreement with their subjects. In a research paper, do not start sentences with conjunctions or finish them with prepositions. When writing formally, it is advisable to never split an infinitive because someone will (wrongly) complain. Avoid clichés like a disease. Always shun irritating alliteration. Use language which is simple and straightforward. Put together a neat summary.

14. Arrangement of information: Each section of the main body should start with an opening sentence, and there should be a changeover at the end of the section. Give only valid and powerful arguments for your topic. You may also maintain your arguments with records.

15. Never start at the last minute: Always allow enough time for research work. Leaving everything to the last minute will degrade your paper and spoil your work.

16. Multitasking in research is not good: Doing several things at the same time is a bad habit in the case of research activity. Research is an area where everything has a particular time slot. Divide your research work into parts, and do a particular part in a particular time slot.

17. Never copy others' work: Never copy others' work and give it your name because if the evaluator has seen it anywhere, you will be in trouble. Take proper rest and food: No matter how many hours you spend on your research activity, if you are not taking care of your health, then all your efforts will have been in vain. For quality research, take proper rest and food.

18. Go to seminars: Attend seminars if the topic is relevant to your research area. Utilize all your resources.

19. Refresh your mind after intervals: Try to give your mind a rest by listening to soft music or sleeping in intervals. This will also improve your memory. Acquire colleagues: Always try to acquire colleagues. No matter how sharp you are, if you acquire colleagues, they can give you ideas which will be helpful to your research.

20. Think technically: Always think technically. If anything happens, search for its reasons, benefits, and demerits. Think and then print: When you go to print your paper, check that tables are not split, headings are not detached from their descriptions, and page sequence is maintained.

21. Adding unnecessary information: Do not add unnecessary information like "I have used MS Excel to draw graphs." Irrelevant and inappropriate material is superfluous. Foreign terminology and phrases are not apropos. One should never take a broad view. Analogy is like feathers on a snake. Use words properly, regardless of how others use them. Remove quotations. Puns are for kids, not grunt readers. Never oversimplify: When adding material to your research paper, never go for oversimplification; this will definitely irritate the evaluator. Be specific. Never use rhythmic redundancies. Contractions shouldn't be used in a research paper. Comparisons are as terrible as clichés. Give up ampersands, abbreviations, and so on. Remove commas that are not necessary. Parenthetical words should be between brackets or commas. Understatement is always the best way to put forward earth-shaking thoughts. Give a detailed literary review.

22. Report concluded results: Use concluded results. From raw data, filter the results, and then conclude your studies based on measurements and observations taken. An appropriate number of decimal places should be used. Parenthetical remarks are prohibited here. Proofread carefully at the final stage. At the end, give an outline to your arguments. Spot perspectives of further study of the subject. Justify your conclusion at the bottom sufficiently, which will probably include examples.

23. Upon conclusion: Once you have concluded your research, the next most important step is to present your findings. Presentation is extremely important as it is the definite medium though which your research is going to be in print for the rest of the crowd. Care should be taken to categorize your thoughts well and present them in a logical and neat manner. A good quality research paper format is essential because it serves to highlight your research paper and bring to light all necessary aspects of your research.

Informal Guidelines of Research Paper Writing

Key points to remember:

- Submit all work in its final form.
- Write your paper in the form which is presented in the guidelines using the template.
- Please note the criteria peer reviewers will use for grading the final paper.

Final points:

One purpose of organizing a research paper is to let people interpret your efforts selectively. The journal requires the following sections, submitted in the order listed, with each section starting on a new page:

The introduction: This will be compiled from reference matter and reflect the design processes or outline of basis that directed you to make a study. As you carry out the process of study, the method and process section will be constructed like that. The results segment will show related statistics in nearly sequential order and direct reviewers to similar intellectual paths throughout the data that you gathered to carry out your study.

The discussion section:

This will provide understanding of the data and projections as to the implications of the results. The use of good quality references throughout the paper will give the effort trustworthiness by representing an alertness to prior workings.

Writing a research paper is not an easy job, no matter how trouble-free the actual research or concept. Practice, excellent preparation, and controlled record-keeping are the only means to make straightforward progression.

General style:

Specific editorial column necessities for compliance of a manuscript will always take over from directions in these general guidelines.

To make a paper clear: Adhere to recommended page limits.

Mistakes to avoid:

- Insertion of a title at the foot of a page with subsequent text on the next page.
- Separating a table, chart, or figure—confine each to a single page.
- Submitting a manuscript with pages out of sequence.
- In every section of your document, use standard writing style, including articles ("a" and "the").
- Keep paying attention to the topic of the paper.

- Use paragraphs to split each significant point (excluding the abstract).
- Align the primary line of each section.
- Present your points in sound order.
- Use present tense to report well-accepted matters.
- Use past tense to describe specific results.
- Do not use familiar wording; don't address the reviewer directly. Don't use slang or superlatives.
- Avoid use of extra pictures—include only those figures essential to presenting results.

Title page:

Choose a revealing title. It should be short and include the name(s) and address(es) of all authors. It should not have acronyms or abbreviations or exceed two printed lines.

Abstract: This summary should be two hundred words or less. It should clearly and briefly explain the key findings reported in the manuscript and must have precise statistics. It should not have acronyms or abbreviations. It should be logical in itself. Do not cite references at this point.

An abstract is a brief, distinct paragraph summary of finished work or work in development. In a minute or less, a reviewer can be taught the foundation behind the study, common approaches to the problem, relevant results, and significant conclusions or new questions.

Write your summary when your paper is completed because how can you write the summary of anything which is not yet written? Wealth of terminology is very essential in abstract. Use comprehensive sentences, and do not sacrifice readability for brevity; you can maintain it succinctly by phrasing sentences so that they provide more than a lone rationale. The author can at this moment go straight to shortening the outcome. Sum up the study with the subsequent elements in any summary. Try to limit the initial two items to no more than one line each.

Reason for writing the article—theory, overall issue, purpose.

- Fundamental goal.
- To-the-point depiction of the research.
- Consequences, including definite statistics—if the consequences are quantitative in nature, account for this; results of any numerical analysis should be reported. Significant conclusions or questions that emerge from the research.

Approach:

o Single section and succinct.
o An outline of the job done is always written in past tense.
o Concentrate on shortening results—limit background information to a verdict or two.
o Exact spelling, clarity of sentences and phrases, and appropriate reporting of quantities (proper units, important statistics) are just as significant in an abstract as they are anywhere else.

Introduction:

The introduction should "introduce" the manuscript. The reviewer should be presented with sufficient background information to be capable of comprehending and calculating the purpose of your study without having to refer to other works. The basis for the study should be offered. Give the most important references, but avoid making a comprehensive appraisal of the topic. Describe the problem visibly. If the problem is not acknowledged in a logical, reasonable way, the reviewer will give no attention to your results. Speak in common terms about techniques used to explain the problem, if needed, but do not present any particulars about the protocols here.

The following approach can create a valuable beginning:

o Explain the value (significance) of the study.
o Defend the model—why did you employ this particular system or method? What is its compensation? Remark upon its appropriateness from an abstract point of view as well as pointing out sensible reasons for using it.
o Present a justification. State your particular theory(-ies) or aim(s), and describe the logic that led you to choose them.
o Briefly explain the study's tentative purpose and how it meets the declared objectives.

Approach:

Use past tense except for when referring to recognized facts. After all, the manuscript will be submitted after the entire job is done. Sort out your thoughts; manufacture one key point for every section. If you make the four points listed above, you will need at least four paragraphs. Present surrounding information only when it is necessary to support a situation. The reviewer does not desire to read everything you know about a topic. Shape the theory specifically—do not take a broad view.

As always, give awareness to spelling, simplicity, and correctness of sentences and phrases.

Procedures (methods and materials):

This part is supposed to be the easiest to carve if you have good skills. A soundly written procedures segment allows a capable scientist to replicate your results. Present precise information about your supplies. The suppliers and clarity of reagents can be helpful bits of information. Present methods in sequential order, but linked methodologies can be grouped as a segment. Be concise when relating the protocols. Attempt to give the least amount of information that would permit another capable scientist to replicate your outcome, but be cautious that vital information is integrated. The use of subheadings is suggested and ought to be synchronized with the results section.

When a technique is used that has been well-described in another section, mention the specific item describing the way, but draw the basic principle while stating the situation. The purpose is to show all particular resources and broad procedures so that another person may use some or all of the methods in one more study or referee the scientific value of your work. It is not to be a step-by-step report of the whole thing you did, nor is a methods section a set of orders.

Materials:

Materials may be reported in part of a section or else they may be recognized along with your measures.

Methods:

- o   Report the method and not the particulars of each process that engaged the same methodology.
- o   Describe the method entirely.
- o   To be succinct, present methods under headings dedicated to specific dealings or groups of measures.
- o   Simplify—detail how procedures were completed, not how they were performed on a particular day.
- o   If well-known procedures were used, account for the procedure by name, possibly with a reference, and that's all.

Approach:

It is embarrassing to use vigorous voice when documenting methods without using first person, which would focus the reviewer's interest on the researcher rather than the job. As a result, when writing up the methods, most authors use third person passive voice.

Use standard style in this and every other part of the paper—avoid familiar lists, and use full sentences.

What to keep away from:

- o   Resources and methods are not a set of information.
- o   Skip all descriptive information and surroundings—save it for the argument.
- o   Leave out information that is immaterial to a third party.

Results:

The principle of a results segment is to present and demonstrate your conclusion. Create this part as entirely objective details of the outcome, and save all understanding for the discussion.

The page length of this segment is set by the sum and types of data to be reported. Use statistics and tables, if suitable, to present consequences most efficiently.

You must clearly differentiate material which would usually be incorporated in a study editorial from any unprocessed data or additional appendix matter that would not be available. In fact, such matters should not be submitted at all except if requested by the instructor.

Content:

- o Sum up your conclusions in text and demonstrate them, if suitable, with figures and tables.
- o In the manuscript, explain each of your consequences, and point the reader to remarks that are most appropriate.
- o Present a background, such as by describing the question that was addressed by creation of an exacting study.
- o Explain results of control experiments and give remarks that are not accessible in a prescribed figure or table, if appropriate.
- o Examine your data, then prepare the analyzed (transformed) data in the form of a figure (graph), table, or manuscript.

What to stay away from:

- o Do not discuss or infer your outcome, report surrounding information, or try to explain anything.
- o Do not include raw data or intermediate calculations in a research manuscript.
- o Do not present similar data more than once.
- o A manuscript should complement any figures or tables, not duplicate information.
- o Never confuse figures with tables—there is a difference.

Approach:

As always, use past tense when you submit your results, and put the whole thing in a reasonable order.

Put figures and tables, appropriately numbered, in order at the end of the report.

If you desire, you may place your figures and tables properly within the text of your results section.

Figures and tables:

If you put figures and tables at the end of some details, make certain that they are visibly distinguished from any attached appendix materials, such as raw facts. Whatever the position, each table must be titled, numbered one after the other, and include a heading. All figures and tables must be divided from the text.

Discussion:

The discussion is expected to be the trickiest segment to write. A lot of papers submitted to the journal are discarded based on problems with the discussion. There is no rule for how long an argument should be.

Position your understanding of the outcome visibly to lead the reviewer through your conclusions, and then finish the paper with a summing up of the implications of the study. The purpose here is to offer an understanding of your results and support all of your conclusions, using facts from your research and generally accepted information, if suitable. The implication of results should be fully described.

Infer your data in the conversation in suitable depth. This means that when you clarify an observable fact, you must explain mechanisms that may account for the observation. If your results vary from your prospect, make clear why that may have happened. If your results agree, then explain the theory that the proof supported. It is never suitable to just state that the data approved the prospect, and let it drop at that. Make a decision as to whether each premise is supported or discarded or if you cannot make a conclusion with assurance. Do not just dismiss a study or part of a study as "uncertain."

Research papers are not acknowledged if the work is imperfect. Draw what conclusions you can based upon the results that you have, and take care of the study as a finished work.

- o You may propose future guidelines, such as how an experiment might be personalized to accomplish a new idea.
- o Give details of all of your remarks as much as possible, focusing on mechanisms.
- o Make a decision as to whether the tentative design sufficiently addressed the theory and whether or not it was correctly restricted. Try to present substitute explanations if they are sensible alternatives.
- o One piece of research will not counter an overall question, so maintain the large picture in mind. Where do you go next? The best studies unlock new avenues of study. What questions remain?
- o Recommendations for detailed papers will offer supplementary suggestions.

Approach:

When you refer to information, differentiate data generated by your own studies from other available information. Present work done by specific persons (including you) in past tense.

Describe generally acknowledged facts and main beliefs in present tense.

The Administration Rules

Administration Rules to Be Strictly Followed before Submitting Your Research Paper to Global Journals Inc.

Please read the following rules and regulations carefully before submitting your research paper to Global Journals Inc. to avoid rejection.

Segment draft and final research paper: You have to strictly follow the template of a research paper, failing which your paper may get rejected. You are expected to write each part of the paper wholly on your own. The peer reviewers need to identify your own perspective of the concepts in your own terms. Please do not extract straight from any other source, and do not rephrase someone else's analysis. Do not allow anyone else to proofread your manuscript.

Written material: You may discuss this with your guides and key sources. Do not copy anyone else's paper, even if this is only imitation, otherwise it will be rejected on the grounds of plagiarism, which is illegal. Various methods to avoid plagiarism are strictly applied by us to every paper, and, if found guilty, you may be blacklisted, which could affect your career adversely. To guard yourself and others from possible illegal use, please do not permit anyone to use or even read your paper and file.

CRITERION FOR GRADING A RESEARCH PAPER (COMPILATION) BY GLOBAL JOURNALS

Please note that following table is only a Grading of "Paper Compilation" and not on "Performed/Stated Research" whose grading solely depends on Individual Assigned Peer Reviewer and Editorial Board Member. These can be available only on request and after decision of Paper. This report will be the property of Global Journals.

Topics	Grades		
	A-B	**C-D**	**E-F**
Abstract	Clear and concise with appropriate content, Correct format. 200 words or below	Unclear summary and no specific data, Incorrect form Above 200 words	No specific data with ambiguous information Above 250 words
Introduction	Containing all background details with clear goal and appropriate details, flow specification, no grammar and spelling mistake, well organized sentence and paragraph, reference cited	Unclear and confusing data, appropriate format, grammar and spelling errors with unorganized matter	Out of place depth and content, hazy format
Methods and Procedures	Clear and to the point with well arranged paragraph, precision and accuracy of facts and figures, well organized subheads	Difficult to comprehend with embarrassed text, too much explanation but completed	Incorrect and unorganized structure with hazy meaning
Result	Well organized, Clear and specific, Correct units with precision, correct data, well structuring of paragraph, no grammar and spelling mistake	Complete and embarrassed text, difficult to comprehend	Irregular format with wrong facts and figures
Discussion	Well organized, meaningful specification, sound conclusion, logical and concise explanation, highly structured paragraph reference cited	Wordy, unclear conclusion, spurious	Conclusion is not cited, unorganized, difficult to comprehend
References	Complete and correct format, well organized	Beside the point, Incomplete	Wrong format and structuring

INDEX
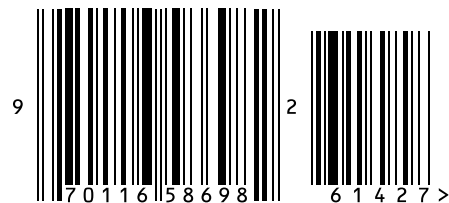
save our planet

Global Journal of Researches in Engineering

Visit us on the Web at www.GlobalJournals.org | www.EngineeringResearch.org
or email us at helpdesk@globaljournals.org